NASA CONTRACTOR REPORT 166268

Study of Aerodynamic Technology for Single-Cruise-Engine V/STOL Fighter/Attack Aircraft

Phase I Final Report

W. H. Foley
A. E. Sheridan
C. W. Smith
General Dynamics Corporation

CONTRACT NAS2-11000
February 1982

NASA CONTRACTOR REPORT 166268

Study of Aerodynamic Technology for Single-Cruise-Engine V/STOL Fighter/Attack Aircraft

Phase I Final Report

W. H. Foley
A. E. Sheridan
C. W. Smith
General Dynamics Corporation
Fort Worth, Texas

Prepared for
Ames Research Center
Under Contract NAS2-11000

National Aeronautics and
Space Administration

Ames Research Center
Moffett Field, California 94035

This Page Intentionally Left Blank

FOREWORD

The study of Aerodynamic Technology for a Single-Cruise-Engine V/STOL Fighter/Attack Aircraft was conducted under contract NAS2-11000, which was jointly sponsored by NASA/ARC, NAVAIR and DTNSRDC. The contract monitor was Mr. D. A. Durston of NASA/ARC. The study was conducted by General Dynamics' Fort Worth Division Aerodynamics Section with Dr. W. H. Foley serving as program manager.

The authors wish to acknowledge the assistance provided by technical contacts, W. P. Nelms, D. A. Durston (NASA/ARC), M. W. Brown (NAVAIR) and J. H. Nichols (DTNSRDC) and General Dynamics engineers, B. B. Beard, M. A. Kaiser, J. D. Pressley, D. C. Rapp and H. L. Roland.

Dimensional quantities in this report are given in U.S. Customary Units. A table for conversion to International System (SI) Units is provided in the Appendix.

This Page Intentionally Left Blank

TABLE OF CONTENTS

TABLE OF CONTENTS (Continued)

LIST OF TABLES

This Page Intentionally Left Blank

LIST OF FIGURES

LIST OF FIGURES (Continued)

LIST OF FIGURES (Continued)

LIST OF FIGURES (Continued)

LIST OF SYMBOLS

A/B	afterburner
a.c.	aerodynamic center, percent MAC
ADEN	augmented deflecting exhaust nozzle
AR	aspect ratio
b	span, in.
$\bar{c}$, MAC	mean aerodynamic chord, in.
C_D	drag coefficient
$C_{D_{o,o}}$	zero-lift/zero-camber drag coefficient
C_L	lift coefficient
$C_{L_{buffet}}$	lift coefficient for constant buffet intensity
$C_{L_{maximum\ usable}}$	maximum usable lift coefficient
C_{L_α}	lift-curve slope
$C_{L_{\delta_e}}$	derivative of lift coefficient with respect to elevator deflection
C_l	rolling-moment coefficient
C_{l_p}	derivative of rolling-moment coefficient with respect to roll rate
C_{l_β}	derivative of rolling-moment coefficient with respect to sideslip angle
$C_{l_{\delta_a}}$	derivative of rolling-moment coefficient with respect to aileron deflection
$C_{m_{x\bar{c}}}$	pitching moment about x percent MAC
C_{m_o}	zero-lift pitching-moment coefficient
C_{m_q}	derivative of pitching-moment coefficient with respect to pitch rate
$C_{m_{\dot{\alpha}}}$	derivative of pitching-moment coefficient with respect to angle-of-attack rate
C_n	yawing-moment coefficient
C_{n_p}	derivative of yawing-moment coefficient with respect to roll rate

LIST OF SYMBOLS (Continued)

C_{n_r}	derivative of yawing-moment coefficient with respect to yaw rate
C_{n_β}	derivative of yawing-moment coefficient with respect to sideslip angle
$C_{n\,\delta_a}$	derivative of yawing-moment coefficient with respect to aileron deflection
$C_{n\,\delta_r}$	derivative of yawing-moment coefficient with respect to rudder deflection
C.P.	center of pressure, percent MAC
$C.P._{\delta e}$	center of pressure of left due to elevon deflection, percent MAC
C_T	thrust coefficient, $\frac{T}{q\,S_{ref}}$
C_y	side-force coefficient
C_{y_r}	derivative of side-force coefficient with respect to yaw rate
C_{y_β}	derivative of side-force coefficient with respect to sideslip angle
$C_{y\,\delta_r}$	derivative of side-force coefficient with respect to rudder deflection
c_r	root chord
c_t	tip chord
D	drag, lb
e	span efficiency factor
ESF	engine scale factor, $\frac{T}{T_{ESF=1.0}}$
h	pressure altitude, ft
k	fraction of fan air exhausting through the ejectors
L	lift, lb
M	Mach number
MAC	mean aerodynamic chord
NPR	nozzle pressure ratio, $\frac{P_t}{P}$
N	normal force, lb

LIST OF SYMBOLS (Continued)

N_Z	limit vertical load factor
OWE	operating weight empty
P_∞	freestream static pressures, lb/ft ^{2}
P_S	specific excess power
P_t	total pressure, lb/ft^2
q	freestream dynamic pressure, lb/ft^2
RCS	reaction control system
SOB	sink over bow, ft
S_{ref}	reference wing area, ft^2
STO	short takeoff
STOL	short takeoff or landing
STOVL	short takeoff/vertical landing
S_{VT}	exposed area of vertical tail, ft^2
T	thrust, lb
TS	Type Specification
t/c	thickness-to-chord ratio (percent)
U_{de}	gust velocity, ft/sec
V	freestream velocity, ft/sec, knots
V_E	equivalent airspeed
V_H	high-speed design airspeed
V_L	design limit airspeed
VSTOL	vertical or short takeoff or landing
VTOL	vertical takeoff or landing
$\dot{w}$	weight flow, lb/sec
WOD	velocity of wind over deck, knots

LIST OF SYMBOLS (Concluded)

α, alpha	angle of attack, deg
α_{LO}	angle of attack at zero lift, deg
β, beta	angle of sideslip, deg
ϕ	ejector measured thrust/isentropic supply thrust (where isentropic supply thrust is the thrust which would be obtained from supplied air at the nozzle exit of pressures and flow rates expanded at isentropically to ambient pressure)
	or
	roll angle, deg
δ_e	elevon deflection, deg
δ_r	rudder deflection, deg
δ_n	thrust vector angle for core ADEN, deg
θ	pitch attitude angle, deg
ψ	yaw angle, deg
γ	flight path angle, deg
λ	taper ratio, $\frac{c_r}{c_t}$
$\sigma_{c.g.}$	r.m.s. buffet intensity at center of gravity
Λ_{LE}	leading-edge sweep angle, deg

1. INTRODUCTION

Early in 1980 General Dynamics began a program to investigate the possibilities of designing a V/STOL fighter/attack aircraft incorporating an existing engine, as opposed to the conventional process of designing conceptual aircraft to given missions, which generally require new engines. The logic behind this was twofold: such a demonstrator aircraft could be built much faster and cheaper than one requiring an engine development.

1.1 PROPULSIVE CONCEPT

One of the propulsion systems that appeared attractive was the ejector system developed under contract to NASA/Ames (References 1 through 4). This ejector system is somewhat more bulky than a short-diffuser type such as the Alperin ejector, but it has the advantage of possessing a respectable, dependable augmentation ratio, ϕ, that has been demonstrated on a large-scale, engine-driven model at Ames.

From the perspective of General Dynamics, the advantage of an ejector system is not just its high augmentation. It is more significant that the ejector exhaust is cool and its velocity is relatively low. Although afterburning systems such as RALS and PCB are capable of equally good augmentations, and although lift engines are probably the most compact systems available, it is our opinion that the environmental and inlet injestion problems associated with the extremely hot and high-velocity exhausts of these other systems have not been fully addressed. Our own investigations indicate that it is not only possible to get into very real problems when operating aircraft based on such systems, but highly probable. Although fixes, such as deck grids, might be found, it seems certain that such fixes will limit the operational usefulness of hot-footprint aircraft. An ejector system simply avoids the problem.

To be sure, an ejector system does present some difficulties, the largest single one being the ram drag of the entrained air at forward speeds. In fact, the original ejector model tested at the Ames 40- by 80-foot wind tunnel was quite marginal in its ability to transition from ejector-borne to wing-borne flight due to ram drag. Although it was demonstrated that this could be overcome by vectoring the ejector nozzles aft, an operational aircraft would require controllable vector angles that in turn would require quite complex actuation systems. One way to avoid this problem is to duct only part of the engine flow to the ejector and to exhaust the rest to a single, vectorable nozzle. Further, if only fan air is used to power the ejector, the problem of ducting hot gasses is eliminated. Therefore, the propulsive system used consists of one wherein the fan air flow powers a set of ejectors forward on the aircraft, while the core air is ducted and vectored separately aft. The concept, wherein the fan and core air is separated, is shown schematically in Figure 1-1.

Figure 1-2 shows the propulsive configuration during hovering flight, while Figure 1-3 shows the transition or STO regime, and Figure 1-4 shows up-and-away flight. (These three figures show the present system as drawn around a General Electric engine. The earlier concepts, which were drawn around Pegasus-type engines, differ slightly; these differences will be pointed out as the history of the configuration is discussed below.)

1.1.1 Operational Assumptions

The ultimate, operational aircraft envisioned will have a mid-1990's IOC. It is not entirely clear what Naval requirements will be at that date, so a number of assumptions have been made:

A. In 1995 the Navy will be using large-decked carriers such as are presently in use. While dispersal requirements may lead the Navy to smaller decks in the early 21st century, it is unlikely that the carrier in that time frame will be much smaller than the Essex class, i.e., 600 Ft decks. The concept of fleet air operations being conducted from a great many small ships fails unless improvements in reliability, maintainability, and command control of orders of magnitude are assumed. Historically, this has only happened in the entire field of engineering once the technology base of a vehicle has been frozen. Witness, for example, the automobile. Reliability has certainly improved between 1920 and today, but the basic technology - the reciprocating engine -has held fairly constant. The history of naval requirements since the time of Nelson has demanded - and been dependent upon - vast growth of technologies in countless areas; on the whole, there is absolutely no reason to assume that this situation will reverse itself.

B. A naval aircraft in the 15,000 to 30,000 lb class is too small a weapons platform to perform primary fleet air defense or deep interdiction missions. It would be more appropriate to assign to it close air defense and close air support.

The first assumption above has led General Dynamics to consider only STOVL concepts. At this point, we shall define the term as we use it - viz, in a military mission sense, the only way takeoff can be achieved is through a STO deck run of roughly 400 ft. Vertical landing capability is defined as coming aboard with a reasonable fuel reserve plus any expensive weapons which might be retained.

By this definition, STOVL accomplishes the prime benefit of V/STOL which is that of greatly increasing AIROPS flexibility and decreasing deck cycle times while, at the same time, removing catapult and arresting gear machinery and support personnel from the carrier. It also eliminates the prime drawback of V/STOL - propulsion size and aircraft cost is not driven to the point where it is cost ineffective.

The second assumption has led General Dynamics to pick a modified Type Specification 169 (TS 169) as the design goal. While it is not yet known to be fully responsive to the needs post-1995 Navy, it nonetheless describes the characteristics of a vehicle designed to perform viable military missions and, thus, provides a good starting baseline.

1.1.2 Type Specification 169 (Modified)

For each general configuration, three aircraft are considered, that is, a flight demonstrator, and two operational aircraft - a threshold and a goal aircraft. Flight demonstrator aircraft are built around existing engines or very near-term derivatives. Their primary purpose is to demonstrate the VL and STO ends of the flight regimes. As such, afterburners are not assumed. However, they have been constrained to possess the same airframe as the operational aircraft so that the only extrapolations required from the flight demonstrator are propulsional. Reaction-control-system power is provided by APU's. Threshold operational aircraft are defined as those whose engine thrusts may be assumed to be developed in the normal course of engine growth during the next fifteen or

so years, but which will require technological advances primarily in the area of reaction control power provided by the engine. The goal operational aircraft require a more advanced engine in order to provide significantly enhanced hover thrust. These definitions are quantified in Table 1-1. The impetus for setting the goal operational aircraft vertical landing weight as the air-to-air weapons plus 4000 lbs. payload was the assumption that, during the time period 1995+, air-to-ground weapons will become sufficiently sophisticated - and expensive - that recovery of unexpended stores will be a requirement. Another modification to TS 169 is that the interdiction mission be flown with internal fuel. This was due to the fuel weight penalties incurred by the increased cruise drag of external tankage, which is especially critical during STO. The last exception is the removal of the gun. It is anticipated that IFF devices will become sufficiently reliable and accurate so that visual recognition will not be required in air-to-air combat. As for strafing, at a time when ground-to-air weapons are being carried at battalion and, possibly, company levels, the exposure time required to strafe will likely present risk to attack aircraft. However, should a gun remain a requirement, it could be accommodated by the goal aircraft by lowering the weight of expendable stores returned to the carrier.

Initially, the hover fuel allowance used was 5 percent of full fuel plus 20 minutes sea level loiter. However, upon reflection such a reserve makes little sense for a STOVL. It does not account for the fact that VL capability will significantly lower landing cycle times. Further, twenty minutes' loiter fuel does not necessarily provide any meaningful hover time, especially with configurations which use afterburners while hovering. For the concepts studies herein, it happens that 20 minutes loiter fuel equates to 4 minutes hover capability. Therefore, the hover fuel reserve was changed to 5 percent plus 4 minutes at intermediate hover. This, however, is a subject which will require more detailed investigation.

The TS 169 point performance for the operational aircraft is shown in Table 1-2; no modifications or exceptions are taken.

Table 1-1

TYPE SPEC 169, MODIFIED

MISSIONS

ESCORT	-	400 MILE RADIUS 2 AIM-9 2 AMRAAM NO GUN 1.05 SFC + 5 PERCENT RESERVE
INTERDICTION	-	550 MILE RADIUS WITH INTERNAL FUEL 2 AIM-9 4 MK 83 NO GUN 1.05 SFC + 5 PERCENT RESERVE

STO*

ESCORT	-	400 FT, ZERO WIND, ZERO SINK
INTERDICTION	-	400 FT WITH SKI JUMP OR 400 FT, 25 KT WOD

VL*

FLIGHT DEMO	-	OWE + 4 MIN. INT. POWER FUEL
THRESHHOLD	-	OWE + FUEL FOR 4 MIN. INT. POWER FUEL + 5 PERCENT TAKEOFF FUEL + 2 AIM-9 + 2 AMRAAM

OPERATIONAL

GOAL	-	OWE + ABOVE FUEL + 2 AIM-9 + 4000 LBS

*TROPICAL DAY, SEA LEVEL

Table 1-2 TYPE SPECIFICATION 169 POINT PERFORMANCE

	THRESHOLD	GOAL
M_{MAX}, DRY POWER, 10000 FT	.98	1.0
COMBAT CEILING, DRY POWER	45000 FT	50000 FT
ACCEL, .8 M TO 1.6 M, 35000 FT	110 SEC.	80 SEC
SUSTAINED G, .65 M, 10000 FT	5.0	5.5
P_S, .9 M, 10000 FT	750 fps	850 fps

✔ POINT PERFORMANCE CALCULATED WITH ESCORT STORES AND 60% FULL FUEL

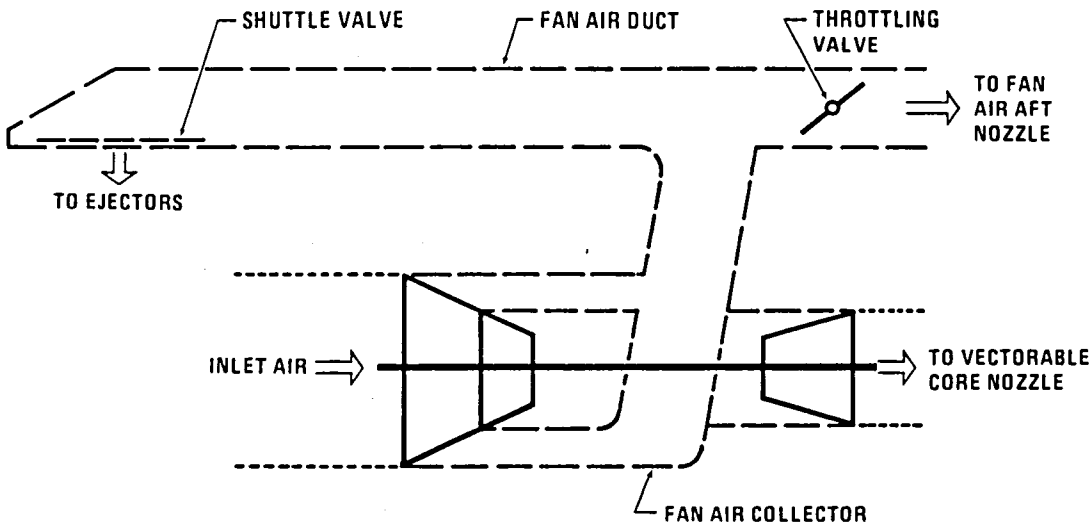

Figure 1-1 Propulsive System Schematic

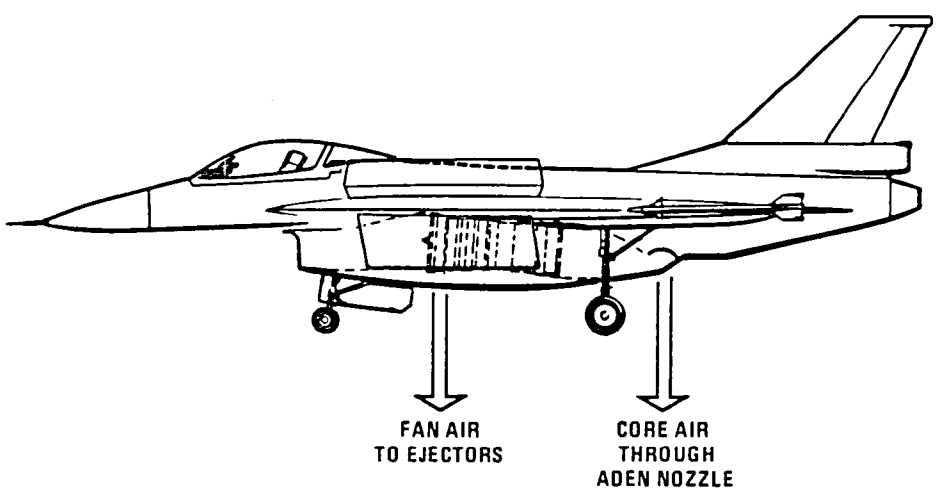

Figure 1-2 Propulsion System — Hover Configuration

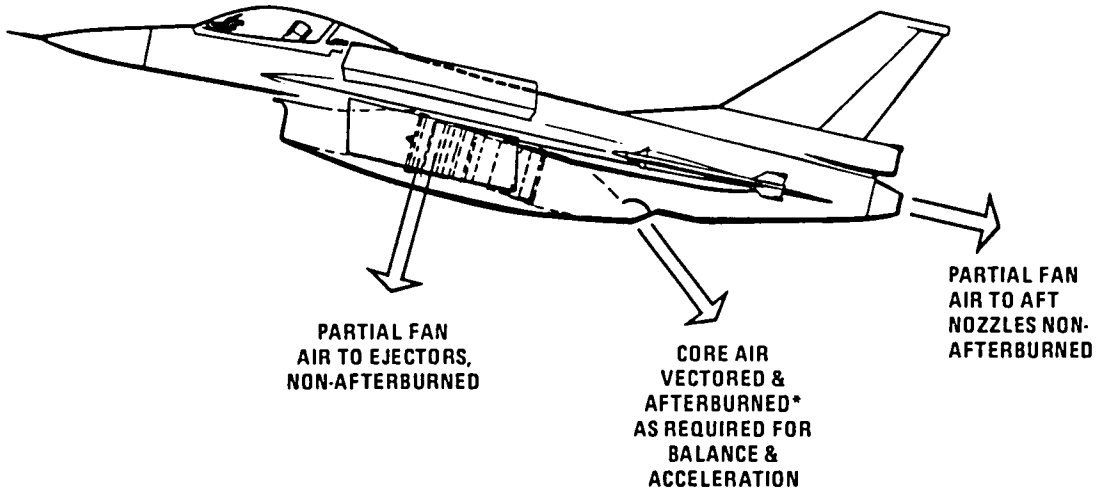

**CORE AFTERBURNED ONLY ON F101-DFE CONFIGURATIONS*

Figure 1-3 Propulsion System — STO and Transition Configuration

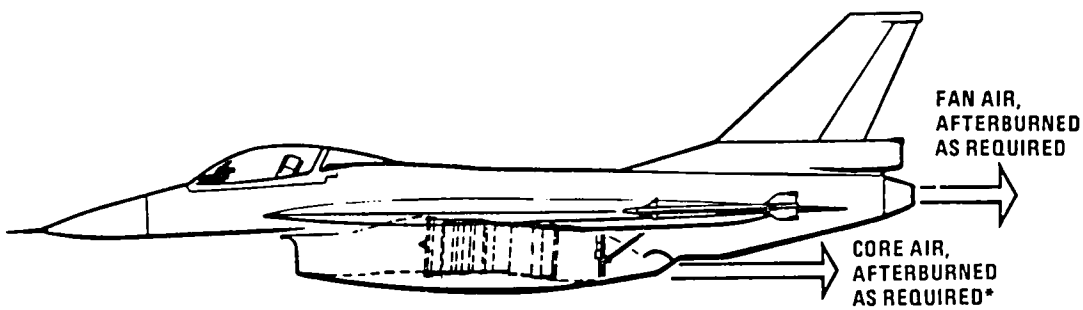

**ONLY ON F101-DFE CONFIGURATIONS*

Figure 1-4 Propulsion System — Up-and-Away Configuration

1.2 ADVANCED PEGASUS CONCEPTS

The initial designs of the E-series were drawn around the Rolls-Royce 11F35 engine, for a flight demonstrator, and a Rolls-Royce J-engine, for the operational aircraft. (The detailed propulsion characteristics of these and the other engines considered in this work are proprietary to the respective engine manufacturers; they are discussed in Reference 5.) In the Rolls-powered configurations, the core flows are not afterburned for the operational aircraft.

1.2.1 Configuration E-1

The first configuration in the series attempted to incorporate the ejector with a VEO-wing . In this design, fan air exhausted over two VEO nozzles when it was not ducted to the ejector. While this may have produced an outstanding STO aircraft, structural design difficulties developed between the wing box and the fan air duct. Thus, this design was refined to avoid the problem.

1.2.2 Configuration E-2

In this configuration (Figure 1-5), the ejectors were placed in oversized, F-16-type strakes. The aft fan air exhaust was ducted to a 2-D, afterburning nozzle, and the core flow exhausted to a vectorable, axisymmetric nozzle. Initial performance indicated that the aircraft could meet most of TS 169 with the exception of point performance. Because of structural interference between the ejectors and the wing box, the wing had to be located aft in a non-optimum position. The resultant impact on the area curve and trim drag was such that the configuration was capable of only subsonic flight. In order to increase the flexibility of locating the ejector relative to the c.g., and the wing with respect to the c.g. and the area curve, a long-root-chord configuration (whose diffuse structure allowed such flexibility) was investigated.

1.2.3 Configurations E-3 and E-4

An F-16E cranked-arrow wing was placed around the E-2 fuselage and propulsion system to become Configuration E-3 (Figure 1-6). Preliminary analysis indicated that, with full-span leading edge devices for maneuver, this J-engine configuration would meet TS 169 escort mission and point performance, while, with the 11F35 engine, a good flight demonstrator could be achieved; takeoff performance for the two is indicated on Table 1-3.

A further refinement of E-3 was attempted in configuration E-4, the aft fan air nozzle was eliminated and the fan air was remixed with the core air through an ADEN nozzle when not being used in the ejectors (Figure 1-7). However, this required that the fan and core pressures be matched. This sufficiently degraded the performance of the Pegasus-type engine that further development of E-4 was stopped and E-3 became the standard for further development of the series.

At this state in the development it became questionable that the 11F35 would be funded for development. Although the 11F35 would make a reasonable flight demonstrator for E-3, it appeared very unlikely that it would also make a satisfactory operational aircraft. Therefore, under a study separate from the present, a search for an alternate engine was initiated (Ref. 5). The General Electric F101/DFE emerged as a very suitable candidate, and was picked as the engine for this study.

Table 1-3 TAKEOFF PERFORMANCE FOR ROLLS ROYCE POWERED E-3

PRELIMINARY ESTIMATES

	PEGASUS 11-F35	J-ENG.
ZERO FUEL WEIGHT	19608	21721
$VTOGW_{max}$	24729	28682
STOGW:*		
400' RUN (USN)	31900	37000
1500 ' (USAF) W. EJEC./W.O. EJEC.	43928/35342	52400/41000

**Fan Air Afterburned, Both Aircraft, During Accel.*

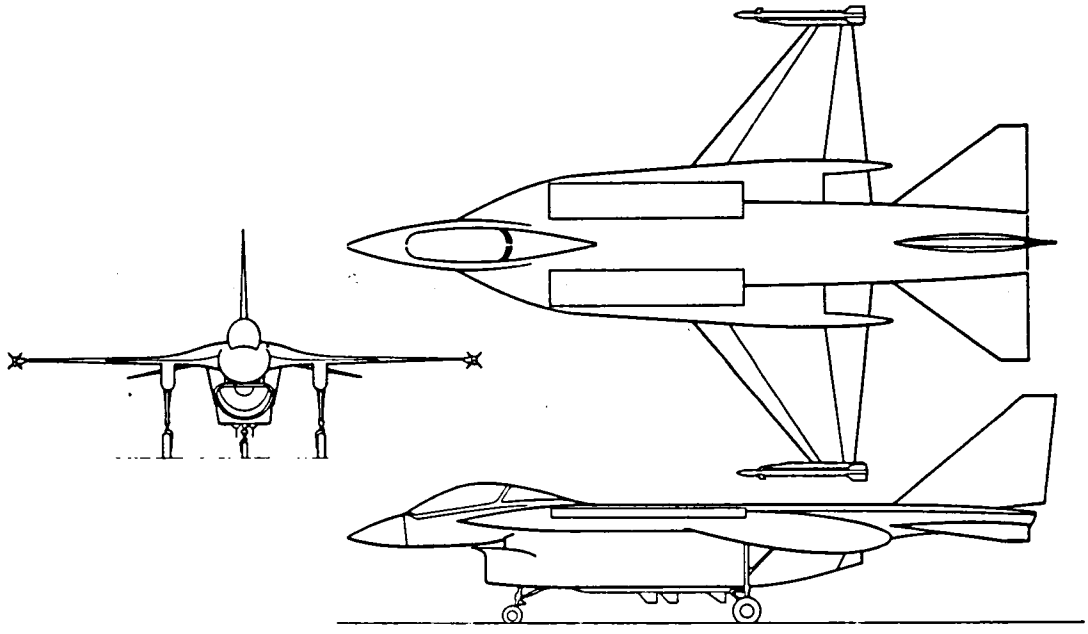

Figure 1-5 Configuration E-2

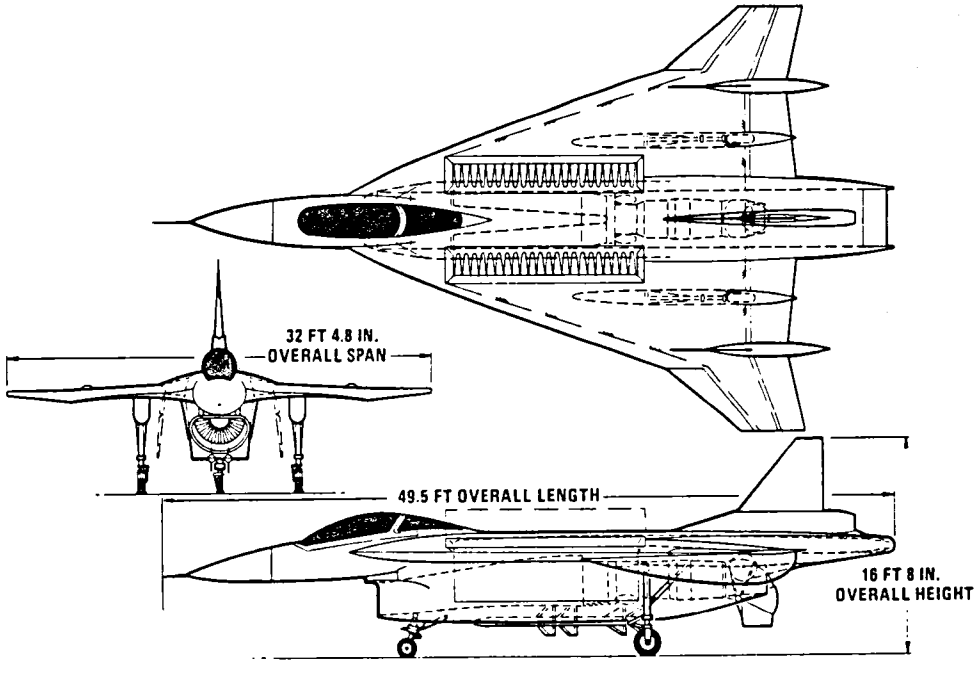

Figure 1-6 Rolls Royce Powered Configuration E-3

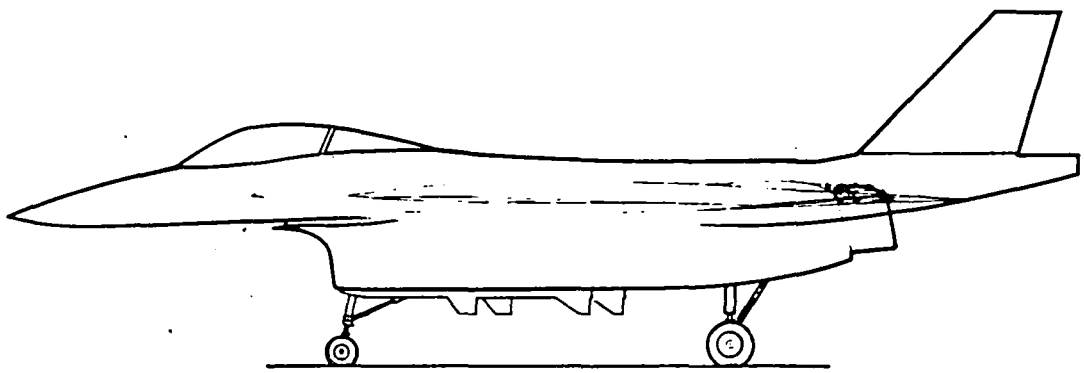

Figure 1-7 Configuration E-4

1.3 F101/DFE CONCEPTS

The previous conceptual design work was conducted under General Dynamics' funding; what follows describes the work sponsored by NASA Contract No. NAS2-11000 of which this is the final report.

1.3.1 Configuration E-3/DFE

The basic differences, as influence an aircraft design, between the Rolls-Royce and General Electric engines under consideration are that the G.E. engine is of lower thrust and lower B.P.R. than the R.R. However, the G.E. engine is more suitable to core air afterburning than the R.R. Thus, the first task in the study was to adapt the E-3 configuration to the G.E. engine. As a result of the lower thrust, the original E-3 wing was sized down by a scale factor of .9 (which gave an S_{ref} of 523 ft^2), and, as a result of the benefit of afterburning the core flow, an ADEN was substituted in place of the previous vectorable axisymmetric nozzle. This required that the 2-D fan air nozzle be replaced by an axisymmetric afterburning nozzle, because the confluence of two 2-D nozzles on this configuration presented unacceptable base drag and fuselage heating problems. The fuselage forebody was changed to one similar to an F-16. One reason for this was economy for the flight demonstrator - the use of a flight-rated F-16 fuselage forward of the pressure bulkhead would entail considerable savings. As for the operational aircraft, the use of phased-array radar would permit the 1981 F-18 radar to be accommodated in an F-16 size nosecone. Also, at this point, the conceptual design mechanism was changed. Whereas the Rolls-powered configurations were drawn by hand, the G.E. powered configurations were done on a ComputerVision system recently put into operation by General Dynamics. This system permitted major configuration variants to be constructed and evaluated much more quickly and thoroughly than had been possible previously.

The flight demonstrator is now based upon the F101/DFE engine; the characteristics of the operational engine, upon which the configuration evolves from this point, will be discussed in Section 2, where the configuration which ultimately evolved is discussed in detail. However, for the remainder of this Section 1, aircraft performance will be discussed in terms of the operational aircraft.

The E-3/DFE configuration is shown on Figure 1-8. The only major difference between it and the Rolls-powered version other than those mentioned above is the change in landing-gear placement, which was necessitated by tip-over angle. A thorough performance analysis of the configuration, however, indicated that it could well exceed the Mach, P_S, and acceleration requirements of TS 169, but could not make the escort range due to the loss of fuel storage volume because of the scaled-down wing size from the Rolls configuration. (It must also be admitted that, at this stage, E-3/DFE was submitted to a much more rigorous performance analysis than was its predecessor.) Further, it fell short of meeting the maneuver requirement. Simple growth of planform size was prohibited by the fact that a cranked-arrow wing is, basically, a relatively heavy structure. This consideration is of utmost importance in a STOVL design, so the further configurations consisted of designs which traded off the excess speed of E-3/DFE for maneuver and range without increasing the airframe weight.

1.3.2 Configuration E-5

E-5, shown in Figure 1-9, was a clipped delta, 65°/-10°, planform with the same thickness ratio and span as E-3 but with S_{ref} = 601 ft^2. While the increased fuel volume in its wing permitted it to make the escort mission on internal fuel, it was still a little shy on maneuver performance. Although the maneuver could have been increased to meet the specification with leading edge devices, this would have detracted from its range. Futhermore, because of the drag encountered with external fuel tanks, the weight of the configuration for the interdiction mission became so large that the aircraft could not be launched in 400 feet, even with a ski jump. Thus, the requirement for meeting the interdiction mission with internal fuel became a driver. Therefore, another increase in wing area as well as aspect ratio was tried and became E-6.

1.3.3 Configuration E-6

E-6, shown in Figure 1-10, is a 60°/-10° clipped delta, again with the same thickness ratio distribution as E-3. The span was increased from that of the E-3/DFE to that of the Rolls-powered E-3. While these changes did not materially affect the aircraft empty weight, they did increase fuel volume and performance to the point where both the escort and interdiction missions as well as the maneuver point could be met with inernal fuel. While acceleration and P_S were less than that of E-5, they still exceeded TS 169 requirements. However, on more detailed analysis, the fuselage fuel volume required to make the ranges limited the volume for avionics to the point where it was most questionable if the avionics required for an F/A-18 equivalency could be accommodated. Further, this design required a large fuel tank in the fuselage aft of the c.g.; at full fuel, takeoff conditions E-6 had a negative static margin. While the pros and cons of an unstable airframe may be debated, it was felt that this was undesirable during short takeoff. Therefore, a final modification was made. Whereas E-6 had a reverse t/c ratio with 4 percent at the tip, E-7 has the same planform with a constant 4 percent t/c. This permitted sufficiently increased fuel volume in the wing to eliminate the stability concern as well as to fully accommodate the equipment in the fuselage. E-7 is the emergent design in this study, and is the topic of the remainder of this report.

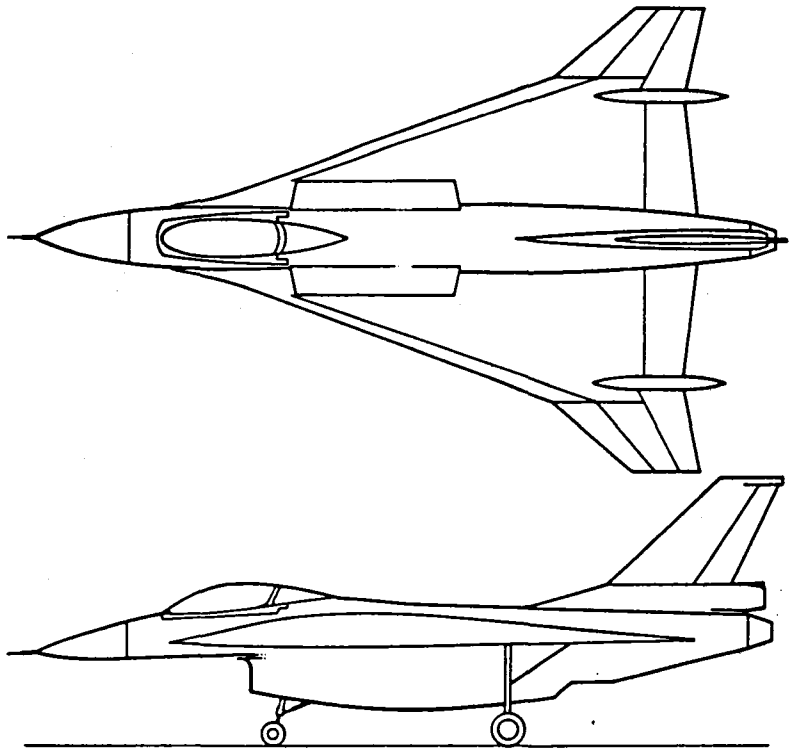

Figure 1-8 Configuration E-3/DFE

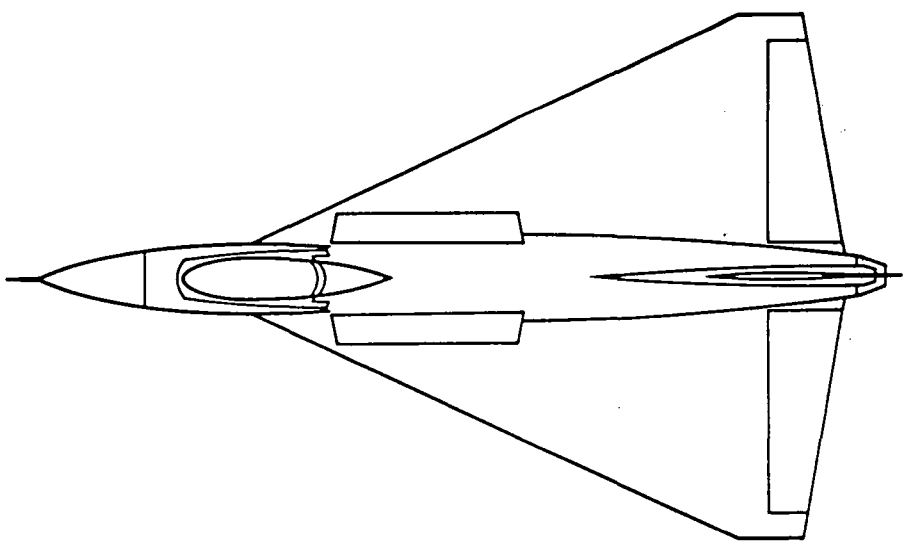

Figure 1-9 Configuration E-5

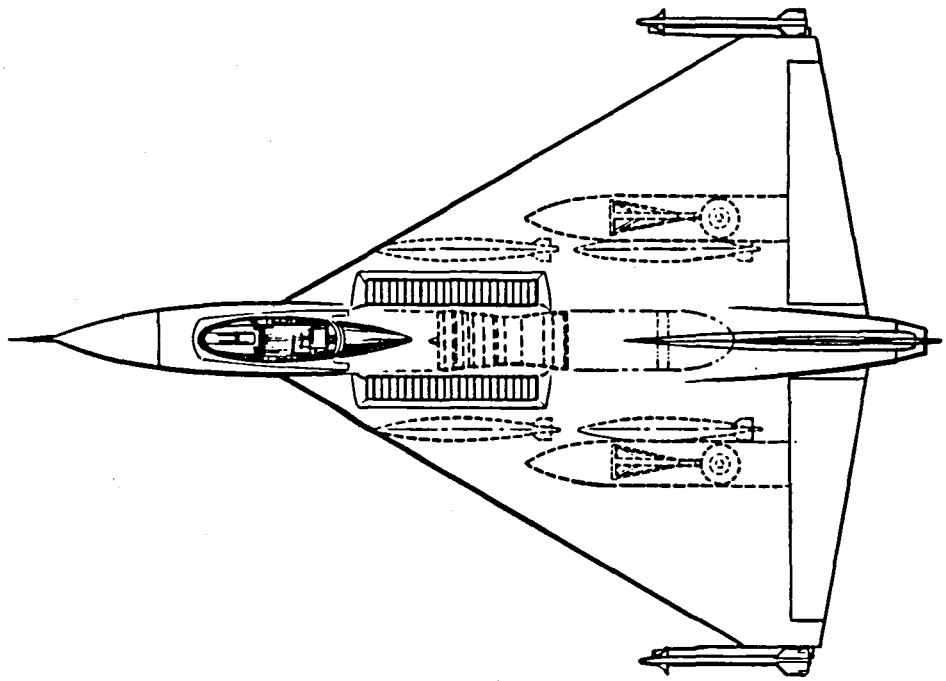

Figure 1-10 Configuration E-6

This Page Intentionally Left Blank

2. AIRCRAFT DESIGN; CONFIGURATION E-7

2.1 PHILOSOPHY

The rationale for General Dynamics' choice of TS 169, STOVL, and propulsion system was discussed in Section 1. The driving philosophy behind the resultant design was twofold. For well over a decade, NASA, the Navy, and industry have been working on V/STOL technology on a number of fronts. It is the belief of General Dynamics that the time has come to attempt to integrate the more promising but disparate technologies into one technology - an aircraft. In a very real sense this is indeed a technology development in itself; due to the tremendous interreliance of the various components of a V/STOL or STOVL aircraft it is impossible to take a technology or design from the laboratory or handbook and "stick it on" an airplane. Rather, these individual invariables must be modified and adapted - often drastically - to work together as a complete system. Witness the number of individual technological innovations which have come, and gone, during the past decades because they could not be integrated into a system.

Next, the emergent flight demonstrator needs to be capable of not only demonstrating hover and the low-speed end for the flight regime at low potential risk, i.e., it must also represent a design which can be translated to a viable military weapons system at low potential risk. The VAK-191, the Convair Pogo, the Hummingbird - the whole list is surprisingly long - all could hover but, to varying degrees, could do little else, nor did they possess the potential to fly military missions without configurational changes so large that it placed the flight demonstrator baseline in question.

2.2 GUIDELINES

The E-7 flight demonstrator was constrained to use the present F101/DFE engine subject to alterations to the engine case to permit the fan air to be ducted off the engine. The engine was then considered as a baseline (ESF = 1.0) and was allowed to grow as required so that the threshold and goal operational aircraft could meet the hover requirements of TS 169 (modified) as discussed in Section 1.1.2.

All aircraft were required to carry 1995 functional equivalency of the F/A-18 avionics (in the case of the flight demonstrator much of this weight would be found in flight test instrumentation.)

The aircraft exterior lines and the ejector interior lines of all aircraft were required to be identical. The lines of the latter were made as close as possible to those of the Reference 1, 2, and 3 ejector.

The flight demonstrator design load criterion was allowed to be set by gust requirements; the operational aircraft were designed for 7.5 g's. The materials used in the flight demonstrator are to be of F-16A technology levels, while operational aircraft were allowed to use 1995 predicted technology levels.

2.3 SIZING

Because all configurations have the same exterior lines, sizing is a fallout of specifying the fixed engine for the flight demonstrator. Thus, while the planform shapes varied in the development of E-7 from E-3/DFE in order to optimize the configuration to TS 169, aircraft weight remained essentially constant.

3. CONFIGURATION E-7 PHYSICAL CHARACTERISTICS

3.1 GEOMETRIC CHARACTERISTICS

The general arrangement for Configuration E-7 is shown in Figure 3-1, and dimensional data are detailed in Table 3-1. The forward fuselage, cockpit and canopy and the vertical tail are geometrically identical to those of the F-16A.

The normal cross-sectional area distribution for the total configuration and major components is given in Figure 3-2. These area distributions are shown with the inlet capture area removed and core nozzle exit areas extended to the aft fuselage limit for use in wave drag analysis. Wetted areas are given in Table 3-2.

The locations of internal components are shown schematically in Figures 3-3 and 3-4 for the operational and flight demonstrator aircraft, respectively. Figure 3-5 shows external stores locations for the operational aircraft escort, interdiction and possible maximum-loading missions.

Table 3-1 CONFIGURATION E-7 DIMENSIONAL DATA

WING	
Area	630.6 ft^2
Aspect Ratio	1.665
Taper Ratio	.115
Span	388.8 in.
Root Chord	419.07 in.
Tip Chord	48.08 in.
Mean Aerodynamic Chord (MAC)	282.68 in.
L.E. Station of MAC	F.S. 228.26
Span Station of MAC	B.L. 71.47
Leading Edge Sweep	60 degrees
Trailing Edge Sweep	-10 degrees
Airfoil	NACA 64A004
Incidence	0 degrees
Dihedral	0 degrees
Twist	0 degrees
Elevon Area	75.67 ft^2
VERTICAL TAIL	
Area	54.75 ft^2
Aspect Ratio	1.294
Taper Ratio	.437
Height	101.0 in.
Root Chord	108.62 in.
Tip Chord	47.5 in.
Leading Edge Sweep	47.5 degrees
Airfoil - Root	5.3 percent thick Biconvex
- Tip	3.0 percent thick Biconvex
Rudder Area	11.65 ft^2
FUSELAGE	
Length	563.61 in.

Table 3-2 WETTED AREAS

	Wetted Areas (ft^2)
Fuselage	506
Canopy	36
Ejector Bodies	205
Main Landing Gear Fairings	99
Dorsal Fairing	47
Wing	729
Vertical Tail	83
Total	1705

This Page Intentionally Left Blank

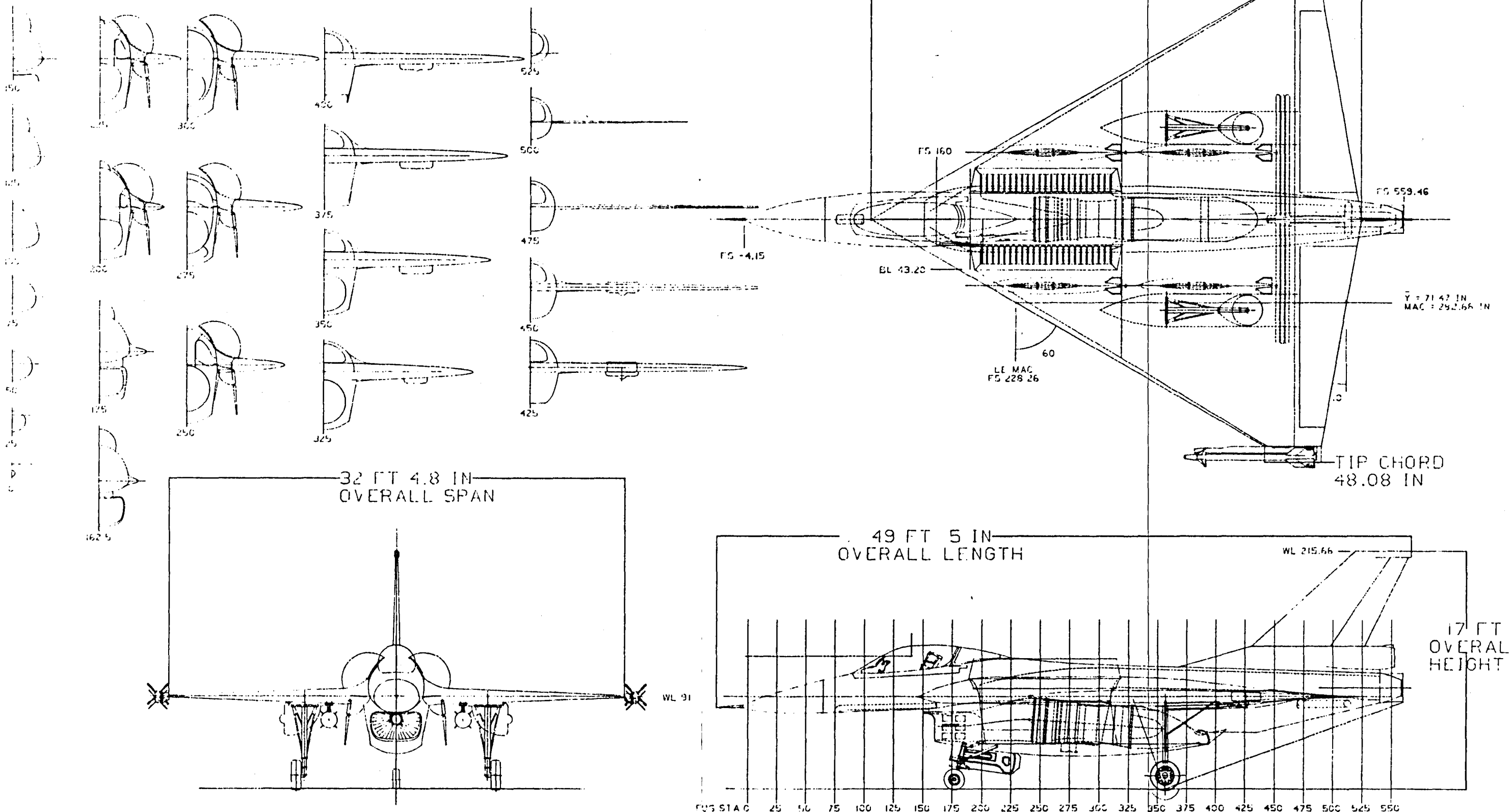

Figure 3-1 **Configuration E-7 — General Arrangement**

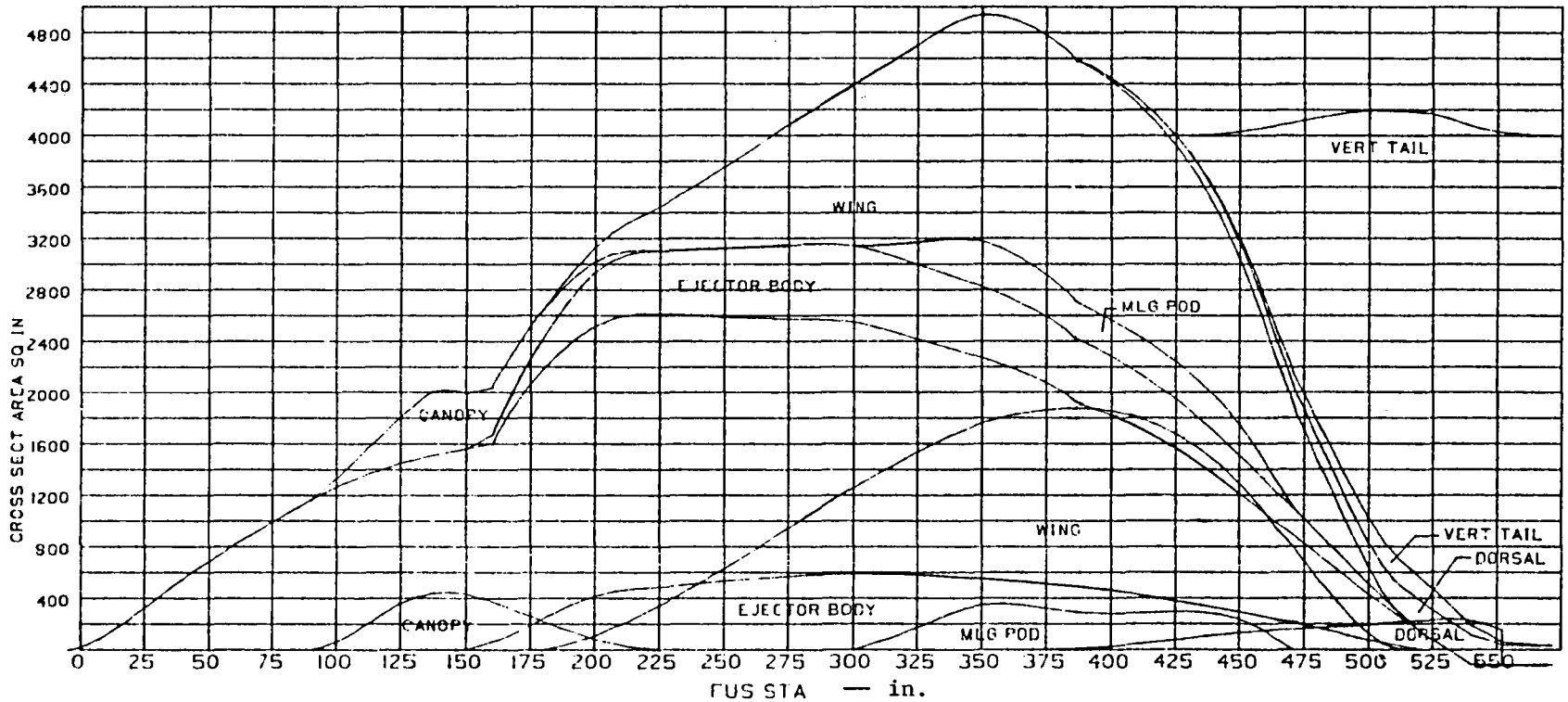

Figure 3-2 Configuration E-7 — Normal Cross-Sectional Area Distribution

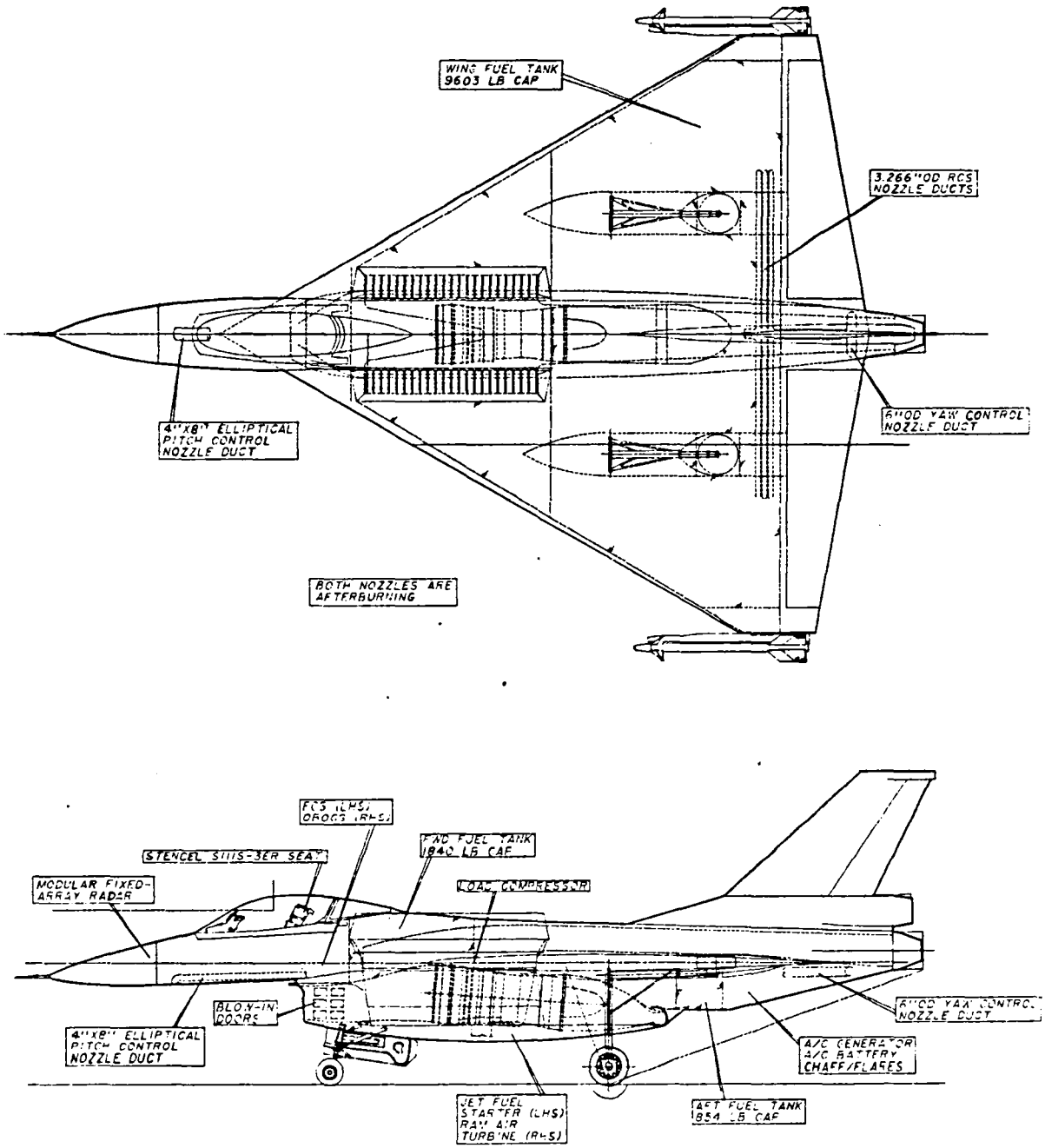

Figure 3-3 E-7 Operational Aircraft — Internal Components

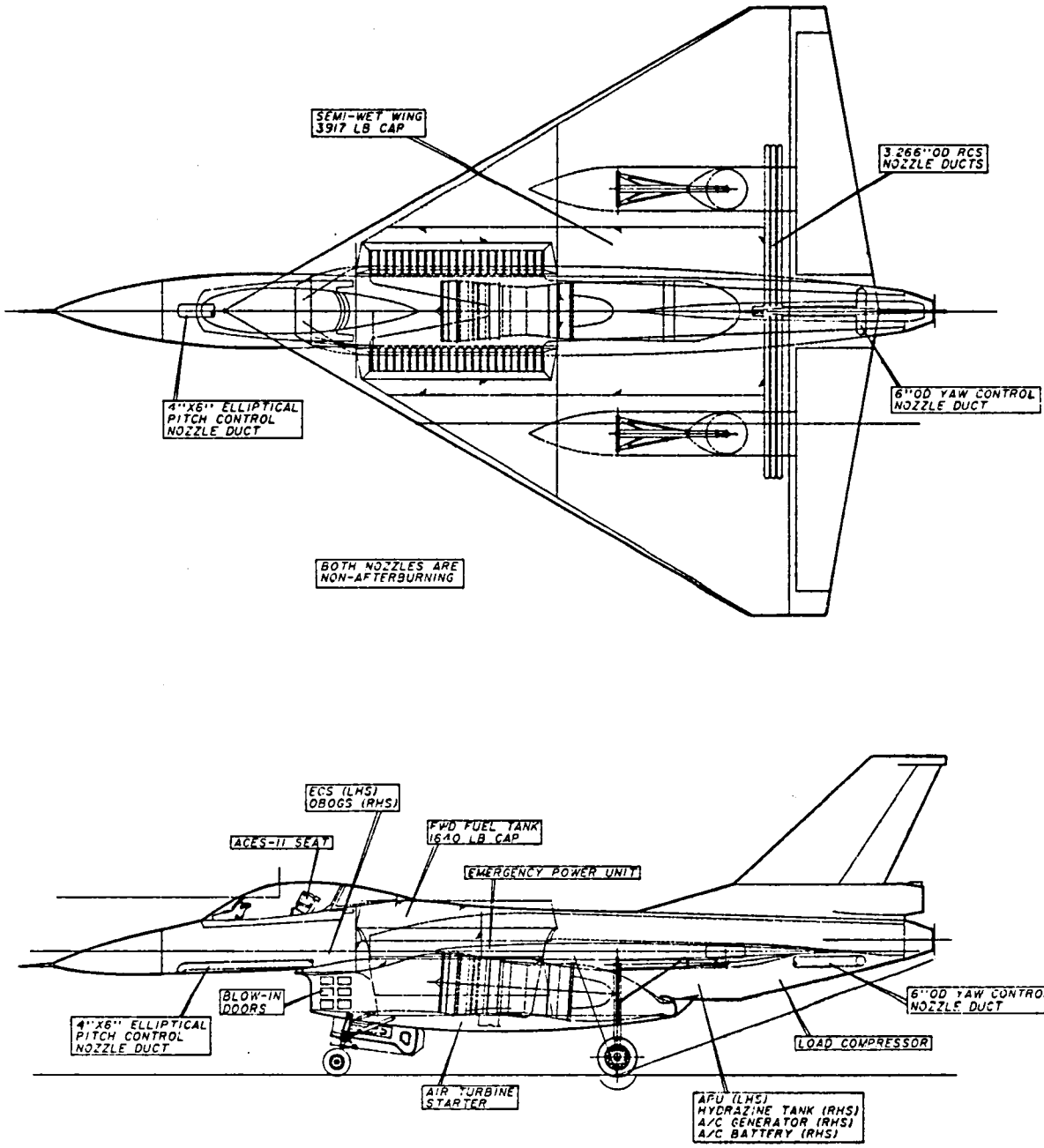

Figure 3-4 E-7 Flight Demonstrator — Internal Components

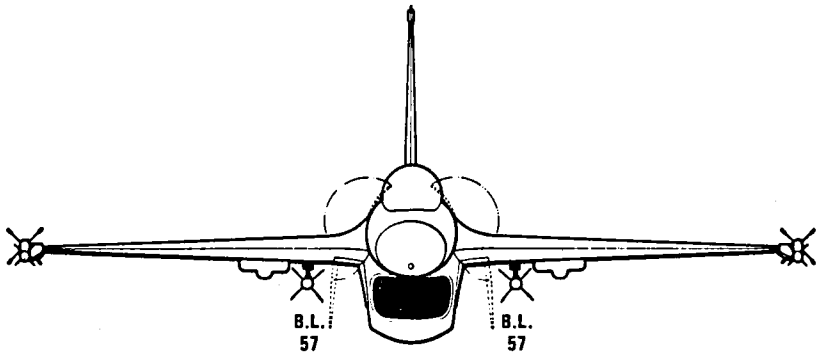

ESCORT LOADING: (2) AMRAAM MISSILES, (2) AIM-9 MISSILES

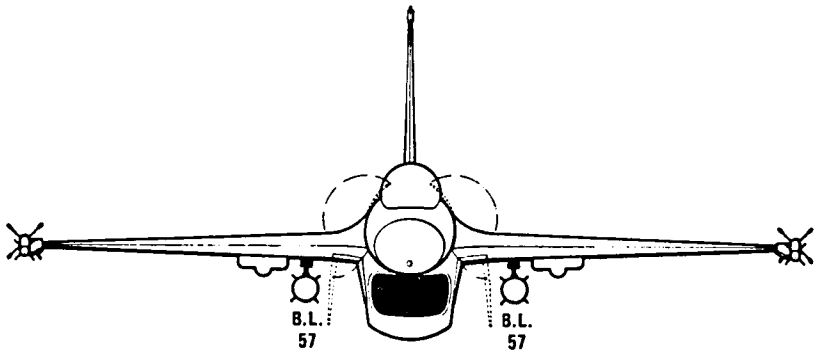

INTERDICTION LOADING: (4) MK-83 BOMBS, (2) AIM-9 MISSILES

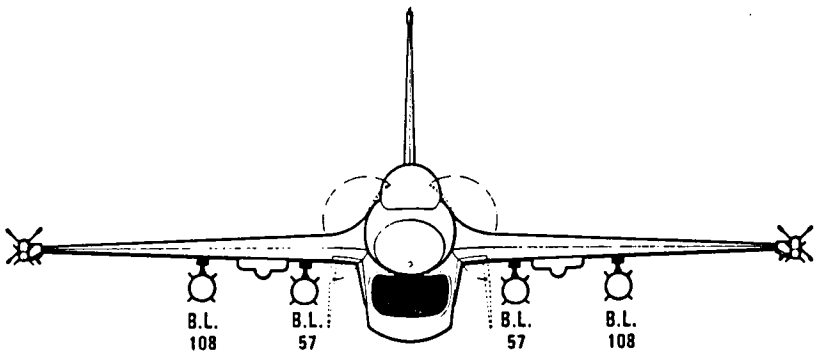

POSSIBLE MAXIMUM LOADING: (6) MK-83 BOMBS, (2) AIM-9 MISSILES

Figure 3-5 Configuration E-7 — Weapons Loadings

3.2 STRUCTURES AND WEIGHTS

This study encompasses the evaluation of both flight demonstrator and operational versions of the aircraft. A combination of four wing planforms and two engines were examined in the configuration matrix as discussed in Section 2 of this report. Further, the scope of this study provided for only conceptual layouts.

Therefore, due to the relatively large number of configurations which were evaluated, and the preliminary nature of the design, the statistical-analytical weight prediction methods of References 6 and 7 were utilized.

The structural methods (Reference 6) are based on a correlation of actual in-service hardware with logical variations of load, geometry and environment parameters (e.g., wing bending material and shear material as a function of beam bending parameters). These methods are for aluminum construction but are adjusted for the use of advanced materials (fibrous composites and metallics) by application of the appropriate technology factors (TF's).

An uncertainty analysis based on the application of the weight prediction methods of References 6 and 7 to 50 in-service aircraft ranging in size from a 6500-pound trainer (T-37) to a 770,000-pound logistic transport (C-5A) shows a weight empty standard-deviation $\pm$2.5 percent range (Reference 8).

Table 3-3 shows a structural weight summary for the operational aircraft structural groups in both conventional aluminum construction and in advanced fibrous composite and advanced metallic materials. The final overall TF for the total structure is .916 (See Table 3-3) or a weight savings of 8.40 percent.

The technology factors have been projected from past hardware design and analytical studies. Extensive use of use has been made of graphite-epoxy design studies on various components for the F-16, F-5, F-111 and other aircraft. One of the most important of these studies is the Graphite Epoxy F-16 Forward Fuselage Program (Reference 9), in which an entire F-16 forward fuselage component was successfully designed, fabricated and tested. Data derived from these tests have been used extensively as a basis for projections of structural concepts, materials data, and weight TF's. Considerable use has also been made of the WICAD study program (F-16 center and aft fuselage, wing and inlet, Reference 10) and work from the original AFTI/F-16 program.

It should be noted that the TF of .916 (Weight saving of 8.4 percent) is somewhat lower than the .85 to .80 TFs (Weight savings of from 15 to 20 percent) normally anticipated for high-fineness-ratio, high-aspect-ratio, low-sweep wing configuration in the 1995 time period. This is the result of having to protect the aft fuselage from the impingement of the hot core air on the aft fuselage and the limited amount of composites that can be used on the lower fuselage due to boil-up of the deflected hot core air. The amount of protection and the materials required for protection of the aircraft structure have not been investigated and are beyond the scope of this study. However, an attempt was made to account for these effects by application of a blast impingement penalty.

3.2.1 Operational Aircraft

The mass properties information of E-7 is presented in a series of tables contained in this section.

Table 3-4 shows the summary of gross weights for several design conditions. Each condition is derived by adding to the Weight Empty of E-7 the appropriate useful load items to obtain the resulting gross weight.

The weights and inertias for design conditions of Table 3-4 and the fighter and attack missions are presented in Table 3-5. The inertias about each axis has been estimated and is shown in units of slug-feet-squared.

Based on TS 169A gudelines for this study, two missions were identified for consideration. The fighter mission (Escort) carries four missiles, while the attack mission (Interdiction) carries two missiles and four conventional bombs.

A group weight statement in MIL-STD-1374 format is included and appears as Table 3-6. The useful load page also contains the buildup for the two primary missions.

Tables 3-7 amd 3-8 give the gross weight and balance information for both the Escort and Interdiction Missions.

Table 3-9 compares the weights of E-7 with the F-16A and F-106A. The F-16A was included because E-7 utilizes the F-16A vertical tail, forward fuselage and similar systems. The F-106A was picked because it has a similar size wing (698 ft^2 vs 630.6ft^2) and also same leading-edge sweep.

3.2.1.1 Basic Structural Criteria (Operational)

The structural design criteria used for weight analysis was based generally on typical TS 169 guidelines and the applicable MIL-A-8860 series structural specifications.

The minimum design symmetrical limit maneuver load factor used was +7.5 and -3.0 g at Basic Flight Design Gross Weight. The Basic Flight Design Gross Weight is based on the Escort Mission Gross Weight less 40 percent of internal fuel. Basic Flight Design Gross Weight and other design gross weight build-ups are shown in Table 3-4. Sink speed has been set at 15 feet/sec (limit) and 18.75 feet/sec (design) at Design Landing Weight. Maximum Design weight has been established assuming stores weight of 10,000 lbs.

The design speed curve (Figure 3-6) is based on the F-16. ($V_H = V_L$) and is based on a constant dynamic pressure (q) line of 2133 psf from M = 1.2 at S.L. (V_E = 794 Kn) to M = 2.0 at (25,500 feet) and then follows a constant standard day inlet duct total temperature line of 308°F to approximately (36,000 feet) at M = 2.2. The maximum Mach number above (36,000 feet) is 2.20 (burst).

3.2.1.2 Propulsion

The basic engine used for this study is a General Electric F101/DFE engine with several modifications. The unit is an advanced technology powerplant which incorporates afterburner, fan-air collector and an augmented deflector engine nozzle (ADEN).

Engine controls, cooling, and accessory gearbox weights are estimated for Configuration E-7 based on existing aircraft hardware.

The starting system has been assumed to be similar to the current F-16A system.

The fuel system has been estimated using Reference 7. The fuel system arrangement consists of fuselage bladder tanks with integral wing fuel tanks. A protected

fuel tank with self-sealing capability has been incorporated according to TS 169 requirments.

Weight estimates for ejectors, plenum, and fan duct are based on the preliminary sizing of these items.

3.2.1.3 Systems and Equipment

Most of the systems and equipment weights estimates are based on existing F-16A and F-16E current system weights and adjusted appropriately for equipment differences, geometry changes and technology factors.

The flight-controls weight is made up of three parts, each estimated separately. Surface-controls weight has been estimated based on E-7 geometry and using Reference 7. The reaction-control-system weight has been estimated based on existing V/STOL aircraft information. The load compressor, which drives the reaction controls, was estimated after a cursory sizing effort was completed.

With an IOC date of 1995, it may be possible for E-7 to be an all-electrical aircraft. Although previous studies have indicated possible weight reductions in an all-electric design versus conventional electric-hydraulic design, no weight reduction has been incorporated. For the purposes of this study the hydraulic system was first estimated using Reference 7 and this weight was then added to the F-16A electrical weight to determine the E-7 system weight.

Table 3-10 presents the avionics equipment for E-7. This suite represents the equipment necessary to be functionally equivalent to an F-18 (not including ECM). It should be noted that this system is an advanced design system that will utilize 1995 technology.

3.2.1.4 Useful Load

The missiles and launchers for both sidewinder (AIM-9L) and the AMRAAM systems are existing designs and hardware utilized in the F-16 programs.

The MK-83 bombs are carried on new ejector racks. Each rack will be mounted directly to the wing and utilize a low-profile ejector unit from the multiple stores ejector rack (MSER). This feature is similar to the current F-16 weapons carriage system.

3.2.2 Flight Demonstrator

The aircraft is geometrically similar to the Operational Aircraft except that the aircraft carries no military payload. It has a considerably reduced fuel load and the limit maneuver load factor and material usage and distribution are changed as described in Section 3.2.2.1.

Weights and center-of-gravity data for the demonstrator aircraft are shown in Table 3-11.

3.2.2.1 Basic Structural Criteria (Demonstrator)

The demonstrator aircraft is of all-metallic construction except for the F-16 vertical tail. The airframe is predominately aluminum with the exception of the two areas where hot air can cause damage to the structure. Like the operational aircraft, the

material required to protect the lower and aft fuselage structure has not been determined. Again, the demonstrator has a blast impingement weight penalty applied to the fuselage to account for these effects.

The other major structural difference between the operational aircraft and the demonstrator aircraft is the maneuver load factor. The basic limit maneuver load factor of 4.0 was set as the result of a gust load study on Configuration E-3. This study was conducted over a range of Mach-altitudes from M=.20 at Sea Level to M=.95 at 40,000 feet and the results are shown in Table 3-12. It has been assumed that the differences in sweep and planform (E-3 Leading-Edge Sweep = 50°/70°; E-7 Leading-Edge Sweep = 60°) has a small effect on lift-curve slope, and hence the results of the gust load study approximate the results for Configuration E-7. It can be seen from Table 3-12 that based on the above rationale, the Demonstrator version of Configuration E-7 would be limited to M = .80 at sea level and M = .90 at 10,000 feet, with no restrictions due to gust above 10,000 feet.

The Demonstrator version of E-7 is designed for a minimum margin of safety of 25 percent on all primary structure. The purpose of this additional margin of safety is to permit safe full flight envelope (with the exceptions stated above) testing without static test. This is the same criterion used successfully in the YF-16 prototype program. The incremental structural weights for the demonstrator aircraft were calculated by increasing the design limit vertical symmetrical load factor by a factor of 1.25.

3.2.2.2 Propulsion

The core engine is the current technology General Electric F101/DFE with fan-air collector and an ADEN. The demonstrator configuration has no afterburners.

The ejectors, plenum, and fan duct weights have been retained from the operational aircraft except for the fan duct. This weight has been increased to compensate for the removal of the fan-air afterburner.

The demonstrator will utilize an air-turbine starter for the purposes of simplicity, weight savings, and cost.

The existing F-16A accessory gearbox will be utilized.

The fuel system has again been estimated using Reference 7 with the appropriate changes for the demonstrator incorporated.

3.2.2.3 Systems and Equipment

The F-16A and F-16E systems have been utiilzed to the fullest extent possible for the demonstrator.

Major changes when compared to the operational aircraft are in the areas of avionics and auxiliary power.

The avionics weight has been reduced from 1278 lb for the operational aircraft to 400 lb for the demonstrator. This weight is consistent with avionics suites in flight-test aircraft in the AFTI-16 and YF-16 programs.

The load compressor for the reaction control system will require an auxiliary power unit. This device has been designated preliminarily to be the AVCO Lycoming AL5512 turbine. This unit is to be installed in the aft fuselage bay that is used as a fuel tank for the operational aircraft.

3.2.2.4 Useful Load

The demonstrator configuration is basically the minimum required for the aircraft except for instrumentation. Based on experiences with other prototype programs, the demonstrator has an allowance of 600 pounds for installed instrumentation.

TABLE 3-3 EFFECT OF ADVANCED MATERIALS ON CONFIGURATION E-7 (OPERATIONAL)

COMPONENT	ALUMINUM CONVENTIONAL CONSTRUCTION	TF	ADVANCED COMPOSITES AND ADVANCED METALS
	lb.		lb.
Wing	4452	.920	4095
Vertical Tail	436*	.90	394
Body	2772	.874	2423
Landing Gear	1390	1.0	1390
Eng. Section Ducts	177	.80	142
Eng. Mounts	50	1.0	50
TOTAL STRUCTURE	9277	.916	8494

*F-16 G/E Vertical Tail converted to an equivalent aluminum construction design - root fairing is modified to contain ECM equipment - estimated weight increase is 60 lb.

Table 3-4 E-7 DESIGN WEIGHT SUMMARY

	Basic Flight Design Gross Weight Fighter	Basic Flight Design Gross Weight Attack	Max. Design Gross Weight	Vertical Landing Design Gross Weight	Landplane Landing Design Gross Weight	Minimum Flying Weight
Weight Empty	18162	18162	18162	18162	18162	18162
Crew	180	180	180	180	180	180
Unusable Fuel	123	123	123	123	123	123
Trapped Fluids	62	62	62	62	62	62
Engine Oil	39	39	39	39	39	39
Parachute	28	28	28	28	28	
Survival Kit	21	21	21	21	21	
Chaff	24	24	24	24	24	
Ram Air Cartridge	20	20	20	20	20	
AIM Provisions	138	138		138	138	
AIM-9L (2)	390	390		390	390	
AMRAAM Provisions	189		189	189		
AMRAAM (2)	600		600	600		
MK-83 Provisions (4)		120				
MK-83 (4)		3940				
Stores Weight			10000		10000	
Fuel						
5%						615
40%					4919	
60%	7378	7378				
100%			12297			
Landing Fuel				1704		
Gross Weight	27354	30625	41745	21680	34106	19181

Table 3-5 E-7 MASS PROPERTIES

CONDITION	WEIGHT	INERTIAS (Slug-Ft^2) ROLL	PITCH	YAW
o Escort Mission TOGW	32273	22701	66538	85666
o Attack Mission TOGW	35544	25146	70067	91371
o Basic Flight Design Gross Weight				
- Fighter	27354	21845	54925	73445
- Attack	30625	24272	58745	79457
o Max Design Gross Weight	41745	31412	77861	105045
o Vertical Landing Weight	21680	16919	52247	65788
o Landplane Landing Weight	34106	26386	64386	86977
o Minimum Flying Weight	19181	10508	47521	54885

Table 3-6 GROUP WEIGHT STATEMENT

GROUP WEIGHT STATEMENT

AIRCRAFT

(INCLUDING ROTORCRAFT)

ESTIMATED

CONTRACT NO.

AIRCRAFT, GOVERNMENT NO.

AIRCRAFT, CONTRACTOR NO.

MANUFACTURED BY

	MAIN	AUX
ENGINE MANUFACTURED BY		
ENGINE MODEL		
ENGINE NO.		
ENGINE TYPE		
PROPELLER MANUFACTURED BY		
PROPELLER MODEL		
PROPELLER NUMBER		

PAGES REMOVED	PAGE NO.

Table 3-6 Continued

1	WING GROUP (INCLUDING EJECTOR DOORS/MECHANISM)					4095
2	BASIC STRUCTURE-CENTER SECTION					
3	-INTERMEDIATE PANEL					
4	-OUTER PANEL					
5	-GLOVE					
6	SECONDARY STRUCTURE-INCL.WING FOLD WEIGHT		0	LBS.		
7	AILERONS - INCL. BALANCE WEIGHT					
8	FLAPS - TRAILING EDGE					
9	- LEADING EDGE					
10	SLATS					
11	SPOILERS					
12						
13						
14						
15						
16						
17						
18						
19	TAIL GROUP					394
20	STRUCT. - STABILIZER					
21	- FIN-INCL.DORSAL				330	
22	VENTRAL					
23	ELEVATOR - INCL.BALANCE WEIGHT					
24	RUDDERS - INCL.BALANCE WEIGHT				64	
25	TAIL ROTOR - BLADES					
26	- HUB & HINGE					
27						
28	BODY GROUP					2423
29	BASIC STRUCTURE - FUSELAGE OR HULL					
30	- BOOMS					
31	SECONDARY STRUCTURE - FUSELAGE OR HULL					
32	- BOOMS					
33	- SPEEDBRAKERS					
34	- DOORS, RAMPS, PANELS & MISC.					
35						
36						
37	ALIGHTING GEAR GROUP - TYPE **					1390
38	LOCATION	RUNNING	*STRUCT.	CONTROLS		
39	MAIN	232	806	162		
40	NOSE	29	106	55		
41	ARRESTING GEAR	---	---	---		
42	CATAPULTING GEAR	---	---	---		
43						
44						
45	ENGINE SECTION OR NACELLE GROUP					52
46	BODY - INTERNAL					
47	- EXTERNAL					
48	WING - INBOARD					
49	- OUTBOARD					
50						
51	AIR INDUCTION GROUP					140
52	- DUCTS					
53	- RAMPS, PLUGS, SPIKES					
54	- DOORS, PANELS & MISC.					
55						
56						
57	TOTAL STRUCTURE					8494

* CHANGE TO FLOATS AND STRUTS FOR WATER TYPE GEAR.

**LANDING GEAR "TYPE": INSERT "TRICYCLE", "TAIL WHEEL", "BICYCLE", "QUADRICYCLE", OR SIMILAR DESCRIPTIVE NOMENCLATURE.

MIL-STD-1374 PART I - TAB
NAME
DATE

GROUP WEIGHT STATEMENT
WEIGHT EMPTY

PAGE
MODEL
REPORT

Table 3-6 Continued

58	PROPULSION GROUP						5672
59	ENGINE INSTALLATION					3801	
60	EJECTOR PLENUM/DUCT					320	
61	FAN DUCT/AFTERBURNER					325	
62	ACCESSORY GEAR BOXES & DRIVE					350	
63	EXHAUST SYSTEM						
64	ENGINE COOLING					34	
65	WATER INJECTION						
66	ENGINE CONTROL					60	
67	STARTING SYSTEM					142	
68	PROPELLER INSTALLATION						
69	SMOKE ABATEMENT						
70	LUBRICATING SYSTEM						
71	FUEL SYSTEM					640	
72	TANKS - PROTECTED						
73	- UNPROTECTED						
74	PLUMBING, ETC.						
75							
76							
77							
78							
79							
80							
81	FLIGHT CONTROLS GROUP						933
82	COCKPIT CTLS.					35	
83	SYSTEMS CONTROLS					398	
84	REACTION CONTROL SYSTEM					500	
85							
86	EMERGENCY POWER PLANT GROUP						160
87	INSTRUMENTS GROUP						128
88	HYDRAULIC & PNEUMATIC GROUP						---
89							
90	ELECTRICAL GROUP						893
91							
92	AVIONICS GROUP						1278
93	EQUIPMENT						
94	INSTALLATION						
95							
96	ARMAMENT GROUP						35
97	FURNISHINGS & EQUIPMENT GROUP						279
98	ACCOMMODATION FOR PERSONNEL						
99	MISCELLANEOUS EQUIPMENT						
100	FURNISHINGS						
101	EMERGENCY EQUIPMENT						
102							
103	AIR CONDITIONING GROUP						275
104	ANTI-ICING GROUP						
105							
106	PHOTOGRAPHIC GROUP						
107	LOAD & HANDLING GROUP						15
108							
109							
110							
111							
112							
113							
114	TOTAL WEIGHT EMPTY - PG 2-1						18162

GROUP WEIGHT STATEMENT
USEFUL LOAD AND GROSS WEIGHT
Table 3-6 Concluded

115	LOAD CONDITION				ESCORT		INTERDICTION
116					MISSION		MISSION
117	CREW				180		180
118							
119	FUEL LOCATION TYPE	GALS.					
120	UNUSABLE	18.1			123		123
121	INTERNAL	1808.4			12297		12297
122							
123	OIL						
124	TRAPPED				62		62
125	ENGINE				39		39
126							
127							
128	MISSILES						
129	AIM PROVISIONS				138		138
130	AIM9L (2)				390		390
131							
132	AMRAAM PROVISIONS				189		
133	AMRAAM (2)				600		
134							
135							
136	BOMBS						
137	PROVISIONS						120
138	MK-83 (4)						3940
139							
140							
141							
142							
143	MISCELLANEOUS						
144	SURVIVAL KIT				21		21
145	PARACHUTE				28		28
146	CHAFF				24		24
147	RAM-AIR-TURBINE CARTRIDGES (2)				20		20
148							
149							
150							
151							
152							
153							
154							
155							
156							
157							
158							
159							
160							
161							
162							
163							
164							
165							
166							
167							
168							
169	TOTAL USEFUL LOAD				14111		17382
170	WEIGHT EMPTY				18162		18162
171	GROSS WEIGHT				32273		35544

* IF REMOVABLE AND SPECIFIED AS USEFUL LOAD.

**LIST STORES, MISSILES, SONOBUOYS, ETC. FOLLOWED BY RACKS, LAUNCHERS, CHUTES, ETC. THAT ARE NOT PART OF WEIGHT EMPTY. LIST IDENTIFICATION, LOCATION, AND QUANTITY FOR ALL ITEMS SHOWN INCLUDING INSTALLATION.

Table 3-7 ESCORT MISSION BALANCE CALCULATIONS

	WEIGHT	CENTER OF GRAVITY F.S.	PERCENT MAC	W.L.
Structure	(8494)	(340.6)		(91.9)
Wing & Carrythrough	3397	390		91
Vertical Tail	394	489		149
Fuselage	2423	275		90
Landing Gear	1390	351		82
Engine Section	192	227		65
Ejector Doors/Provisions	698	255		89
Propulsion	(5672)	(310.3)		(73.4)
Engine/Nozzle	3801	312		67
Duct/Afterburner	325	467		106
Ejectors/Plenum	320	253		100
Cooling	34	325		67
Accessory Gearbox	350	270		46
Engine Controls	60	200		100
Starting	142	250		50
Fuel System	640	300		100
Systems and Equipment	(3996)	(240.5)		(89.1)
Flight Controls/RCS	933	324		84
Emergency Power System	160	240		100
Instruments	128	176		97
Electrical	893	300		83
Avionics	1278	175		92
Armament	35	350		92
Furnishings and Equipment	279	163		100
Air-Conditioning	275	160		90
Load and Handling	15	275		107
Weight Empty	18162	309.4	28.6	85.6
	(824)	(269.5)		(94.1)
Crew	180	138		106
Unusable Fuel	123	300		100
Engine Oil	79	293		80
Fluids	22	293		80
Parachute	28	160		110
Chaff	24	500		100
Survival Kit	21	150		120
Ram-Air Cartridges	20	240		100
AIM Provisions	138	432		91
AMRAAM Provisions	189	247		82
Operating Weight	18986	307.6	28.1	85.6

Table 3-7 (Continued)

	WEIGHT	CENTER OF GRAVITY F.S.	PERCENT MAC	W.L.
	(990)	(316.9)		(80.7)
AIM-9L (2)	390	432		91
AMRAAM (2)	600	242		74
Zero Fuel Weight	19976	308.1	28.2	85.4
Fuel at 6.8 lb/gallon	12297	343		92
Takeoff Gross Weight	32273	321.5	33.0	87.7

Table 3-8 INTERDICTION MISSION BALANCE CALCULATIONS

	WEIGHT	CENTER OF GRAVITY F.S.	PERCENT MAC	W.L.
Weight Empty	18162	309.4	28.6	85.6
	(755)	(282.8)		(95.5)
Crew	180	138		106
Unusable Fuel	123	300		100
Engine Oil	79	293		80
Fluids	22	293		80
Parachute	28	160		110
Chaff	24	500		100
Survival Kit	21	150		120
Ram-Air Cartridges	20	240		100
AIM Provisions	138	432		91
MK-83 Provisions	120	318		84
Operating Weight	18917	308.3	28.3	85.6
	(4330)	(328.3)		(75.5)
AIM-9L (2)	390	432		91
MK-83 (4)	3940	318		74
Zero Fuel Weight	23247	312.0	29.6	83.7
Fuel at 6.8 lb/gallon	12297	343		92
Takeoff Gross Weight	35544	322.8	33.5	86.4

Table 3-9 WEIGHT EMPTY COMPARISON

Description	E-7 Area (ft^2)	E-7 Unit Wt. (lb/ft^2)	E-7 Weight	F-16A (PR106) Area (ft^2)	F-16A (PR106) Unit Wt. (lb/ft^2)	F-16A (PR106) Weight	F-106A Area (ft^2)	F-106A * Unit Wt. (lb/ft^2)	F-106A Weight
Structure			(8494)			(7642)			(10742)
Wing and Carrythrough	630.6	5.39	3397	300.0	7.45	2235	697.8	5.31	3704
Horizontal Tail			-	63.7	6.84	436			-
Ventrals			-	16.1	2.30	37			-
Vertical Tail	54.75	7.20	394	54.75	6.10	334	105.0	6.70	703
Fuselage	586	4.13	2423	749	4.39	3271	985	4.51	4445
Landing Gear			1390			974			1235
Engine Section			192			355			655
Ejector Doors/ Mech. (Wing)			698			-			-
Propulsion			(5672)			(3799)			(7111)
Engine Installation			3801			3054			5817
Exhaust			-			-			319
Cooling			34			34			45
Lube System			-			-			52
Accessory Gearbox			350			162			-
Controls			60			32			27
Starting			142			142			59
Fuel System			640			375			792
Ejector Nozzles/Plenum			320			-			-
Fan Duct/Afterburner			325			-			-
Systems and Equipment			(3996)			(4145)			(6171)
Flight Controls			933			728			444
Emergency Power Systems			160			172			-
Instruments			128			106			193
Hydraulics			-			313			428
Electrical			893			522			600
Avionics			1278			1132			2821
Armament			35			593			656
Furnishings and Equipment			279			314			512
Air-Conditioning			275			264			411
Load and Handling			15			1			106
Weight Empty			18162			15586			24024

Table 3-10 E-7 AVIONICS EQUIPMENT

Description	Installed Weight
Fixed Array Radar	205
HUD	44
Mission Computer	72
Stores Management System	45
Threat Warning	120
Blanker	7
Chaff	39
INS	41
Carrier Landing System	
Beacon	8
Augmented Receiver	8
ILS	16
Magnetic Compass	4
Service Life Monitor	35
Radar Altimeter	14
Air Data	30
Multi-Function Display (2)	65
UHF/ADF	15
Communications Antennas (5)	10
FLIR Provisions	9
ASPJ Provisions	97
Horizontal Situation Display	23
Signal Processors	140
Integrated Communications/Navigation/Identification	170
AMRAAM Provisions	54
Flight Sensors	7
Total Weight	1278

Table 3-11 E-7 FLIGHT DEMONSTRATOR BALANCE CALCULATIONS

	WEIGHT	CENTER OF GRAVITY F.S.	PERCENT MAC	W.L.
Structure	(7978)	(332.3)		(91.1)
Wing & Carrythrough	2702	389		91
Vertical Tail	394	489		149
Fuselage	2716	275		90
Landing Gear	1241	348		81
Engine Section	227	224		65
Ejector Doors/Provisions	698	255		89
Propulsion	(4404)	(299.0)		(72.8)
Engine/Aft Nozzle	3301	300		67
Fan Duct	170	425		106
Ejectors/Plenum	320	253		100
Cooling	34	325		67
Accessory Gearbox	162	270		46
Engine Controls	45	200		100
Starting	39	250		50
Fuel System	333	300		100
Systems and Equipment	(3991)	(294.9)		(85.4)
Flight Controls	933	362		89
APU/EPU	1076	392		79
Instruments	108	176		97
Hydraulics	327	275		83
Avionics	400	97		92
Armament	566	300		83
Furnishing & Equipment	291	163		100
Air Conditioning	275	175		75
Load and Handling	15	275		107
Weight Empty	16373	314.3	30.4	84.8
Useful Load	(1031)	(349.4)		(99.3)
Crew	180	138		106
Unusable Fuel	58	300		100
Engine Oil	79	293		80
Fluids	22	293		80
Parachute	23	160		110
Instrumentation	600	450		100
EPU Fuel	56	225		100
Oxygen	13	160		100
Operating Weight	17404	316.3	31.2	85.7

Table 3-11 (Continued)

	WEIGHT	CENTER OF GRAVITY F.S.	PERCENT MAC	W.L.
Payload	-	-	-	-
Zero Fuel Weight	17404	316.3	31.2	85.7
Fuel at 6.8 lb/gallon	5757	315.1	-	94
Takeoff Gross Weight	23161	316.0	31.1	87.7

Table 3-12 GUST LOAD FACTORS FOR E-3/DFE FLIGHT DEMONSTRATOR

M	Alt Ft	C_L per Deg	V_E Knots	U_{de} Ft/Sec	N_z=1 + N_z (GW=18,300 lb)	N_z=1 - N_z (GW=18,300 lb)	N_z=1 + N_z (GW=23,800 lb)	N_z=1 - N_z (GW=23,800 lb)
.2	SL	.036	132.2	66	1.7	.3	1.57	.43
.4		.0361	264.4		2.41	-.41	2.15	-.15
.6		.036513	396.6		3.12	-1.12	2.74	-.74
.8		.03782	528.8		3.93	-1.93	3.39	-1.39
.9		.0393	594.9		4.40	-2.40	3.78	-1.78
.95		.040472	627.95		4.68	-2.68	4.01	-2.01
.2	10,000	.036	109.65	66	1.61	.39	1.49	.51
.4		.0362	219.31		2.23	-.23	1.99	.01
.6		.03683	328.96		2.87	-.87	2.51	-.51
.8		.038444	438.61		3.58	-1.58	3.09	-1.09
.9		.0401	493.44		4.01	-2.01	3.44	-1.44
.95		.041514	520.85		4.28	-2.28	3.65	-1.65
.2	20,000	.036	89.64	66	1.52	.48	1.41	.59
.4		.03625	179.27		2.04	-.04	1.83	.17
.6		.037081	268.91		2.59	-.59	2.28	-.28
.8		.038932	358.55		3.22	-1.22	2.78	-.78
.9		.04075	403.36		3.60	-1.60	3.09	-1.09
.95		.042355	425.77		3.84	-1.84	3.28	-1.28
.2	30,000	.036	72.05	57	1.37	.63	1.29	.71
.4		.0363	144.11		1.74	.26	1.59	.41
.6		.0373	216.16		2.15	-.15	1.91	.09
.8		.0393	288.22		2.60	-.60	2.28	-.28
.9		.04145	324.24		2.89	-.89	2.51	-.51
.95		.043002	342.26		3.07	-1.07	2.65	-.65
.2	40,000	.036	56.86	47	1.25	.75	1.19	.81
.4		.03635	113.72		1.50	.50	1.39	.61
.6		.0374	170.57		1.77	.23	1.61	.39
.8		.0397	227.43		2.08	-.08	1.86	.14
.9		.04185	255.86		2.28	-.28	2.01	-.01
.95		.0436	270.08		2.40	-.40	2.11	-.11

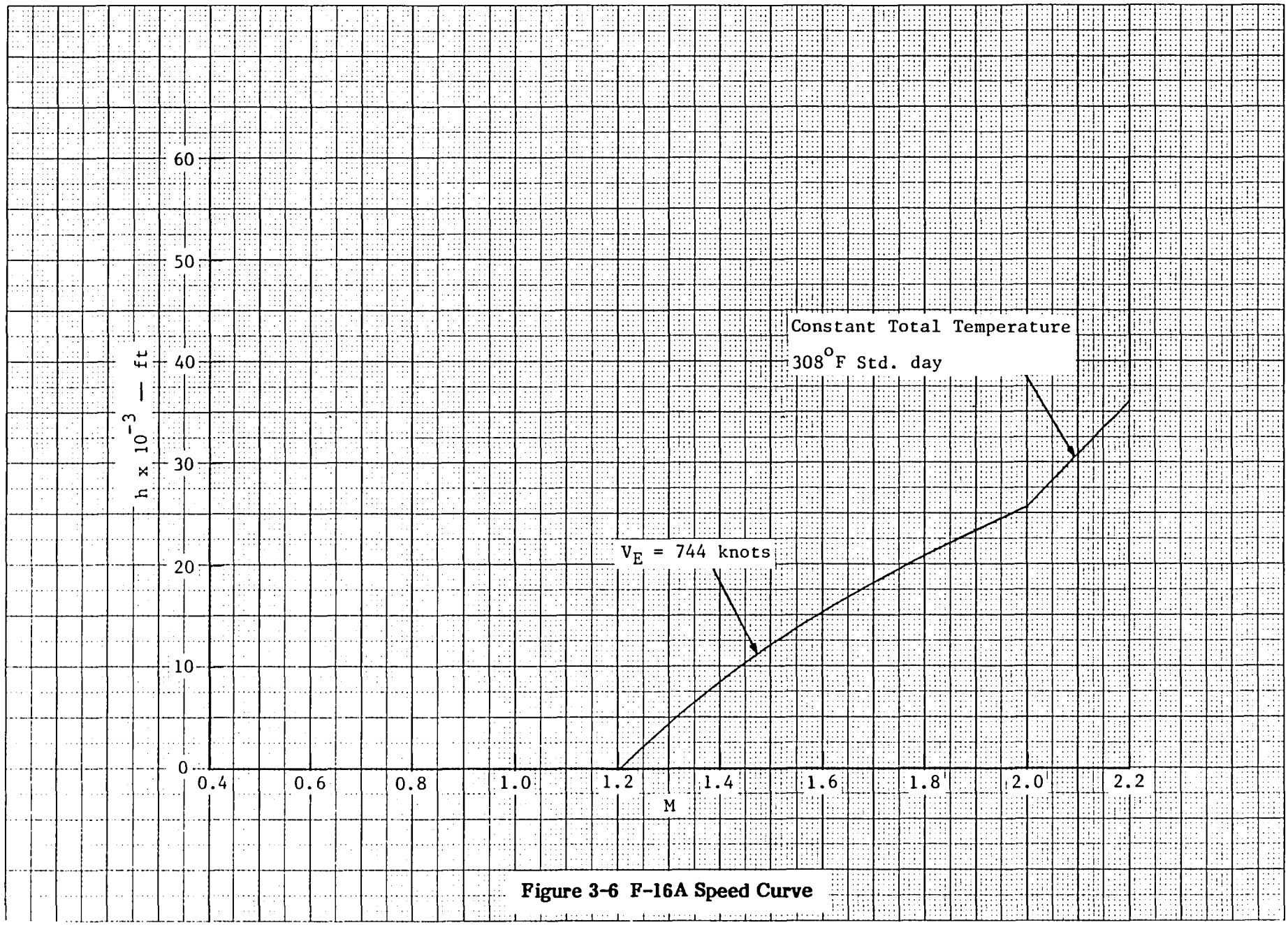

Figure 3-6 F-16A Speed Curve

This Page Intentionally Left Blank

4. AERODYNAMIC ANALYSIS

The aerodynamic analyses of all of the F101/DFE STOVL configurations are tied to the extensive experimental data base accumulated during other General Dynamics high-performance aircraft programs, namely the F-16E, F-16A, F-106 and B-58 programs.

The F-16E configuration shares with the STOVL configurations a highly-swept, long-root-chord wing planform and a similar fuselage-inlet arrangement with the same forward fuselage and vertical tail (Figure 4-1). This configuration has evolved over the last five years having undergone 2489 hours of wind-tunnel testing; therefore, an extensive aerodynamic data base exists from which realistic comparative evaluations can be made.

The F-16A, F-106 and B-58 aircraft are or have been operational aircraft in the U.S. Air Force inventory. As such, they have undergone extensive wind-tunnel and flight testing, from which large aerodynamic data bases exist.

Planform views of the F-106A and B-58A are shown in Figure 4-2. Note that these planforms are very similar to that of configuration E-7.

Aerodynamics data are presented in this section for the operational aircraft with tip missiles installed. These data may also be applied to the flight-demonstrator aircraft.

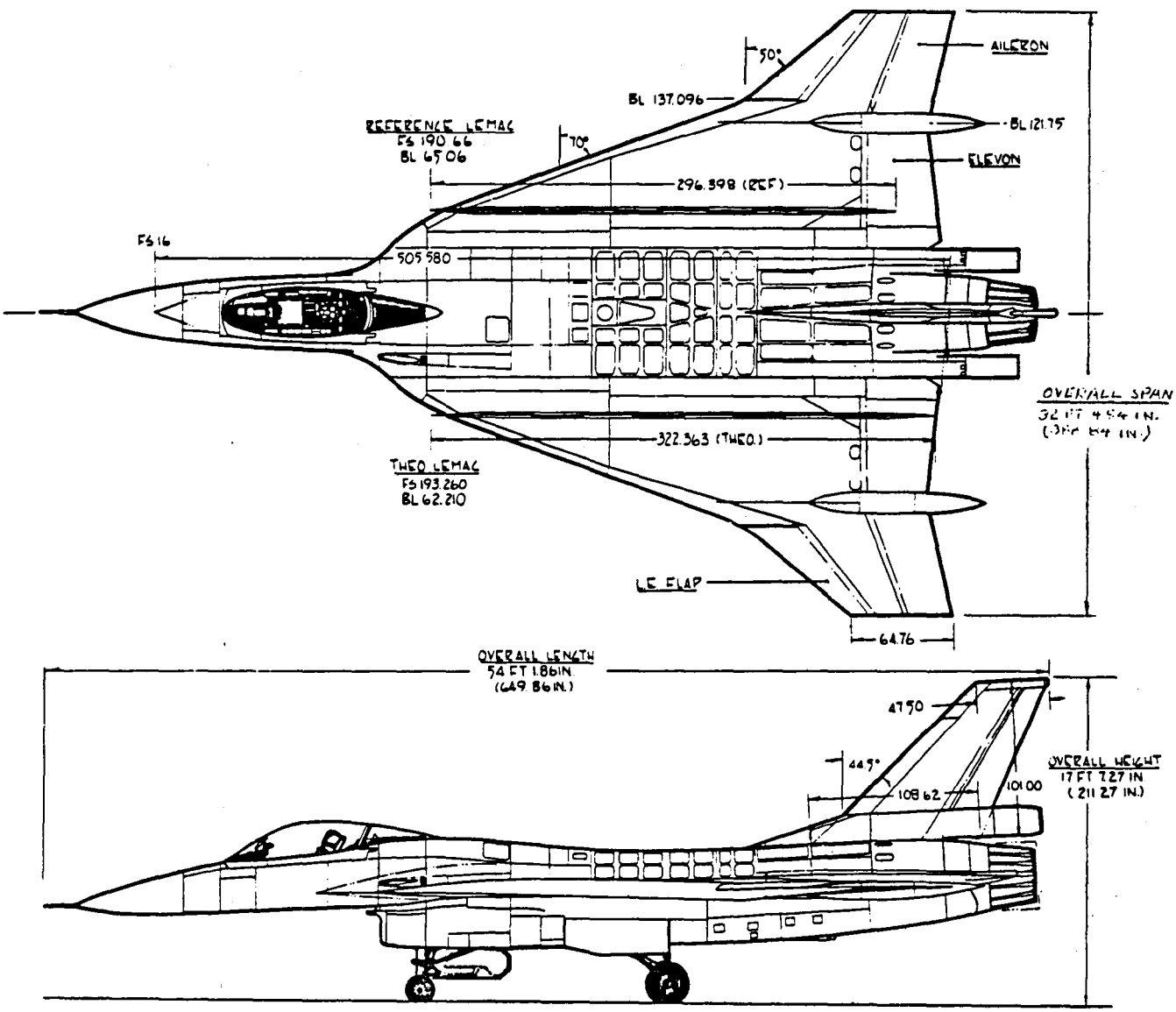

Figure 4-1 F-16E Configuration

linear dimensions in inches

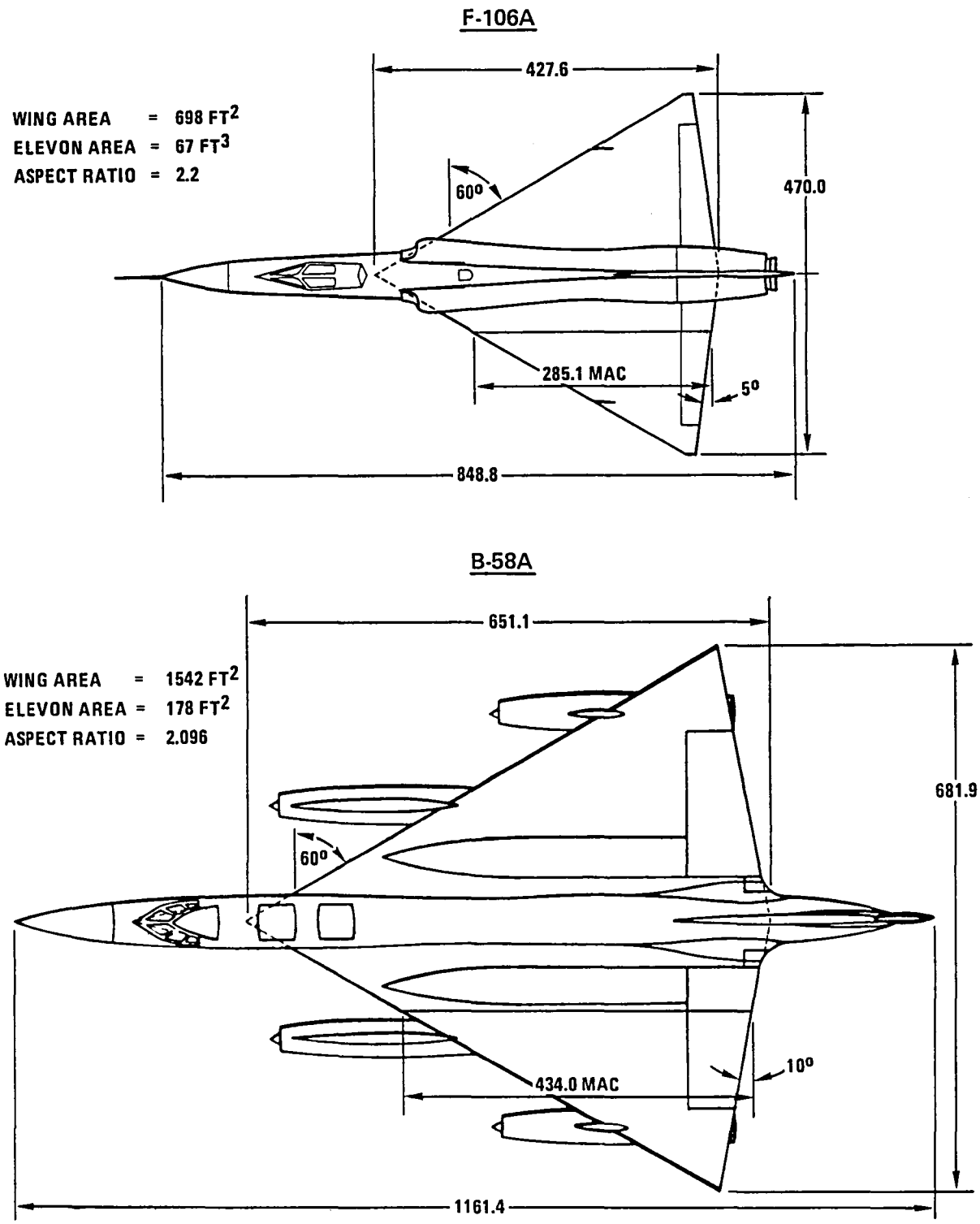

Figure 4-2 F-106A and B-58A Planform Comparison

4.1 ZERO-LIFT/ZERO-CAMBER DRAG

Zero-lift/zero-camber drag ($C_{D_{0,0}}$) estimates are based on emperical and analytical prediction methods and past experiment. Contributions of various drag components to $C_{D_{0,0}}$ are summarized in Table 4-1 and the resulting $C_{D_{0,0}}$ is presented as a function of Mach number in Figure 4-3. The variation of $C_{D_{0,0}}$ with altitude due to Reynolds number changes is shown in Figure 4-4 as increments from the baseline value at 30,000 ft. A thrust-drag bookkeeping system is utilized that places all thrust-dependent drag items in the propulsion package. The zero-lift drag levels of Figure 4-3 are representative of an inlet capture area ratio (A_0/A_i) of 1.0 and a cylindrical nozzle aft of the nozzle hinge line on the core nozzle and the nozzle connect point on the fan nozzle. Spillage drag, nozzle pressure drag and the effects of the nozzle plume on the airframe are accounted for in the thrust data.

Friction, form and interference drag estimates are computed using an automated emperical prediction method described in Reference 11. This method is designed for rapid and accurate prediction of aerodynamic characteristics of aircraft or wind-tunnel models at subsonic, transonic and supersonic speeds.

Supersonic wave drag predictions result from a modified NASA-Harris supersonic area-rule procedure (Reference 12) using an equivalent-body-of-revolution representation of the configuration. The fuselage, the ejector body, engine nacelle, canopy, main landing-gear fairings, and dorsal fairing are each input as bodies of revolution to the procedure. Ejector bodies are defined outboard of the fuselage and inboard of butt line 43.2; the nacelle is arbitrarily defined as the fuselage below waterline 78.0. Cross-sectional areas for the wing and tail are determined by the procedure from airfoil ordinate inputs. The total cross-sectional area distribution is presented in Figure 3-2 with the inlet area removed and the core-nozzle exit area extended to the fuselage aft limit.

Drag (D/q) increments for the inlet boundary-layer diverter, secondary air system, inlet-cowl bluntness, drag-chute base area and miscellaneous protuberances are taken directly from F-16A test data, since these items are the same as for the F-16 or would be approximately the same for similarily sized aircraft (Reference 13). Wing-tip missile and launcher drag (D/q) are taken from F-16E wind tunnel data. Roughness and mismatch drag increments are based on F-16A test data adjusted by the ratio of wetted areas. Supersonic drag due to wing leading-edge bluntness is calculated based on the method of Reference 14. Scrubbing drag on the ramp aft of the core nozzle was calculated based on flow conditions at the core nozzle exit.

The low-speed drag increment for extended landing gear is $C_{D_{gear}} = .0198$. This estimate is based on measured drag values from the B-58A and F-16A flight tests for the main and nose gears respectively, nondimensionalized by landing-gear frontal area.

The drag increment for deployment of the ejector diffuser doors is .0149. This estimate corresponds to an approximate C_D value of 1.0 (Reference 15) based on frontal area of the diffuser.

Figure 4-5 presents store drag increments as functions of Mach number for design escort and interdiction missions of the operational aircraft. These estimates are taken from F-16E wind tunnel test data.

TABLE 4-1 ZERO-LIFT/ZERO-CAMBER DRAG BUILDUP

	MACH NUMBER					
DRAG COMPONENT	0.2	0.6	0.9	1.2	1.6	1.95
Friction	.00767	.00636	.00583	.00537	.00480	.00428
Form	.00051	.00043	.00038	-	-	-
Interference	.00031	.00041	.00127	-	-	-
Wave	-	-	-	.01515	.01362	.01480
B.L. Diverter	-	-	-	.00031	.00071	.00066
L.E.Bluntness	-	-	-	.00004	.00007	.00011
Secondary Air System	.00027	.00027	.00024	.00025	.00025	.00025
Protuberence & Roughness	.00107	.00112	.00132	.00203	.00174	.00157
Cowl Bluntness	-	-	-	.00013	.00020	.00016
Drag Chute Base	-	-	-	.00031	.00031	.00031
Tip Missiles & Launchers	.00124	.00114	.00076	.00171	.00133	.00124
Scrubbing	.00121	.00010	.00002	-	-	-
Total	.01228	.00983	.00982	.02530	.2303	.02338

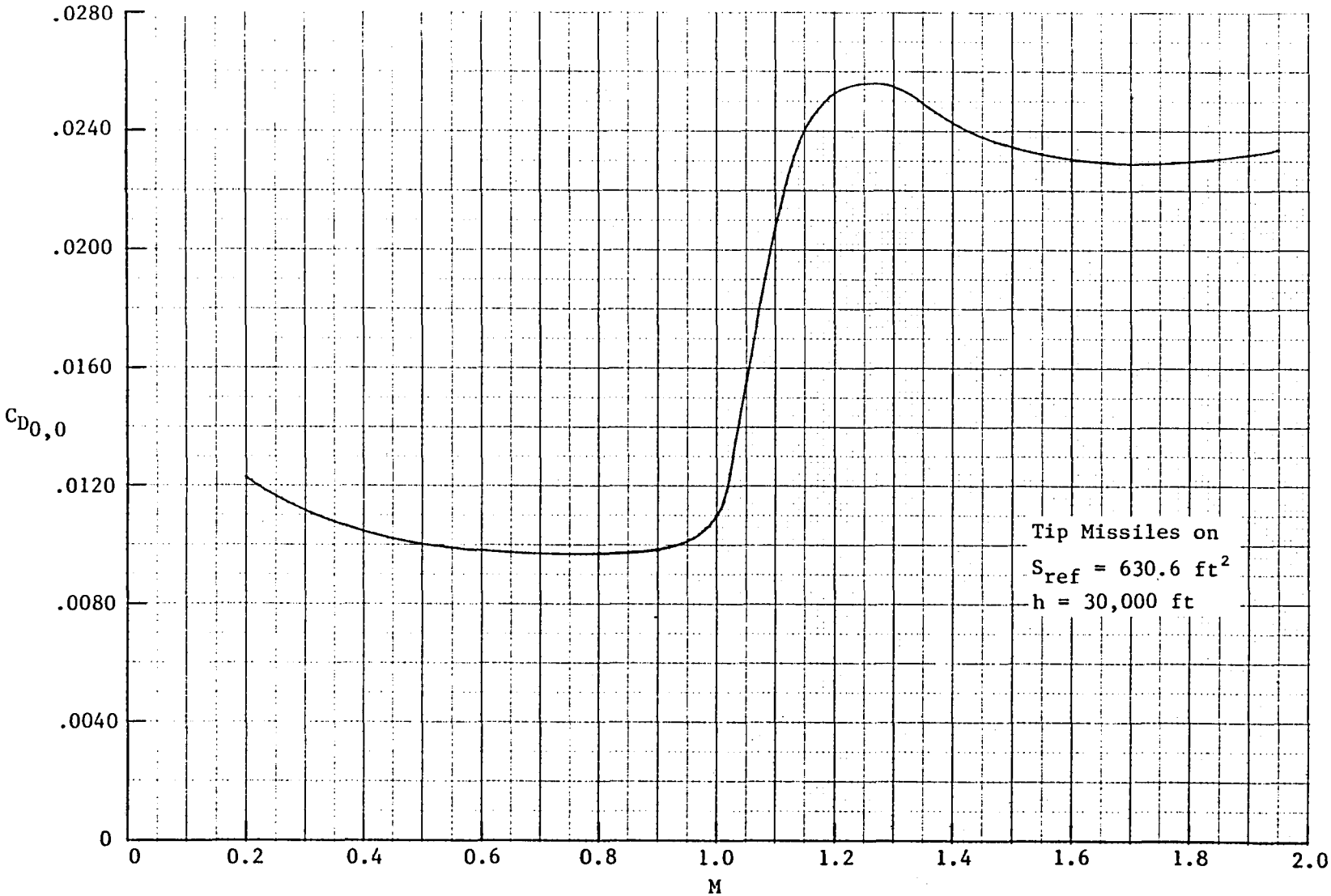

Figure 4-3 Variation of Zero-Lift/Zero-Camber Drag Coefficient with Mach Number

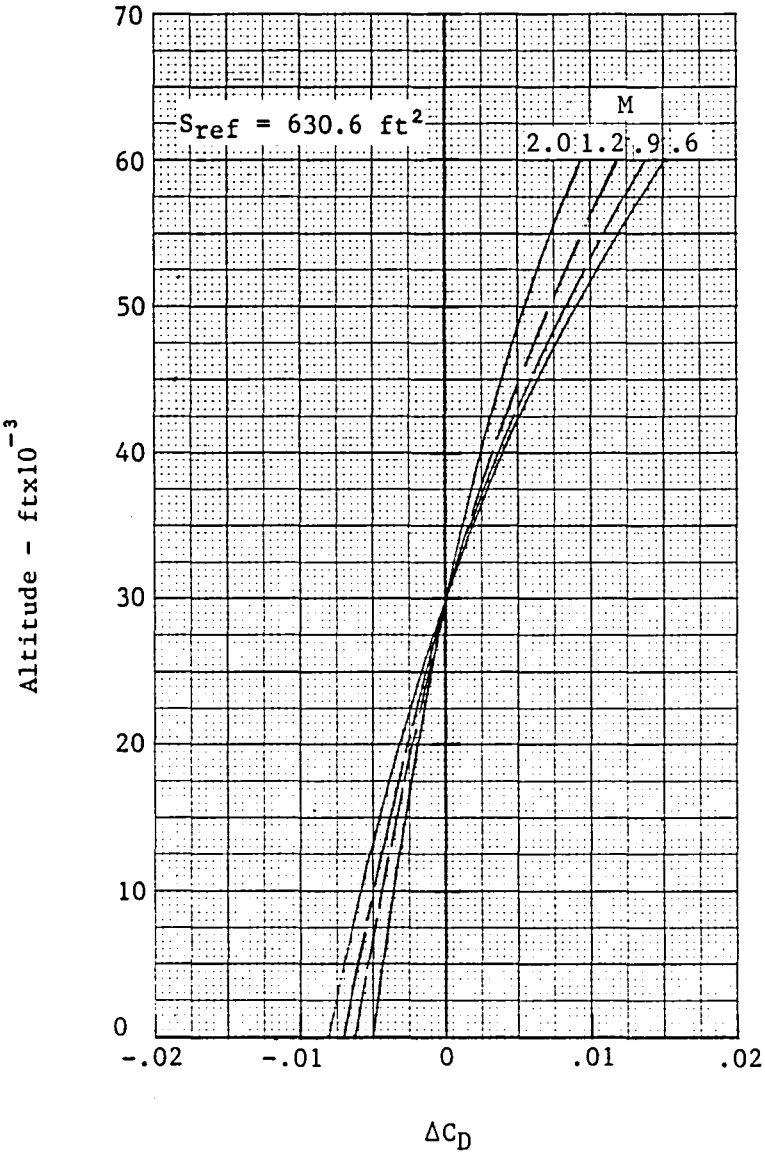

Figure 4-4 Variation of Zero-Lift/Zero-Camber Drag Coefficient with Altitude

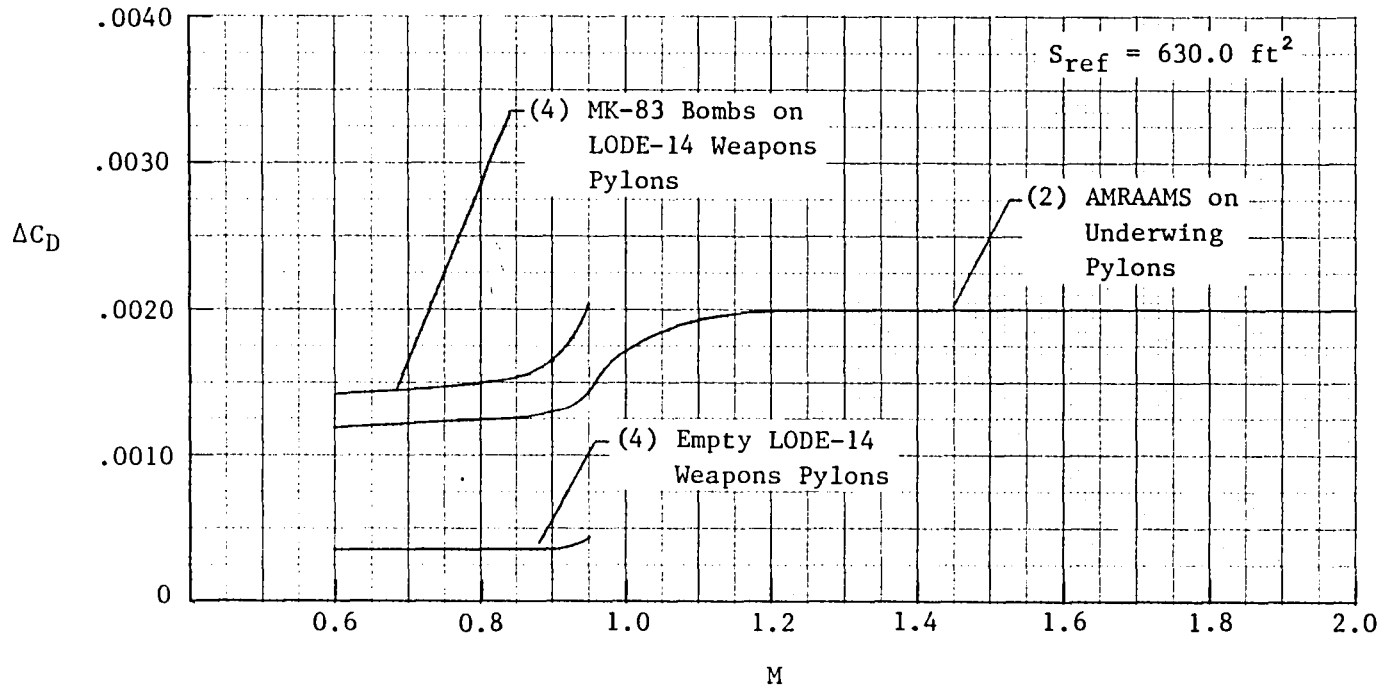

Figure 4-5 **Variation of Drag Coefficient Increment with Mach Number for Escort- and Interdiction-Mission Weapons Loadings**

4.2 LIFT-DEPENDENT AERODYNAMICS

Lift-dependent aerodynamic characteristics are determined primarily from F-16E wind-tunnel test data with linear-lifting-surface-theory increments to account for planform differences and B-58/F-106 wind tunnel data to account for elevon-deflection effects.

The Cunningham kernel-function method (References 16 and 17) is used to predict effects of planform differences between the E-7 and F-16E configurations. This method is based on linear lifting-surface theory and uses assumed pressure functions with unknown coefficients to solve the kernal-function integral equation. The program is applicable to multiple interfering surfaces in subsonic, transonic or supersonic flow; they may be coplanar or non-coplanar. Local linearization is used to treat non-uniform transonic flow problems. For cases with imbedded shocks, appropriate normal-shock boundary conditions are added to account for flow discontinuities. Loads induced by shock movement are accounted for by including a "shock doublet", whose strength is found as part of the solution. A modified Polhamus suction analogy is used to obtain the vortex lift contribution due to leading-edge separation. A method for imposing pressure-coefficient limits is used as a means of realistically spreading vortex lift and high leading-edge loading that occur with subsonic leading edges. The method is verified for highly-swept wings by comparison with experiment in Reference 17.

4.2.1 High Speed

Untrimmed tip-missiles-on lift and drag characteristics for the F-16E configuration were obtained in transonic and supersonic wind-tunnel tests reported in References 18 through 22. These data were adjusted for the E-7 planform using the Cunningham method. Elevon deflection required to trim and the resulting effects on lift and drag are based on B-58 wind-tunnel data. The B-58 utilized nearly the same planform as E-7 with same elevon-to-wing area ratio. Drag due to lift and camber (C_D-$C_{D_{0,0}}$) is presented as a function of lift coefficient at Mach numbers of 0.6, 0.9, 1.2, 1.6 and 2.0 in Figure 4-6.

4.2.2 Low Speed

Low-Speed tip-missiles-on F-16E wind-tunnel data are reported in References 23 and 24. These data are adjusted for the E-7 planform using the Cunningham method. Lift and drag increments due to elevon deflection are derived from B-58, F-106 and F-16E wind-tunnel data. Free-air lift curves and drag-due-to-lift-and-camber polars for various elevon deflections are presented in Figures 4-7 and -8.

The influence of ground effect on lift and drag is obtained by adjusting the F-16E test increments for the theoretical (Reference 15) effect of changing to the E-7 wing height-to-span ratio. Ground-effect lift curves and drag-due-to lift-and-camber polars for various elevon deflections are shown in Figures 4-9 and -10.

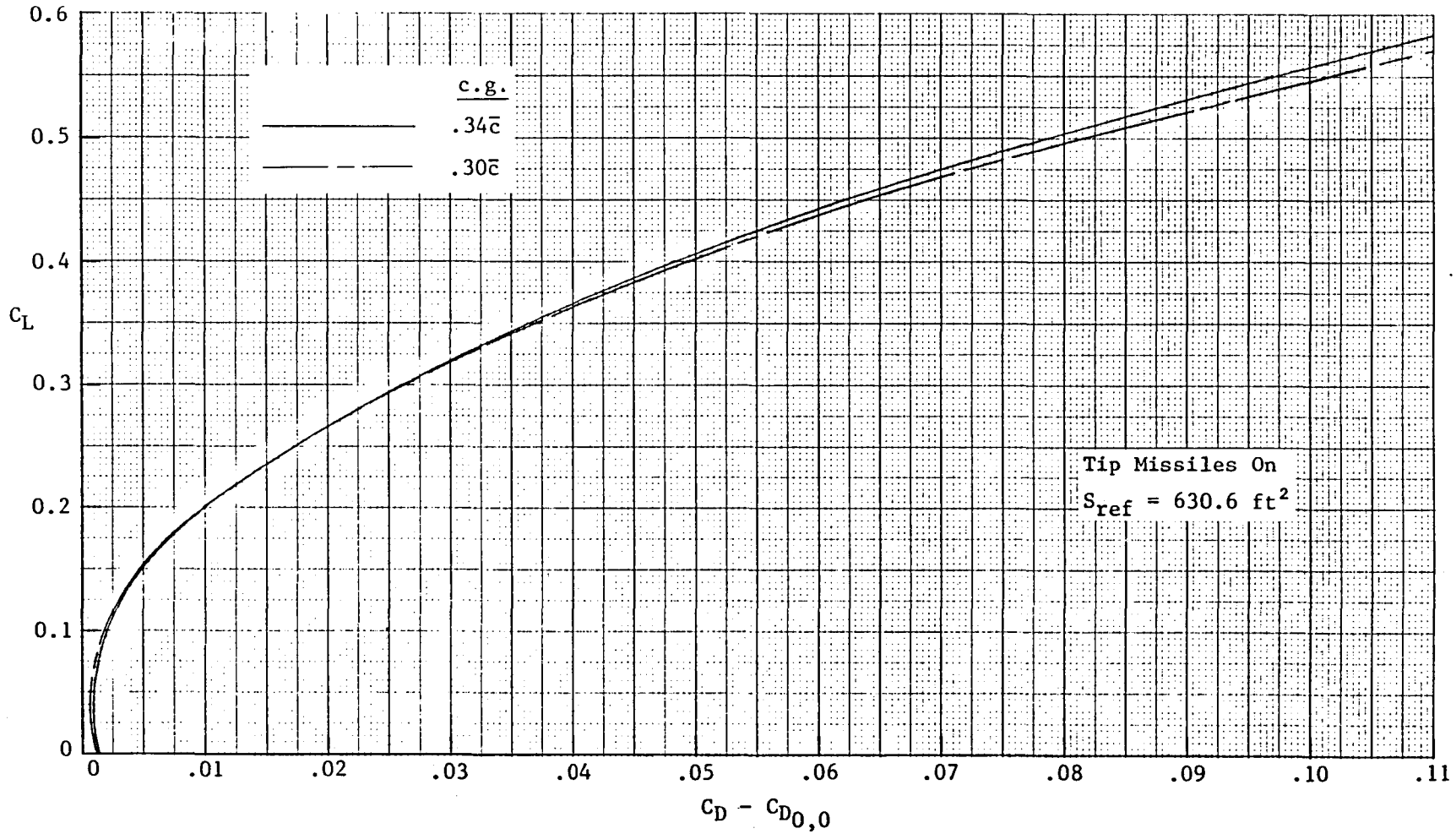

a) M = 0.6

Figure 4-6 Variation of Trimmed Drag Due to Lift and Camber with Lift Coefficient

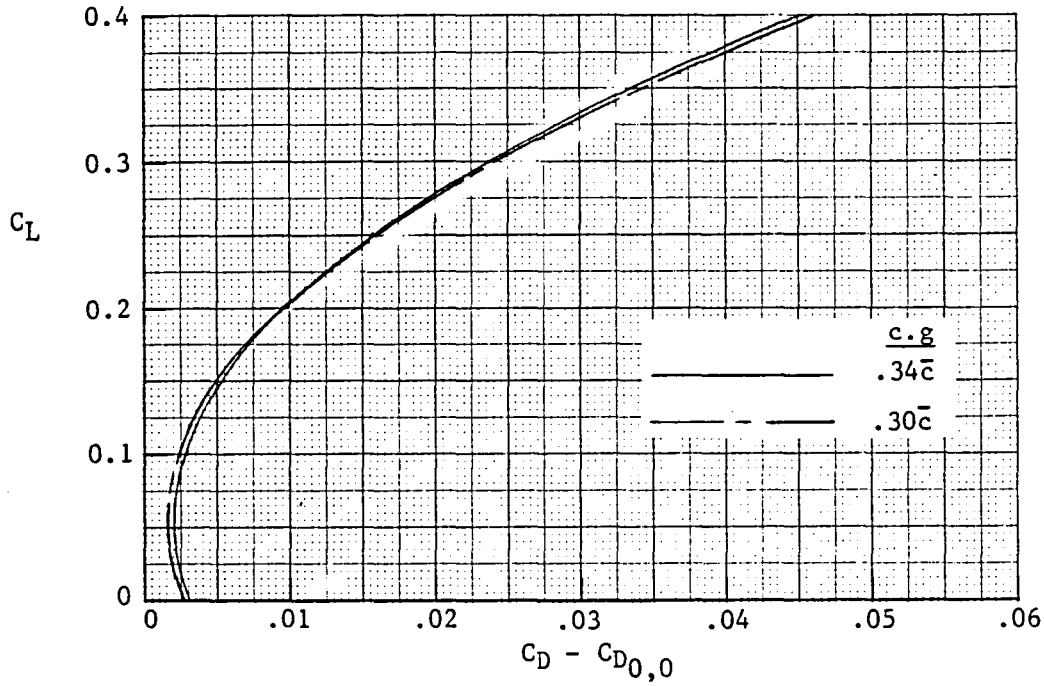

b) M = 0.9

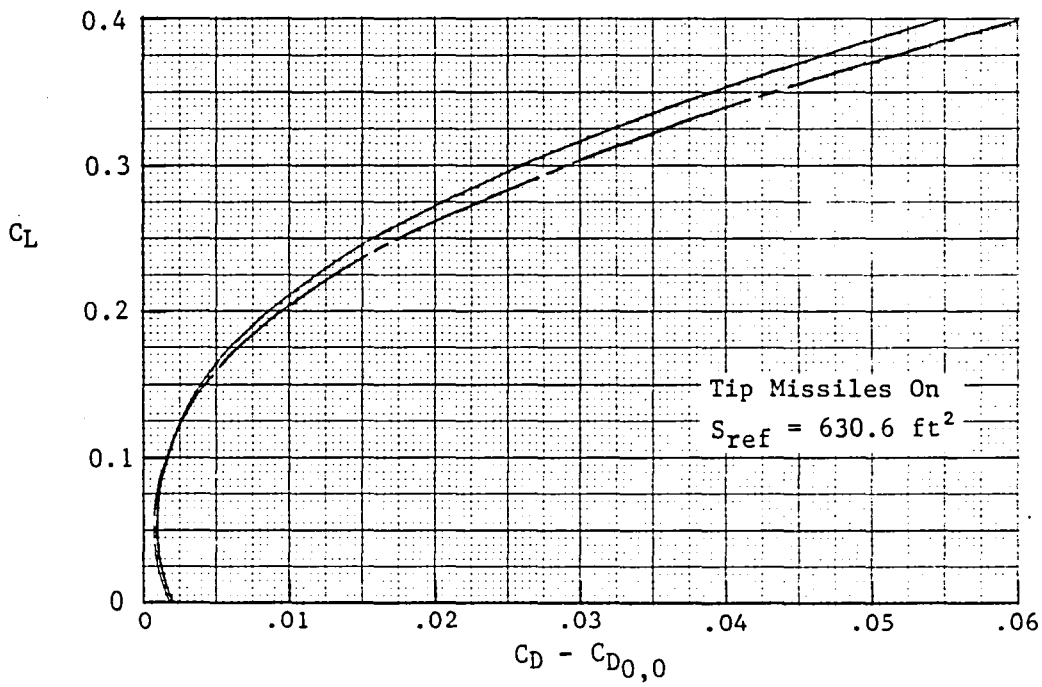

c) M = 1.2

Figure 4-6 Continued

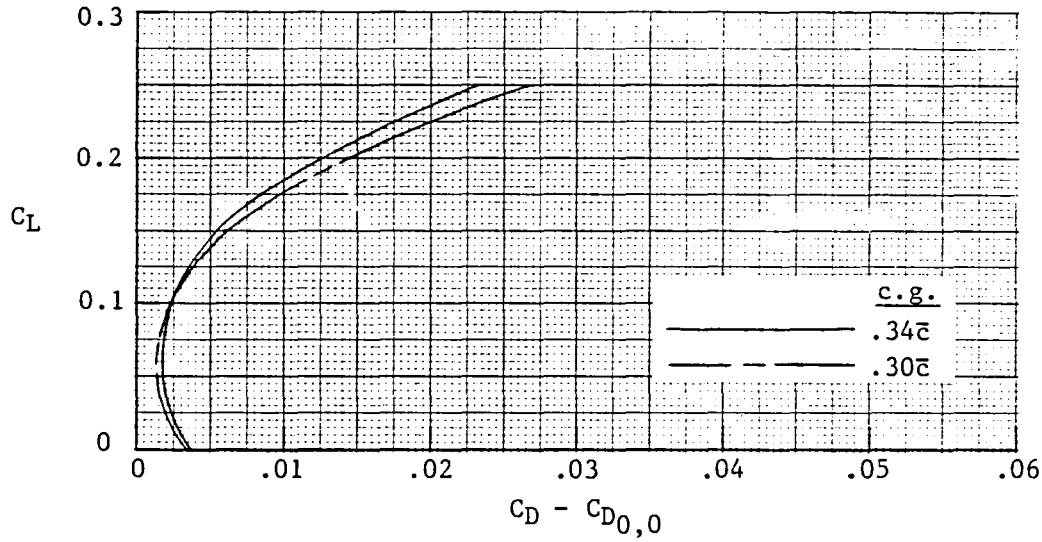

d) M = 1.6

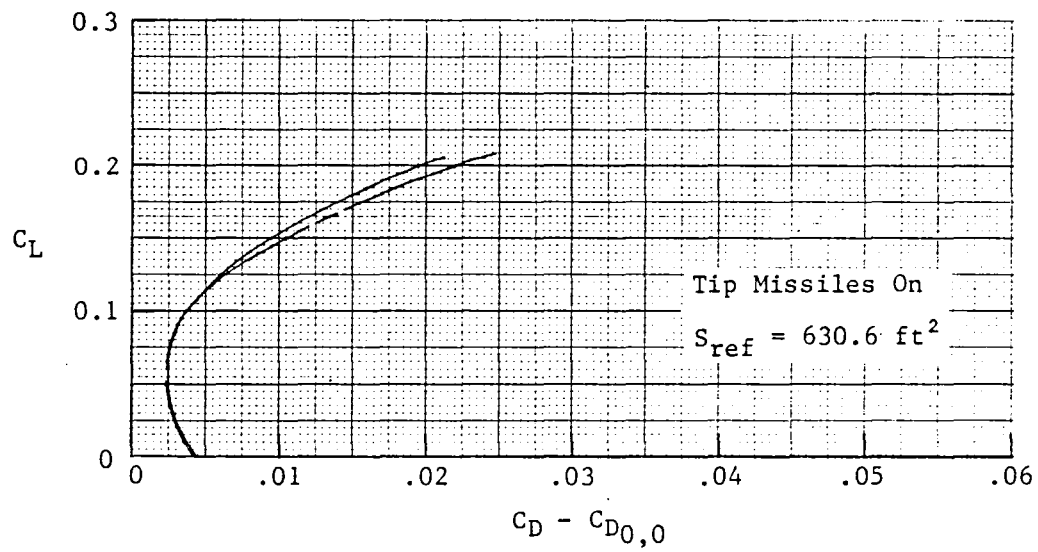

e) M = 2.0

Figure 4-6 Concluded

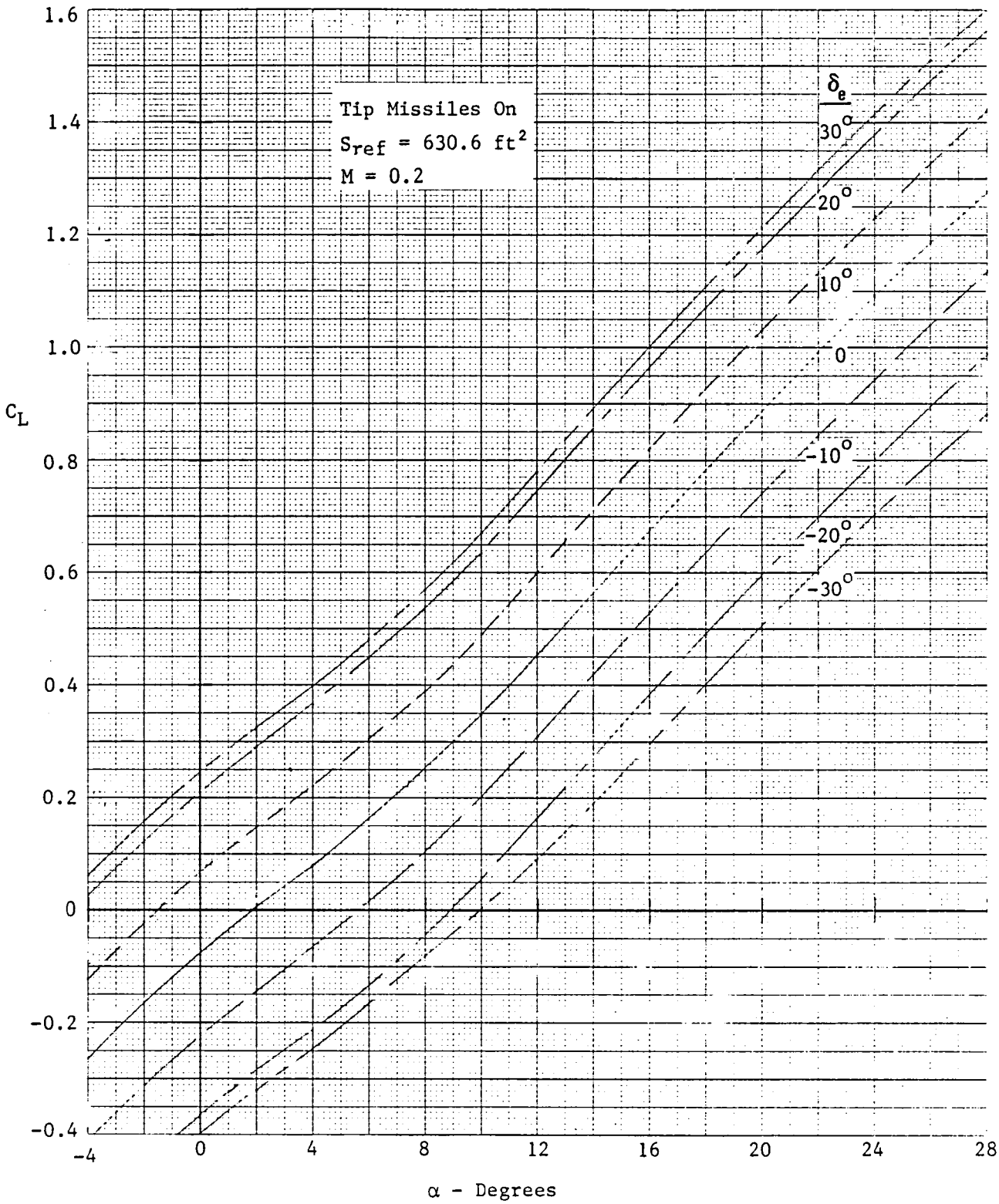

Figure 4-7 Variation of Low-Speed Lift Coefficient with Angle of Attack and Elevon Deflection in Free Air

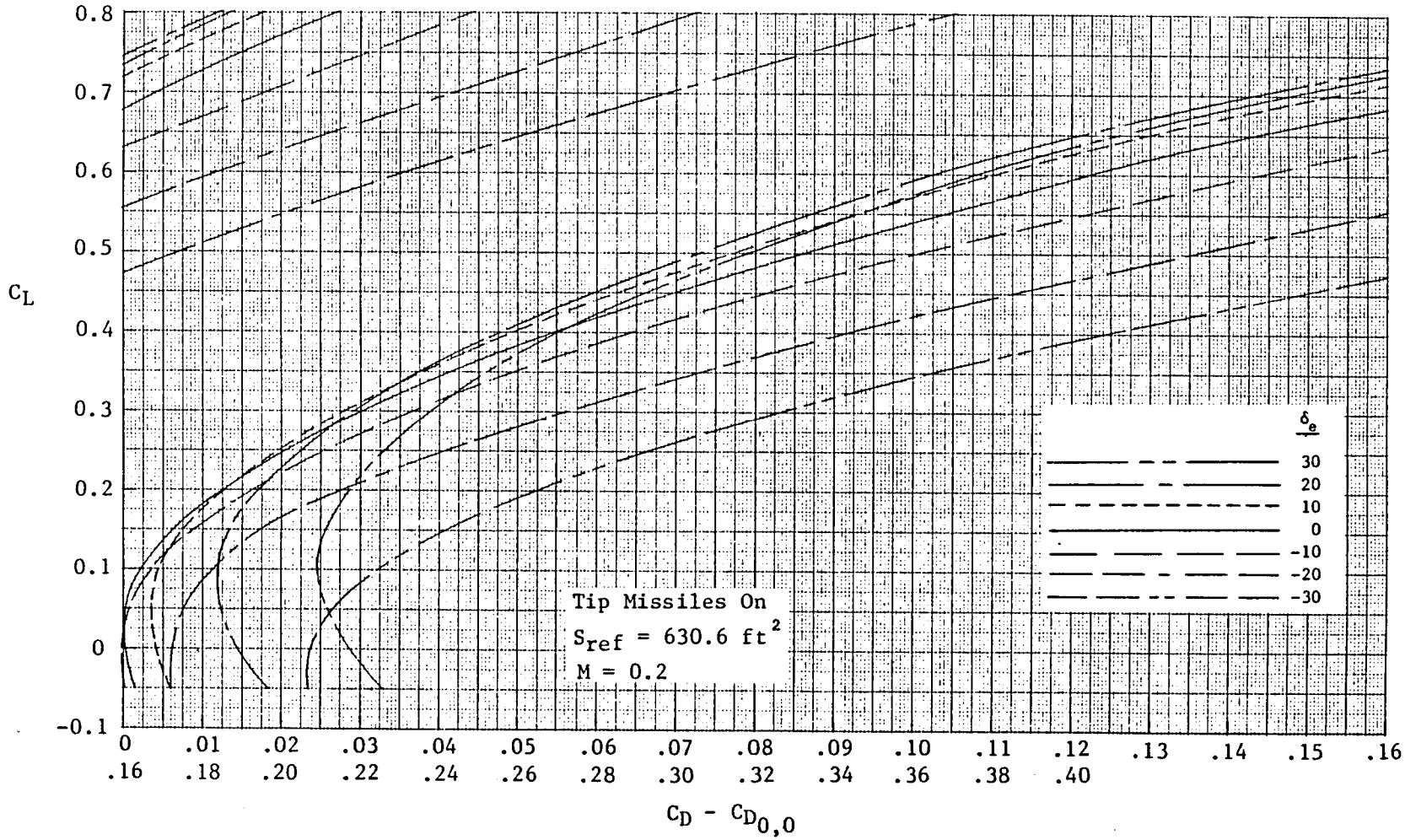

Figure 4-8 Variation of Low-Speed Drag Due to Lift and Camber with Lift Coefficient and Elevon Deflection in Free Air

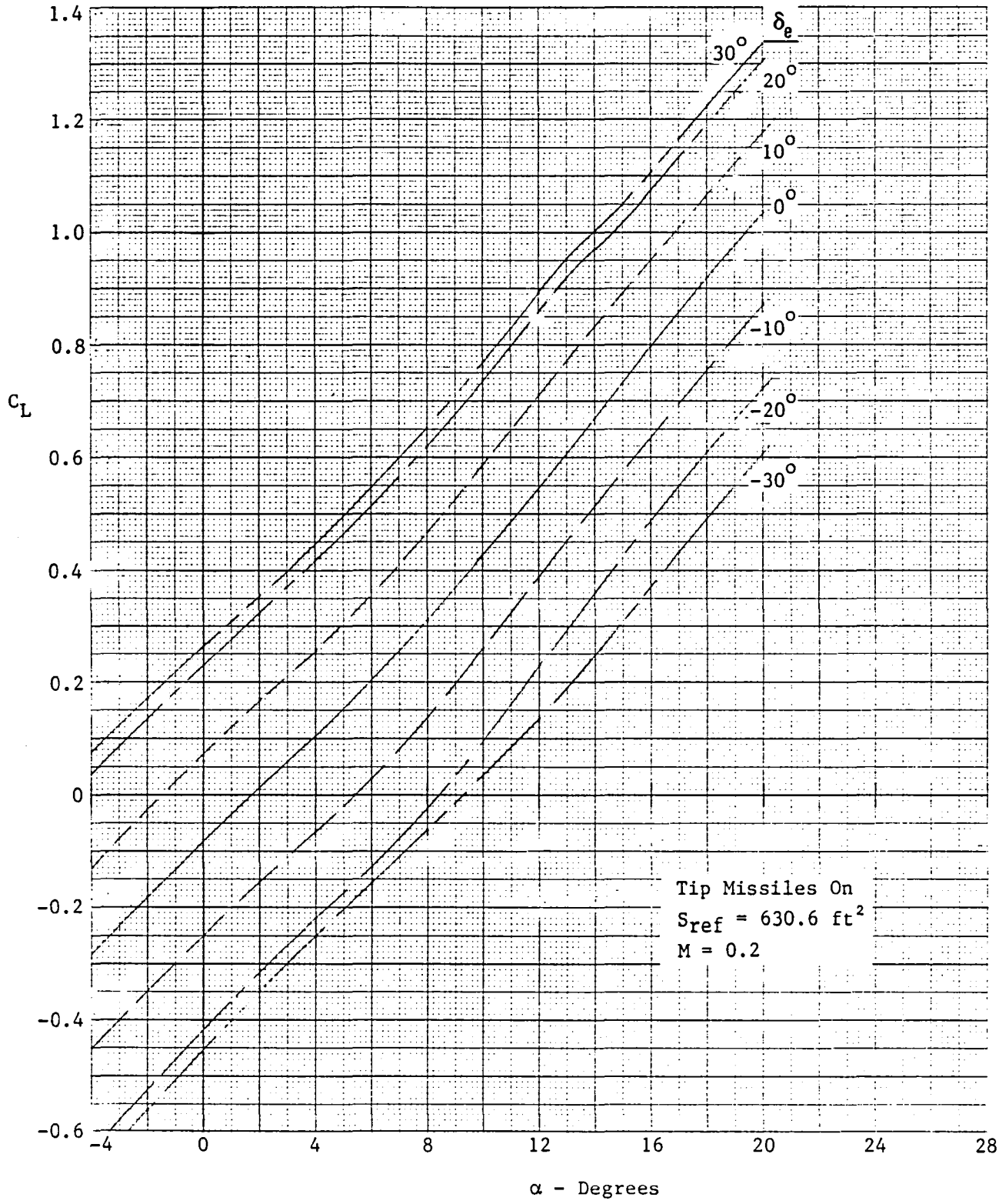

Figure 4-9 Variation of Low-Speed Lift Coefficient with Angle of Attack and Elevon Deflection in Ground Effect

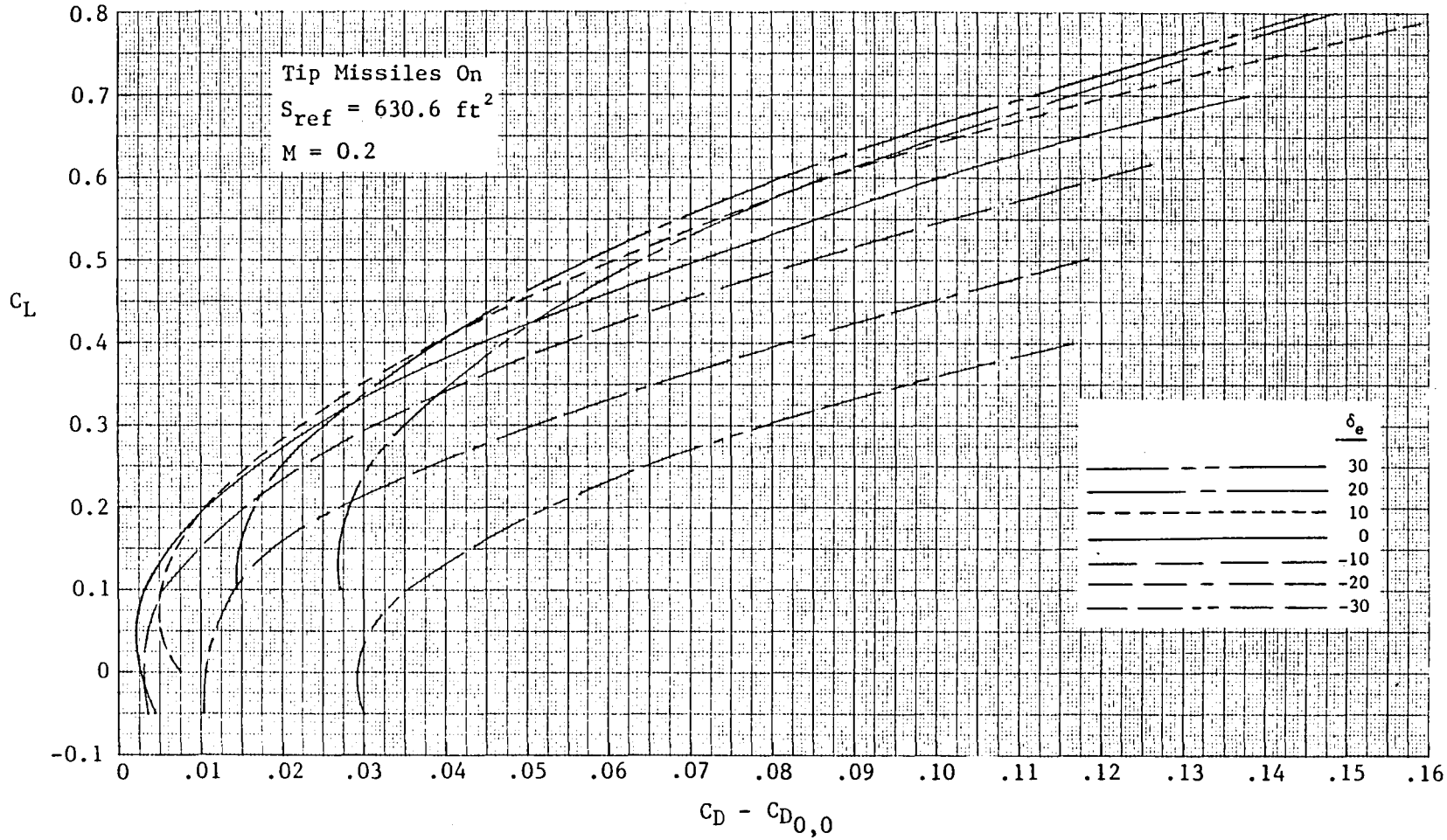

Figure 4-10 Variation of Low-Speed Drag due to Lift and Camber with Lift Coefficient and Elevon Deflection in Ground Effect

4.3 PROPULSION - INDUCED EFFECTS

Effects of the flow through the ejectors on power-off aerodynamic characteristics presented in Figures 4-7 through -10 have not been addressed. Data taken at NASA/Ames Research Center on the DeHavilland ejector configuration, Reference 2, showed a slightly favorable effect of the ejector flow on the aerodynamic lift. Since E-7 has significant configuration differences from the NASA/Ames model, a conservative approach was selected that assumed no effect of the ejector flow on transition lift and drag characteristics. These effects could be determined experimentally using a 1/6-scale powered model.

The classical hover ground effects, suckdown, fountains, and ejector back pressure, have been addressed for inclusion in the estimated hover thrust levels. Data from the NASA/Ames test, Reference 2, were used to define the thrust loss due to back pressure and to estimate the extent and magnitude of the favorable positive pressure region on the aircraft under surface between the ejectors. Suckdown effects over the remainder of the wing and fuselage lower surface were not included due to the uncertain characteristics of the ejector/core nozzle flow field. Additional discussion of the propulsion induced effects is presented under aerodynamic uncertainties in Section 7.

4.4 STABILITY AND CONTROL

During the contract period, initial predictions of basic stability and control parameters were completed for Configuration E-7. In general, the aircraft will be controlled through an electronic flight control system. The full-span trailing-edge control surfaces will supply the pitch control, differential deflection of these surfaces will provide the roll control, and a conventional rudder will provide directional control. The aircraft will be flown in the conventional mode at neutral longitudinal static stability through an automatic fuel management system with manual override. Currently, center-of-gravity (c.g.) positions yielding positive or neutral static stability only are permitted.

A substantial effort has been devoted to the formulation of an actual flight control system for the configuration. This was done at this early stage because of the complex interfaces between the flight control system, the propulsion system, and the reaction control system (RCS). A preliminary estimate of the reaction control requirements has been conducted and development of the flight control system has progressed to the point where full six-degrees-of-freedom (DOF) analysis can be conducted. This will allow detailed studies of the aircraft response with the full RCS operating. Detailed studies of the aircraft response during transition with the ejector system operating can be undertaken, although the impact of the ejectors on the airframe aerodynamics is an unknown factor. This problem will, of course, be present until actual powered-model wind-tunnel results become available.

4.4.1 Prediction of Stability and Control Characteristics

Stability and control predictions for Configuration E-7 in the clean configuration are based on the large amount of data accumulated on delta wing configurations such as the F-102, F-106, and B-58. These programs have produced wind-tunnel and flight test results which are directly applicable to the STOVL Configuration E-7.

In Figures 4-11 and -12, values are shown of pitching moment at zero lift and aerodynamic center location (a.c.) as a function of Mach number. Values for the pitching moment at zero lift were estimated based on recent wind-tunnel testing for the F-16E configuration camber design. This same camber design is incorporated in the airfoil design of Configuration E-7. Values for a.c. location are based on the wind-tunnel and flight test results for the delta-wing designs referenced above with some small modification for the clipped tip based on Falkner lifting-surface theory. The clipped tip provides a place to mount an air-to-air missile and based on recent wind-tunnel experience from the F-16 will produce a small incremental aft shift in a.c. location as illustrated in Figure 4-12.

Comparisons of the a.c. location of Figure 4-12 with the center of gravity locations (c.g.) of Section 3-2 illustrate the care that has been taken to insure neutral or positive static stability for the configurations with various loadings.

Predictions for lift curve slope and angle of attack for zero lift are shown in Figures 4-13 and -14.

The elevon effectiveness is illustrated in Figures 4-15 and -16. Figure 4-15 defines the change in lift as a function of deflection, and Figure 4-16 illustrates the location of the center of pressure (C.P.) as a function of deflection. These levels were obtained from available B-58 data which has the same geometric relationships for elevon area to wing area and hinge line location in percent of mean aerodynamic chord (MAC).

Values for changes in pitching moment due to pitch rate and angle-of-attack rate are shown in Figures 4-17 and -18. These levels were estimated based on results for delta wings.

The estimated values for directional stability, side force and yawing moment due to sideslip, illustrated in Figures 4-19 and -20 were evaluated from F-16A data. This was accomplished by adjusting the vertical-tail-off values for the increase in fuselage side area. This essentially increased the value of tail-off directional instability by 7 percent. The contribution of the vertical tail only (less ventrals) was then added to obtain the total value of directional stability.

The additional lateral stability derivatives for the clean configuration illustrated in Figures 4-21 through -29 were obtained from the B-58 configuration and will be incorporated in the lateral-directional analysis and simulations. The net effect of ejector performance on these derivatives will be established from wind-tunnel testing and will be incorporated as data become available.

General Dynamics has accumulated wind-tunnel results up to very high angles of attack on clipped delta configurations. Figure 4-30 presents some longitudinal results taken in the General Dynamics low-speed tunnel at San Diego. A wing planform with 64-degree leading-edge sweep, -4-degree trailing-edge sweep and taper ratio of 0.1 was tested up to 66 degrees angle of attack. Data for elevator deflections of zero and +20 degrees are shown, and the data demonstrate that for all angles of attack, the configuration will exhibit a longitudinal restoring moment. It is anticipated that Configuration E-7 with the -10-degree trailing-edge sweep will exhibit the same general characteristics at the very high angles of attack.

No applicable data were obtained for the lateral-directional stability characteristics or for lateral or directional control capability. Wind-tunnel testing must be accomplished to establish these characteristics at the very high angles of attack.

4.4.2 STOVL Flight Control and Reaction Control Systems

The control system for E-7 will be a combination of aerodynamic surfaces and a RCS. The aerodynamic surfaces (elevons and rudder) will be used in conventional wing-borne flight and will be used in conjunction with the RCS during transition. The RCS will provide all control during hover.

The RCS consists of five thrusters used to provide pitch roll and yaw control during low-speed flight. A downward thruster in each wing tip provides roll control when operated individually. Simultaneous operation of the roll thrusters provides pitch control. Another thruster under the cockpit also acts as pitch control. Two outward facing thrusters near the tail produce yaw control. The thrusters operate continuously when the RCS is in use and are operated differentially to produce the necessary control moments.

The initial RCS thruster sizing was accomplished using a single DOF model. Each thruster set (pitch, yaw, and roll) was analyzed separately with no kinematic coupling or thruster dynamics considered. The results of this analysis are presented along with the applicable response criteria in Figures 4-31 through -33. The sources of the requirements were MIL SPEC 83300 and Reference 25.

The pitch and yaw thruster magnitudes Figures 4-31 and -32 are only dependent upon thruster placement (moment arm of the thruster with respect to the aircraft c.g.) and the

vehicle inertia properties. Resulting values of pitch and yaw thrust required are 400 and 600 pounds respectively.

Roll thruster magnetudes are determined by the 1-DOF model and gust response requirements. The 1-DOF analysis in Figure 4-33 shows the roll thrust requirement for control to be 70 lb. MIL SPEC 83300 calls for a side gust of 30 knots up to a sideslip angle of 25 degrees. Figure 4-34 shows these results for the RCS alone. As the forward velocity increases from hover, the aerodynamic surfaces become effective and can be used to overcome the gust. The combined aerodynamic/RCS results are presented as Figure 4-35 and indicate a more reasonable situation. From these combined results, the roll thrust requirement was found to be 180 lbs to compensate for a side gust. Therefore, the total roll-channel thrust would be 250 lbs.

All of the thruster values are dependent upon the thruster moment arms and vehicle inertia, and will vary accordingly. The values presented are for a specific thruster location and could change as the overall vehicle evolves.

In Figure 4-36, values of sideslip angle resulting from a crosswind are illustrated. Because of the high angles of attack which occur during carrier takeoff, lateral control requirements will be greatest to overcome rolling moment due to sideslip. Figure 4-36 illustrates a possible angle-of-attack schedule as a function of airspeed for a gross weight of 28,000 pounds. The sideslip angle resulting from a steady sidegust of 30 kts is determined and the resulting aileron deflection to overcome the rolling moment due to sideslip is defined. Aileron deflections with and without RCS operating are illustrated.

Aerodynamic data used in this analysis are for a clean configuration. Aileron deflection and RCS requirements to overcome sidegust at low speed will be continuously upgraded as wind-tunnel test data for the configuration with the ejector system operating become available.

Carrier takeoff and landing requirements as discussed in Reference 25 present a harsh environment for STOVL aircraft. As this program progresses, six degrees of freedom dynamic analysis and simulation will be performed to realistically evaluate the controlability of the aircraft in unsteady airflow conditions.

A substantial effort has involved development of both longitudinal and lateral-directional 3-DOF models. These models are being constructed using the program EASY4 (Reference 26) to study the dynamic response to the system. Block diagrams of the general control system are presented in Figures 4-37 and -38 to demonstrate incorporation of the RCS into the conventional control system. Note thruster dynamics and kinematic coupling within the 3-DOF are included in these analyses.

The EASY4 program provides the capability of performing linear analyses and dynamic systems simulations. Using the 3-DOF models with EASY4 yields a simple, cost effective tool to study the overall control system and define the aircraft characteristics prior to implementation of a fully coupled 6-DOF model. These models will permit the initial definition and evaluation of translational velocity feedback instead of rate feedback for the hover task. Other observers in the field of V/STOL have indicated advantages of this type of control system for precision hovering tasks (Reference 27).

All the values predicted for the control thrusters are based upon criteria set forth in MIL SPEC 83300. Another source of V/STOL response requirements is Reference 25 by AGARD. The AGARD values are less stringent in several cases, especially the sideslip criteria. Due to uncertainty about the aerodynamics of the aircraft operating at low

speeds and high sideslip angles, a more elaborate definition of the RCS parameters was postponed until wind-tunnel results are available.

The successful completion of the complex maneuver involved in transition and hover task associated with STOVL flight is dependent upon the information available to the pilot and the workload associated with the task. The motivation in designing the overall control system is to minimize both the workload and the amount of information with which the pilot must cope to achieve the desired response.

One of the prime objectives in reducing workload is to provide the pilot with a few well defined controls. To do this, the controls need to provide uncoupled responses (e.g., changing throttle position in the hover mode should not alter pitch trim). This suggests integration of the propulsion controls with an automatic flight control system. By incorporating all of the control system inputs and aircraft dynamic information in an onboard flight computer, attitude control can be decoupled from height control. The pilot would be presented with a minimum of controls and would be able to concentrate more on a particular flight task.

Development of this type of integrated flight control system would require a sophisticated fly-by-wire approach. This type of control system will be most important in the development of a successful program which will be able to operate in the demanding environment of Navy carrier operations.

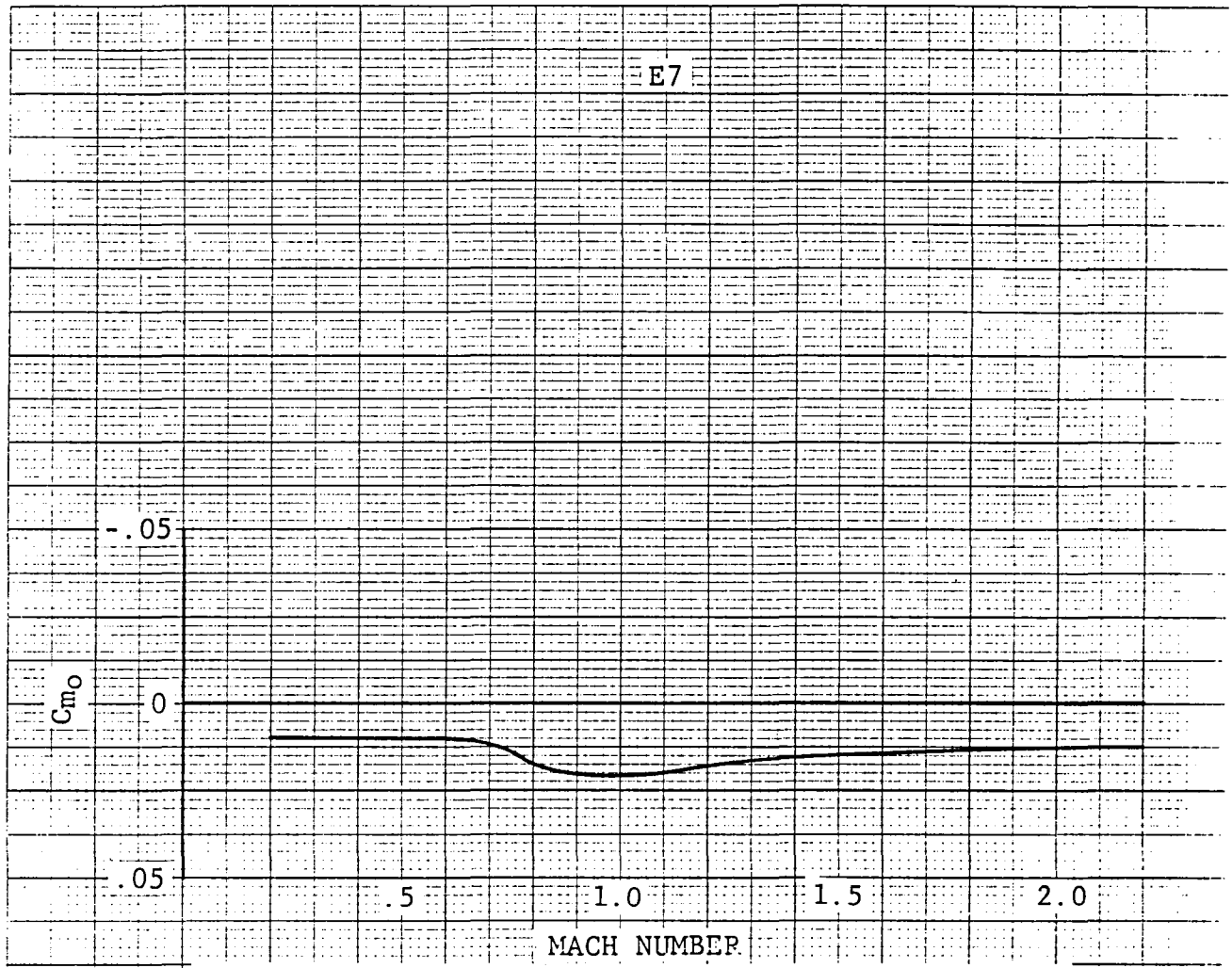

Figure 4-11 Pitching Moment at Zero Lift Versus Mach Number

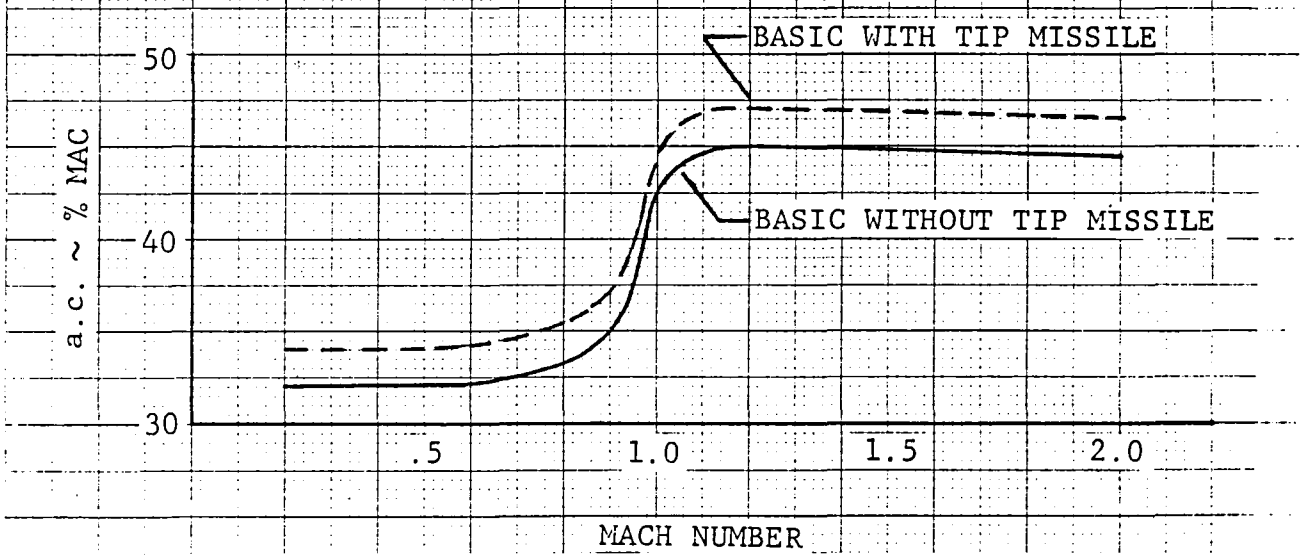

Figure 4-12 Aerodynamic Center Location Versus Mach Number

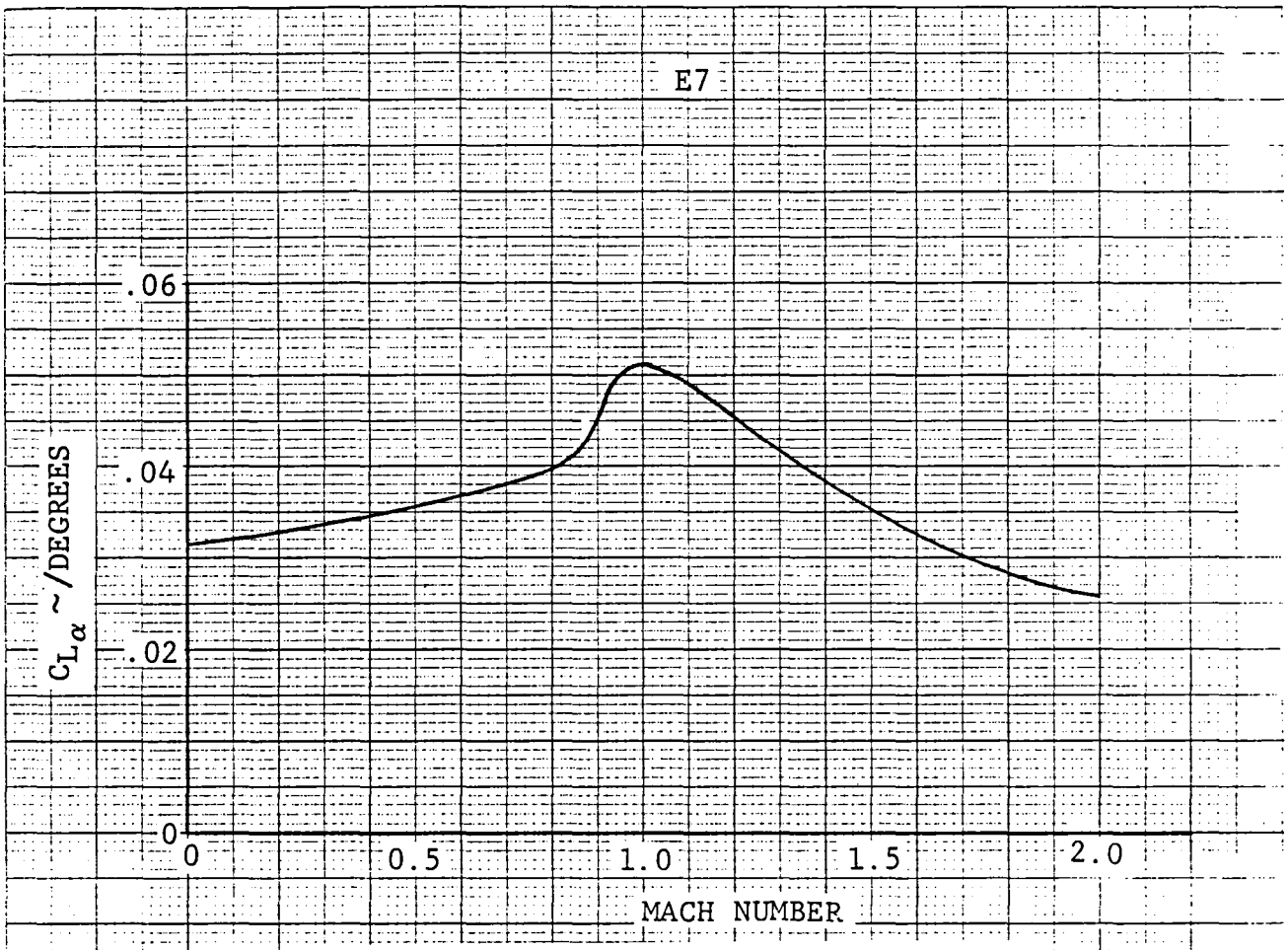

Figure 4-13 Lift Curve Slope Versus Mach Number

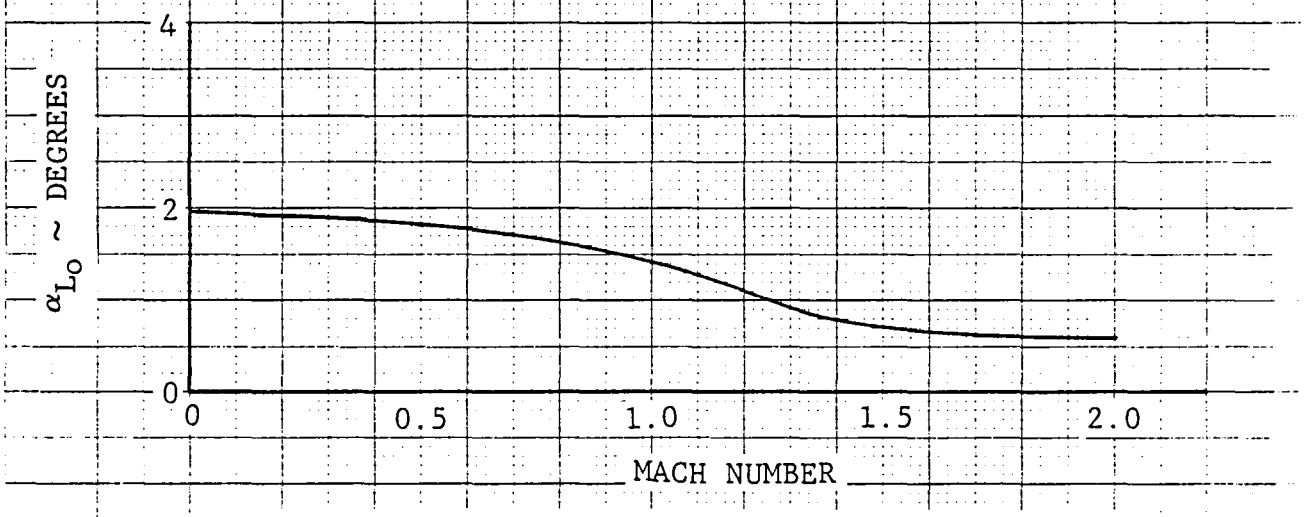

Figure 4-14 Angle of Attack at Zero Lift Versus Mach Number

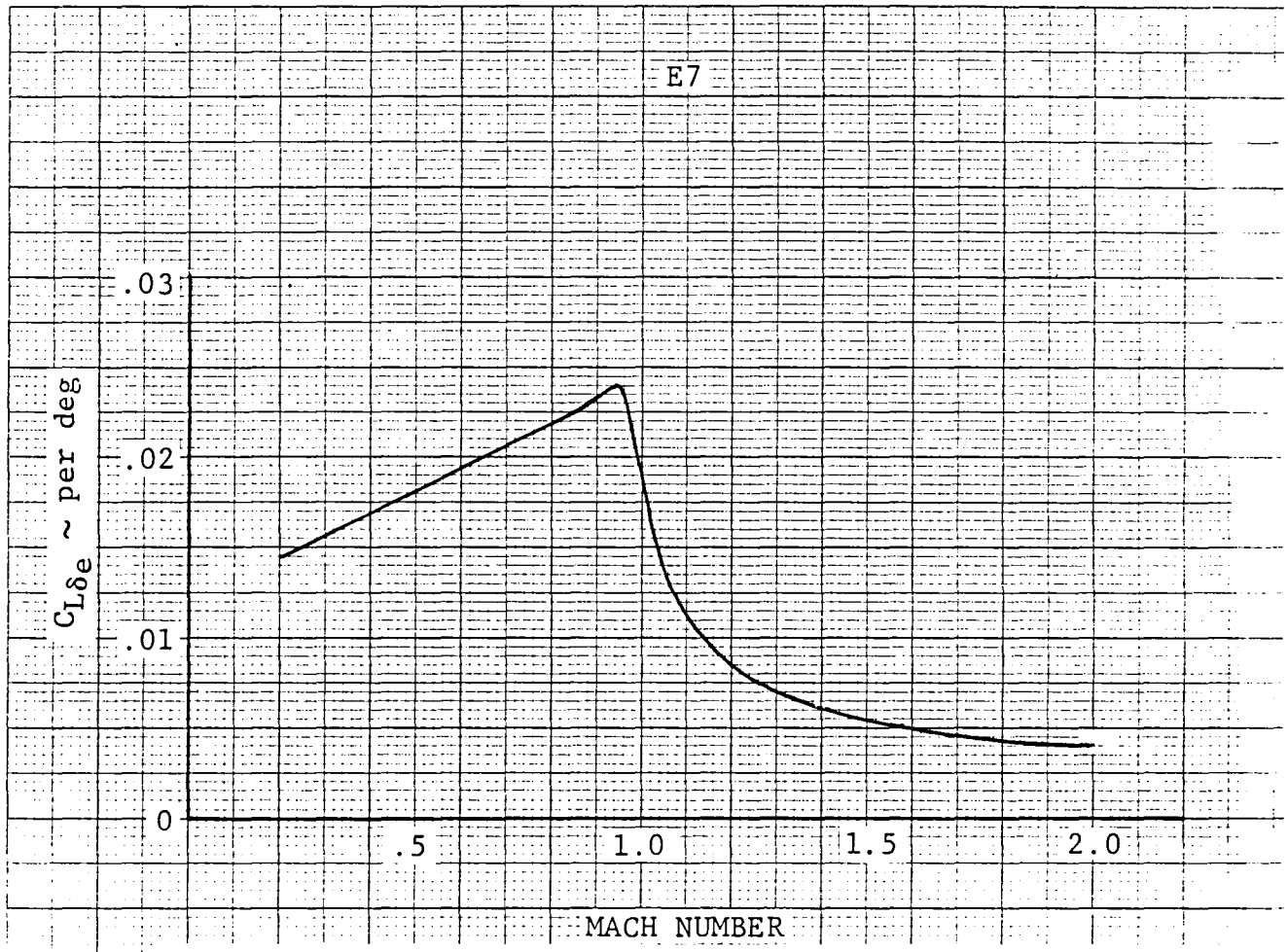

Figure 4-15 Change in Lift with Elevator Deflection Versus Mach Number

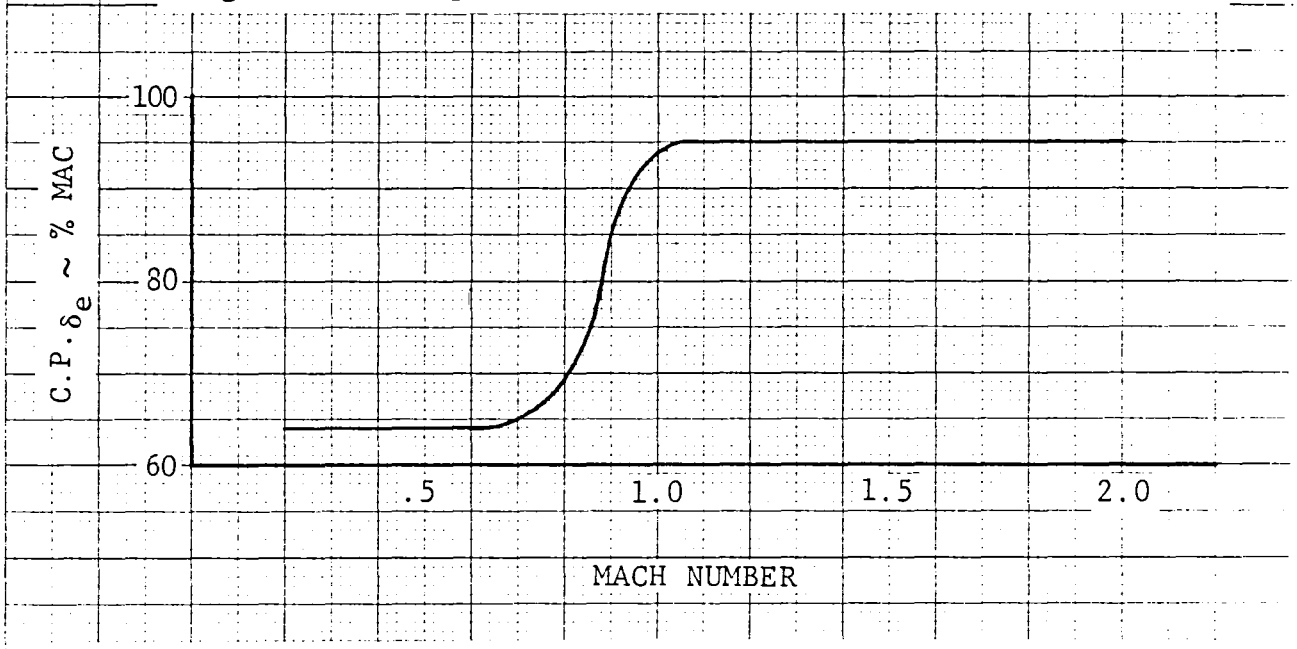

Figure 4-16 Center of Pressure of Lift due to Elevator Deflection Versus Mach Number

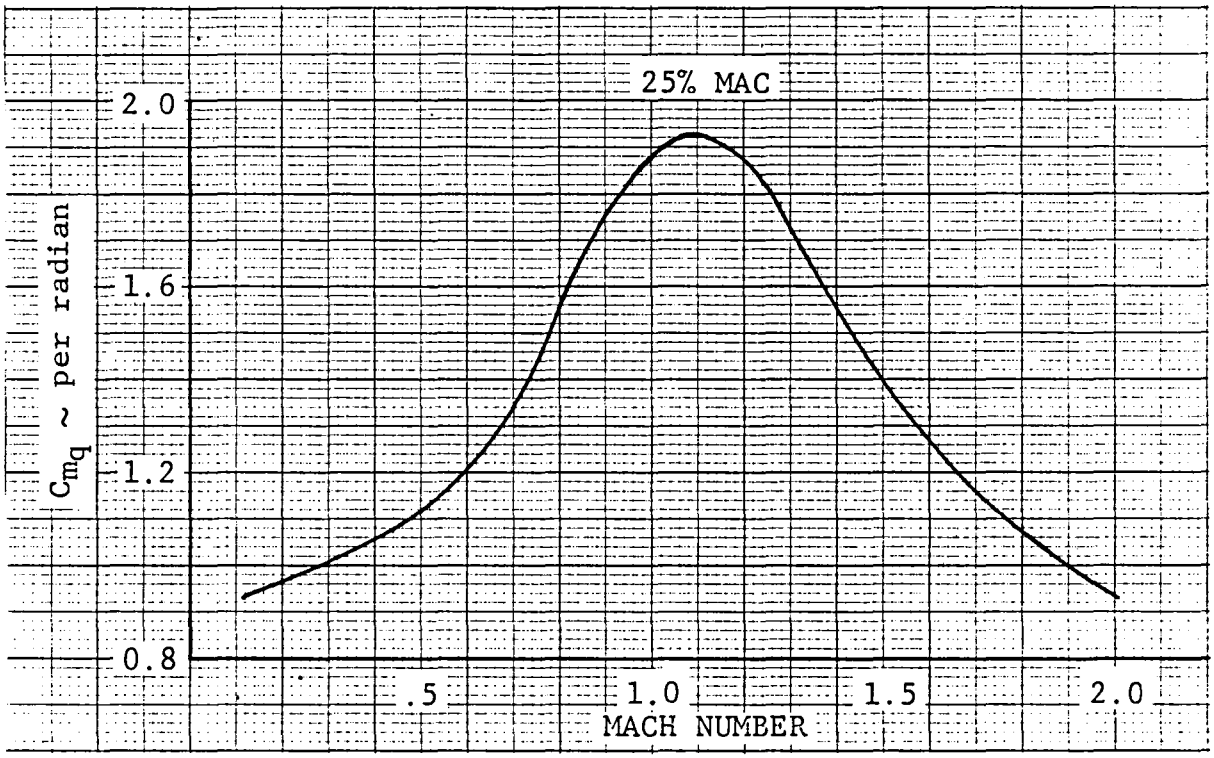

Figure 4-17 Change in Pitching Moment due to Pitch Rate Versus Mach Number

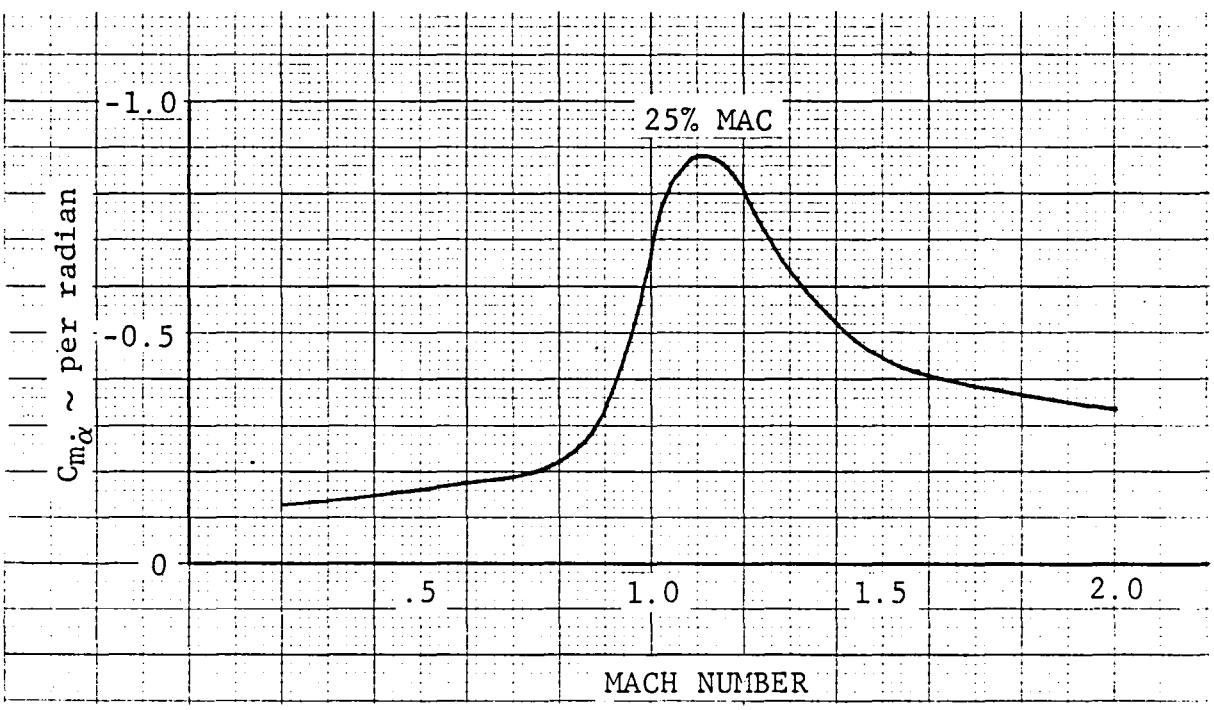

Figure 4-18 Change in Pitching Moment due to α Rate Versus Mach Number

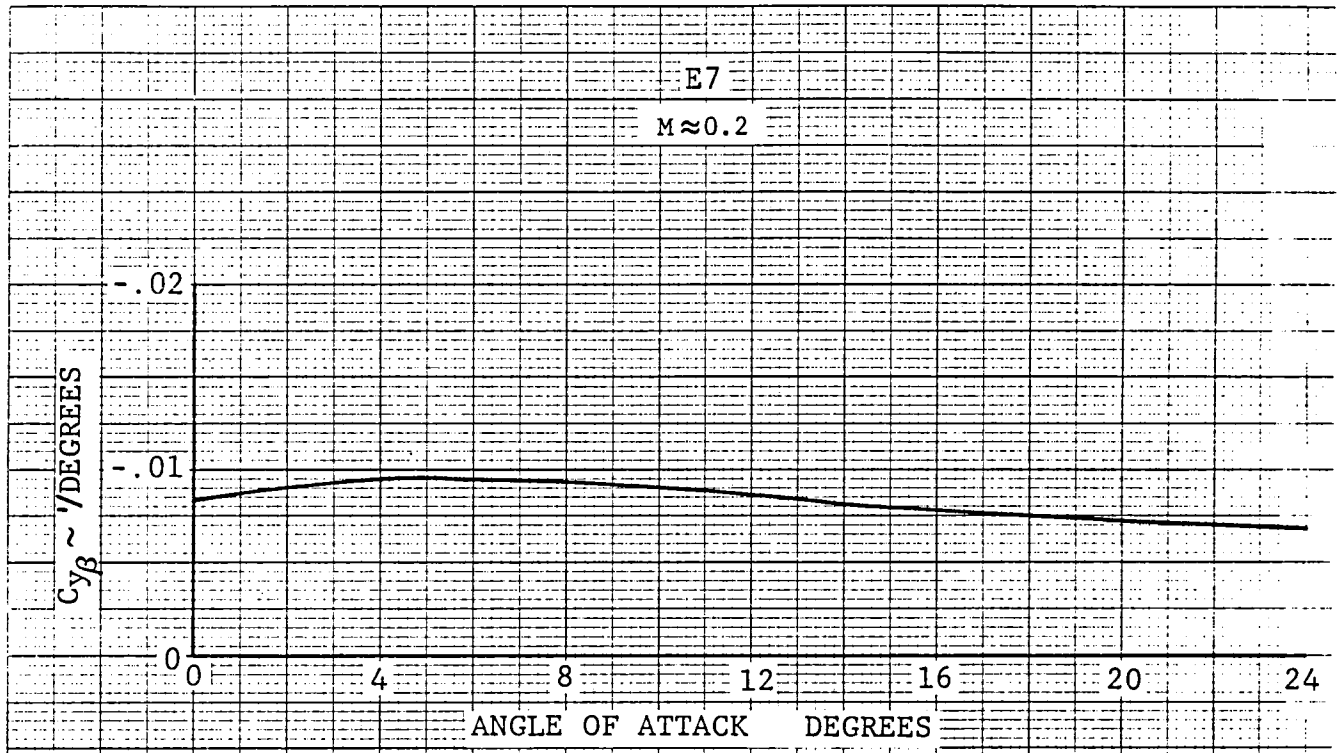

Figure 4-19 Sideforce due to Sideslip

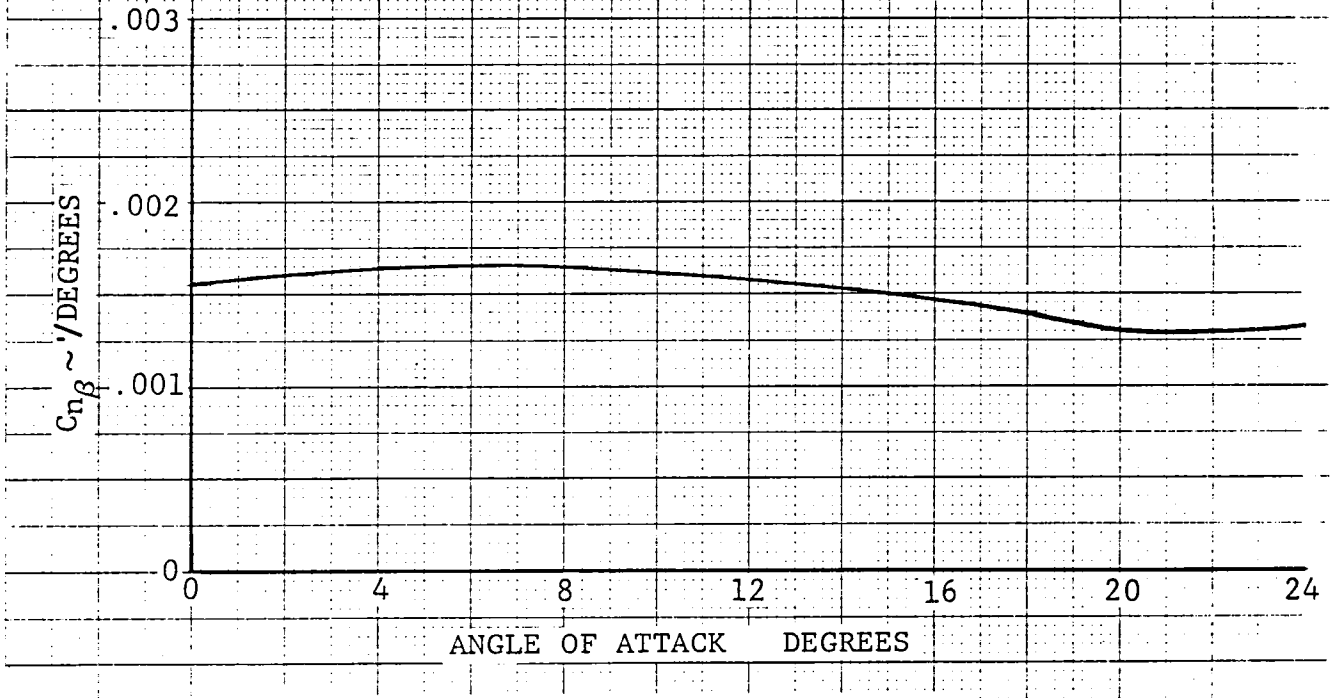

Figure 4-20 Yawing Moment due to Sideslip

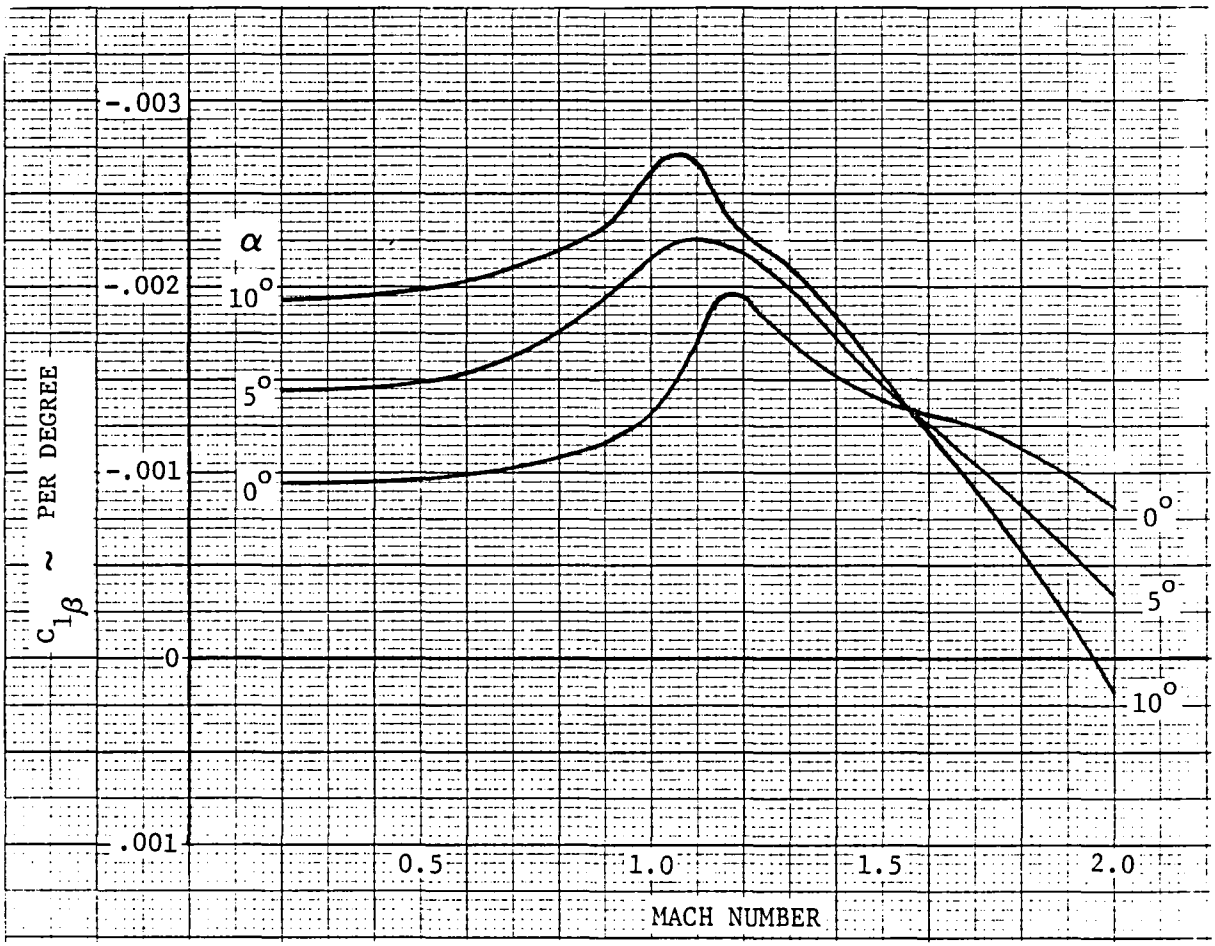

Figure 4-21 Rolling Moment due to Sideslip

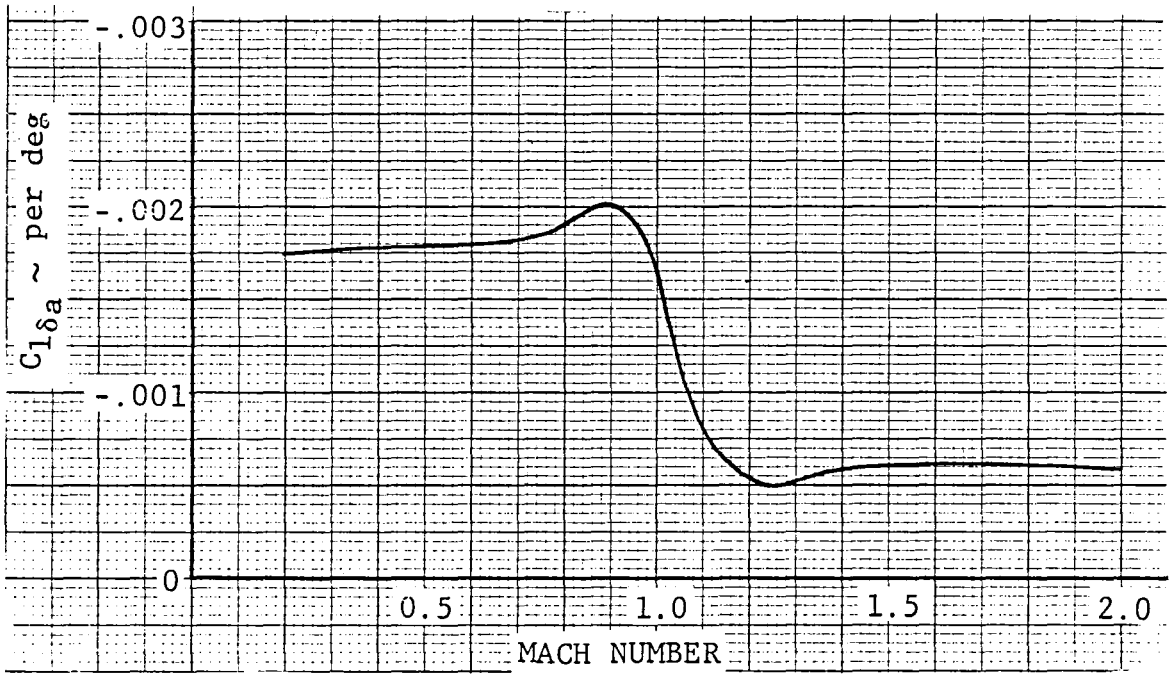

Figure 4-22 Rolling Moment due to Aileron Deflection

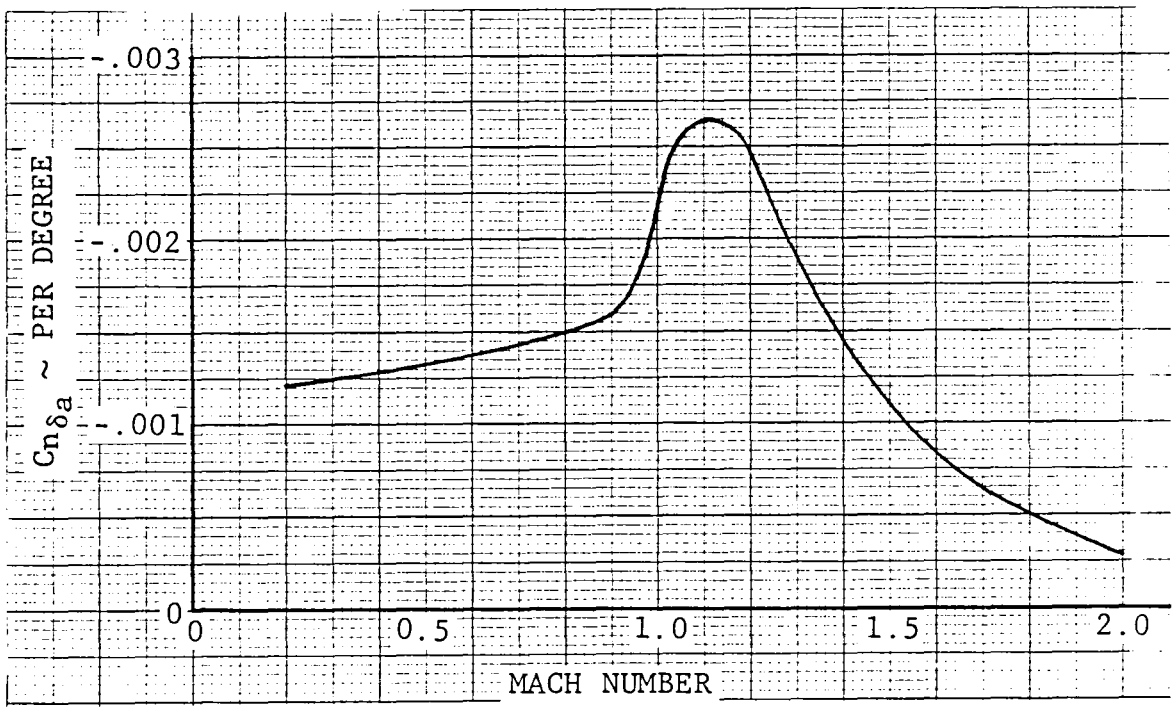

Figure 4-23 Yawing Moment due to Aileron Deflection

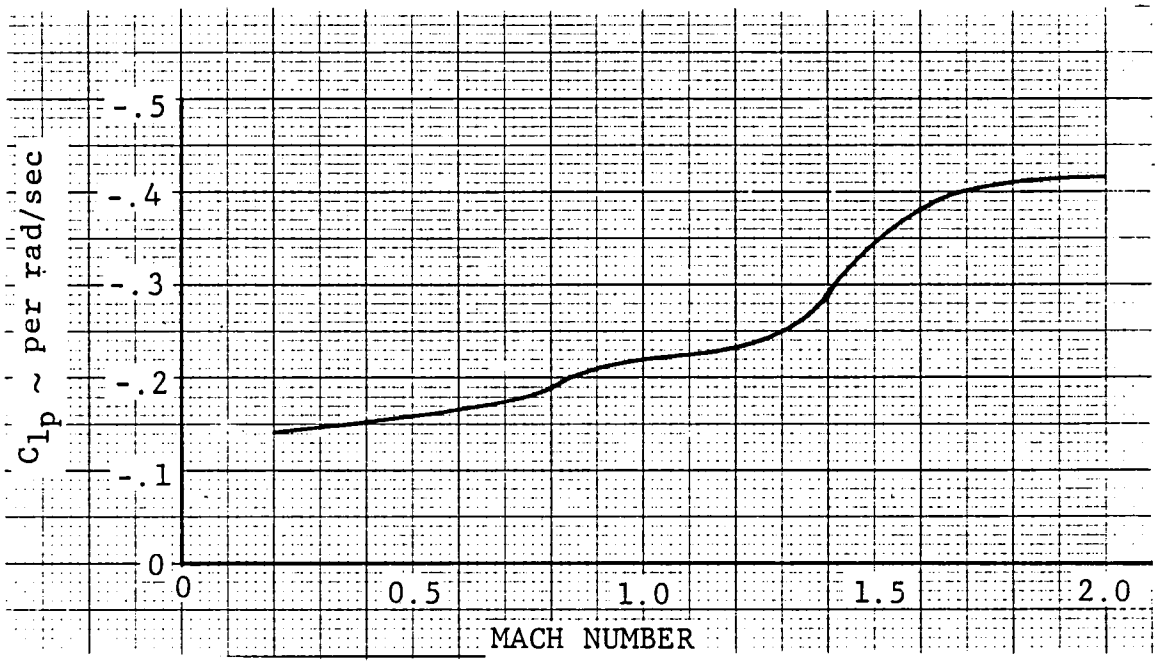

Figure 4-24 Rolling Moment due to Roll Rate

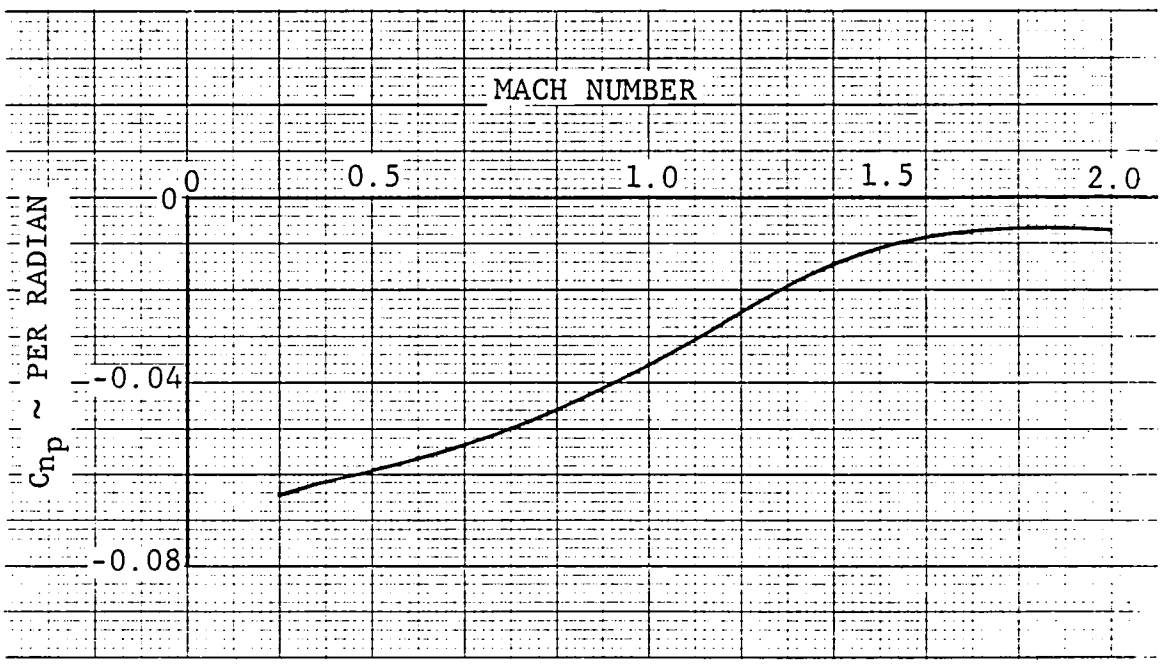

Figure 4-25 Yawing Moment due to Roll Rate

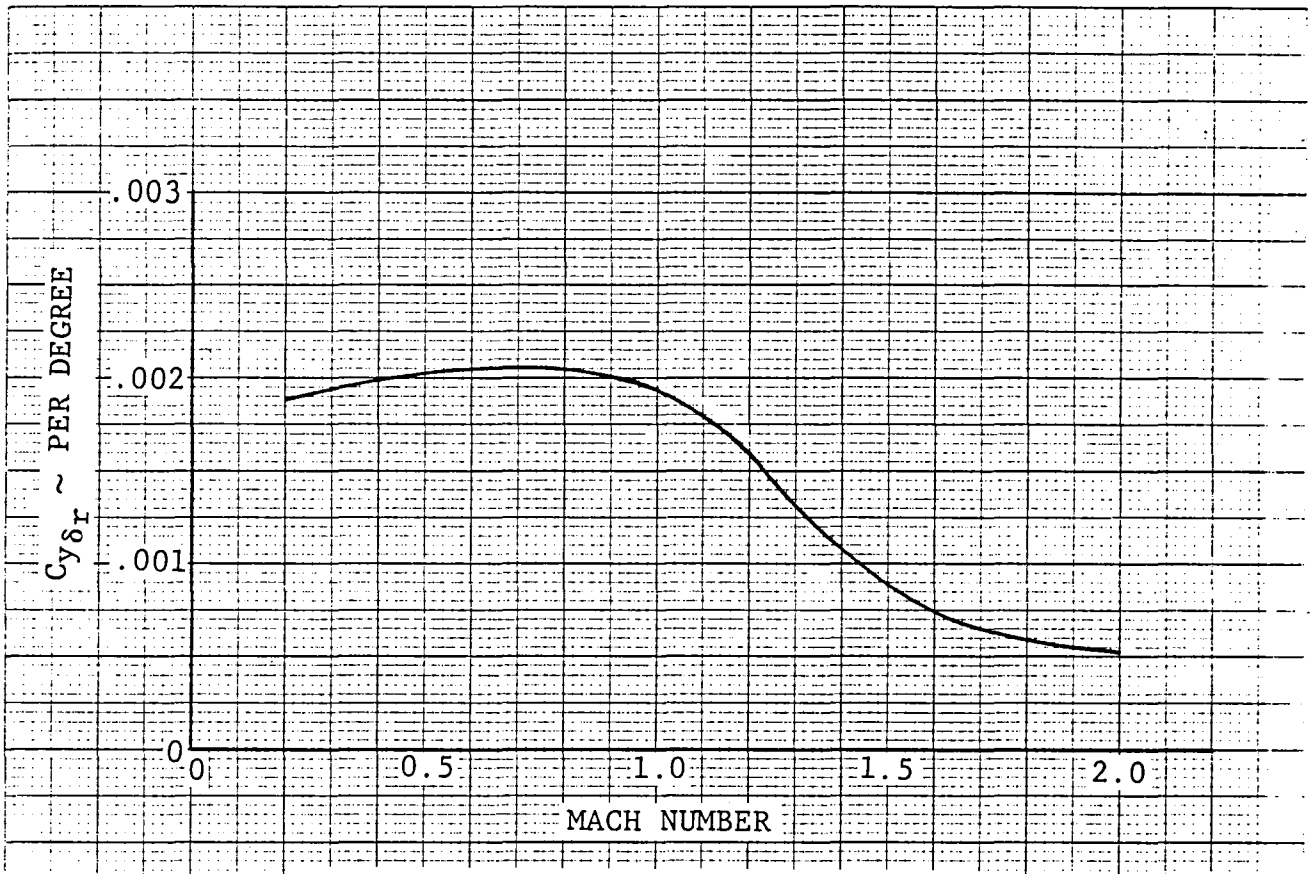

Figure 4-26 Sideforce due to Rudder Deflection

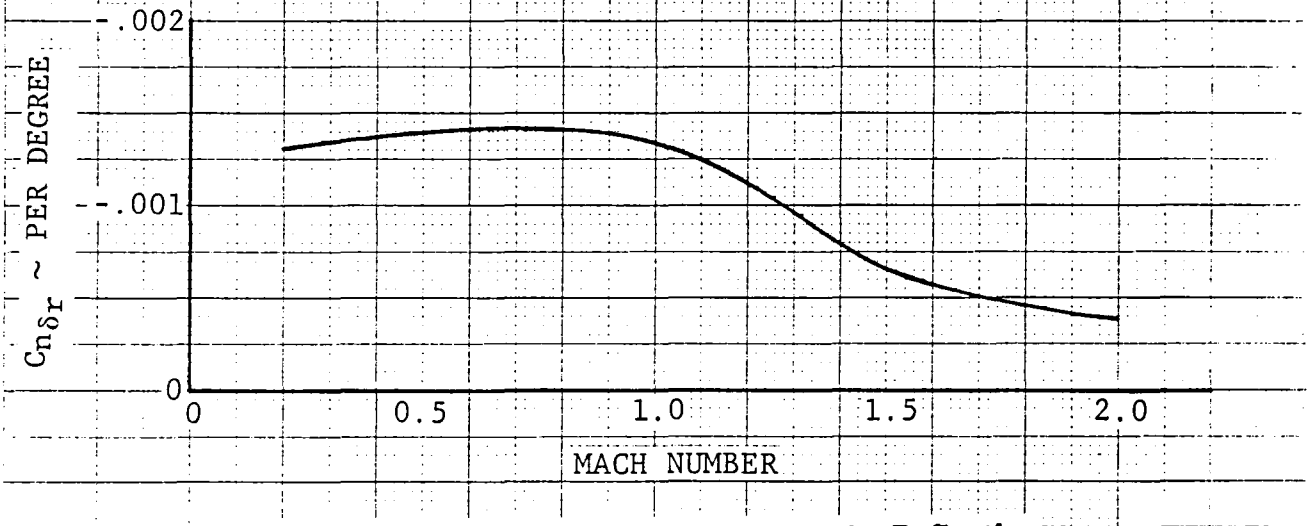

Figure 4-27 Yawing Moment due to Rudder Deflection

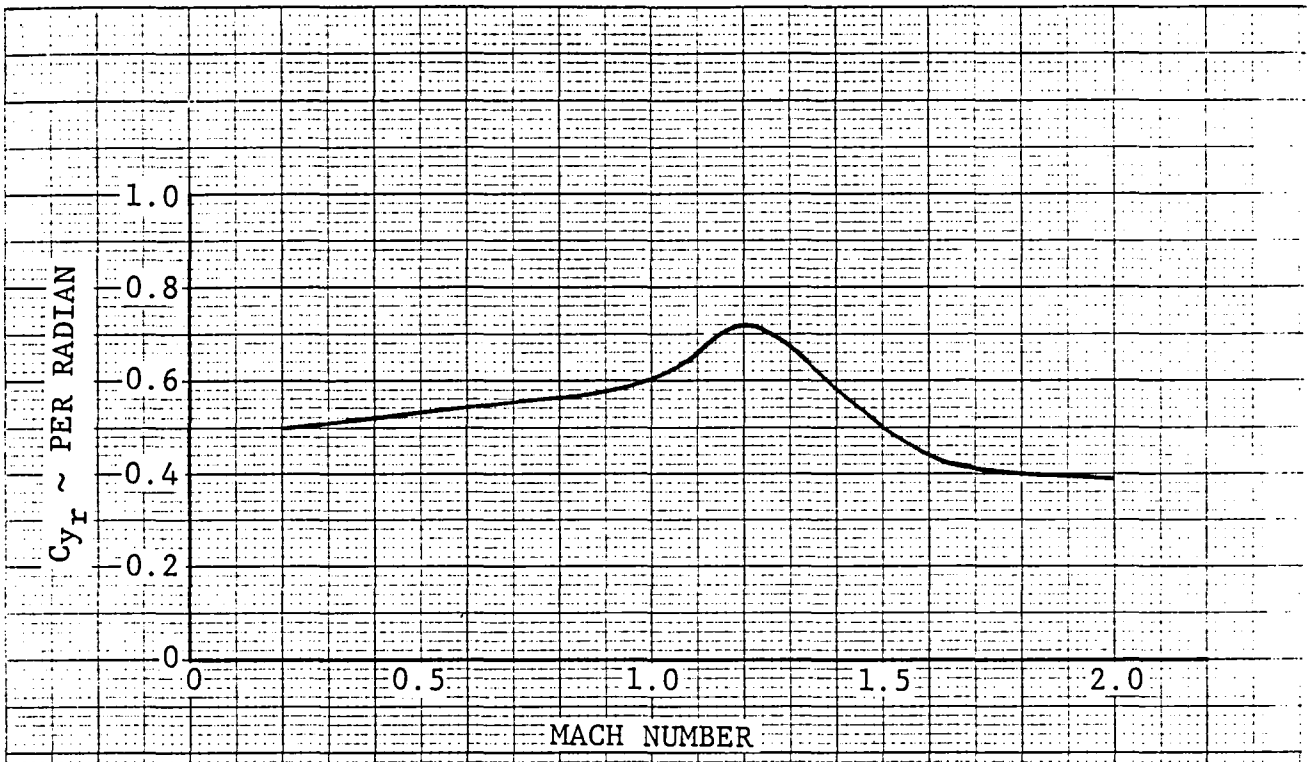

Figure 4-28 Sideforce due to Yaw Rate

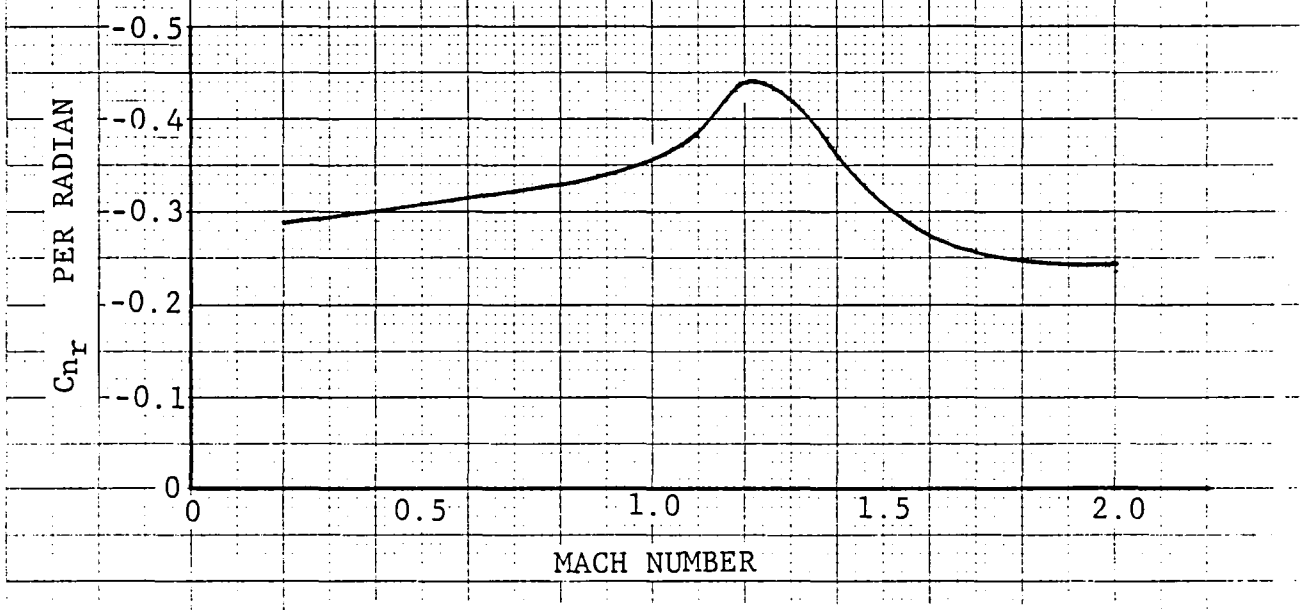

Figure 4-29 Yawing Moment due to Yaw Rate

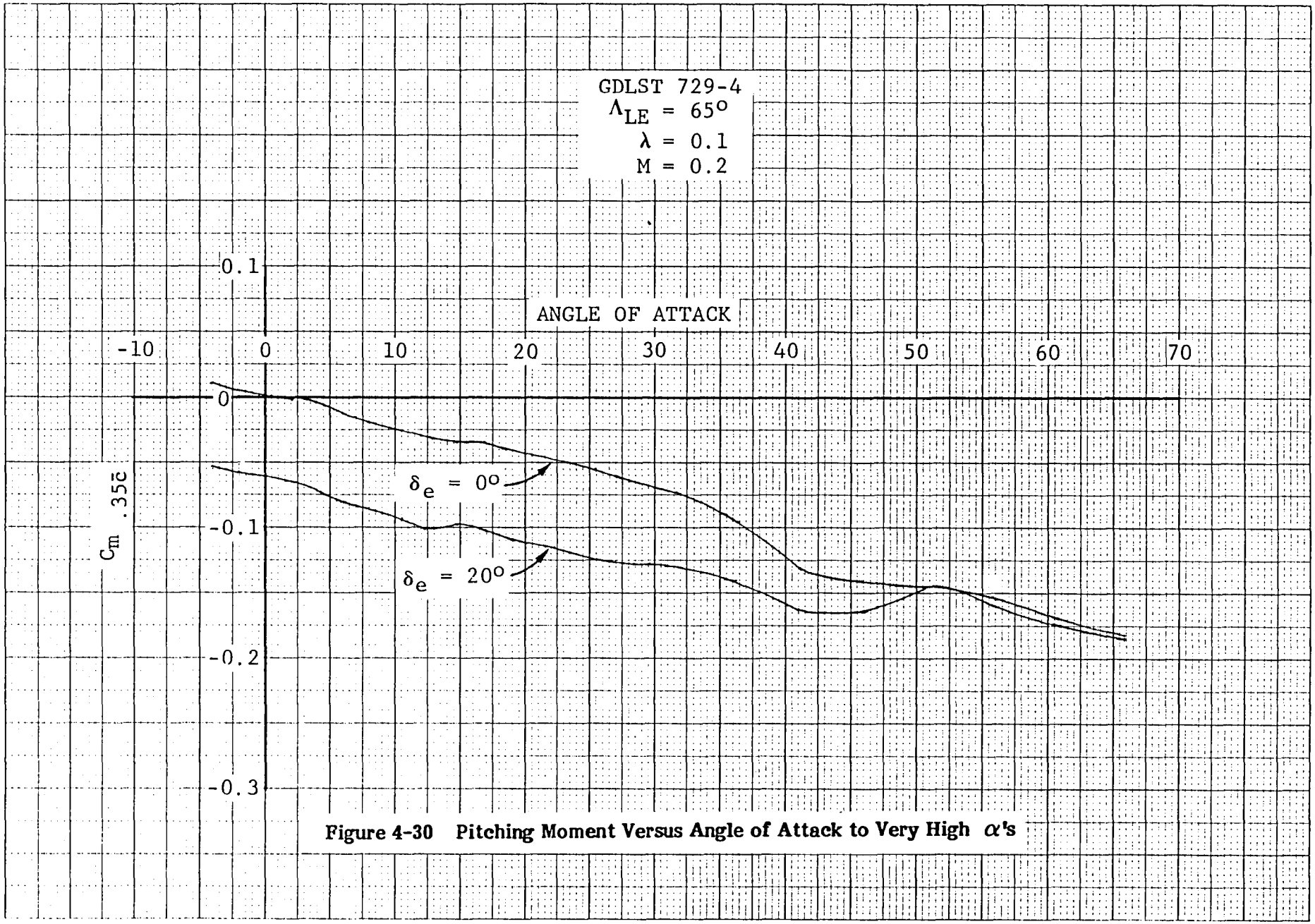

Figure 4-30 Pitching Moment Versus Angle of Attack to Very High α's

PITCH ANGLE VARIATION
FOR A STEP RCS INPUT

1-D UNCOUPLED ANALYSIS

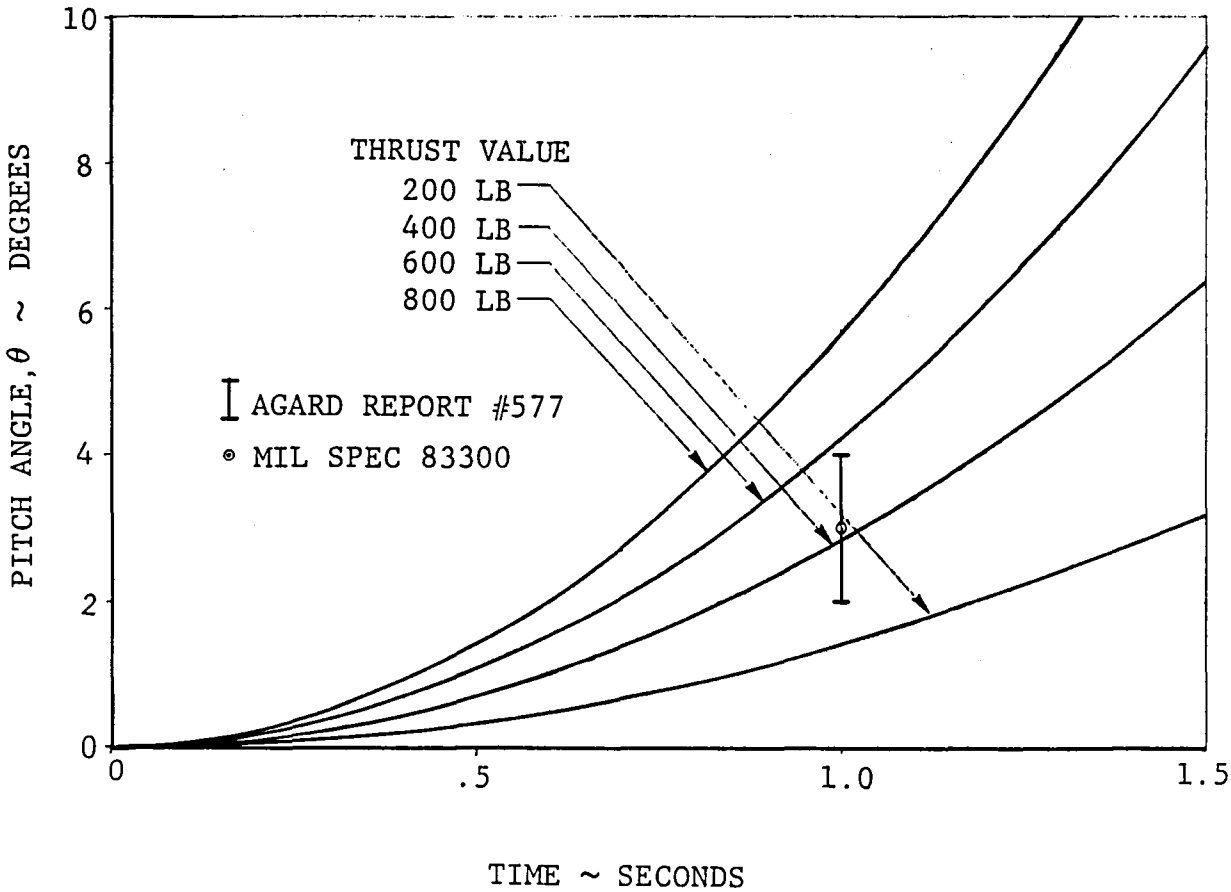

Figure 4-31 Change in Pitch Angle for a Step RCS Input

YAW ANGLE VARIATION
FOR A STEP RCS INPUT

1-D, UNCOUPLED ANALYSIS

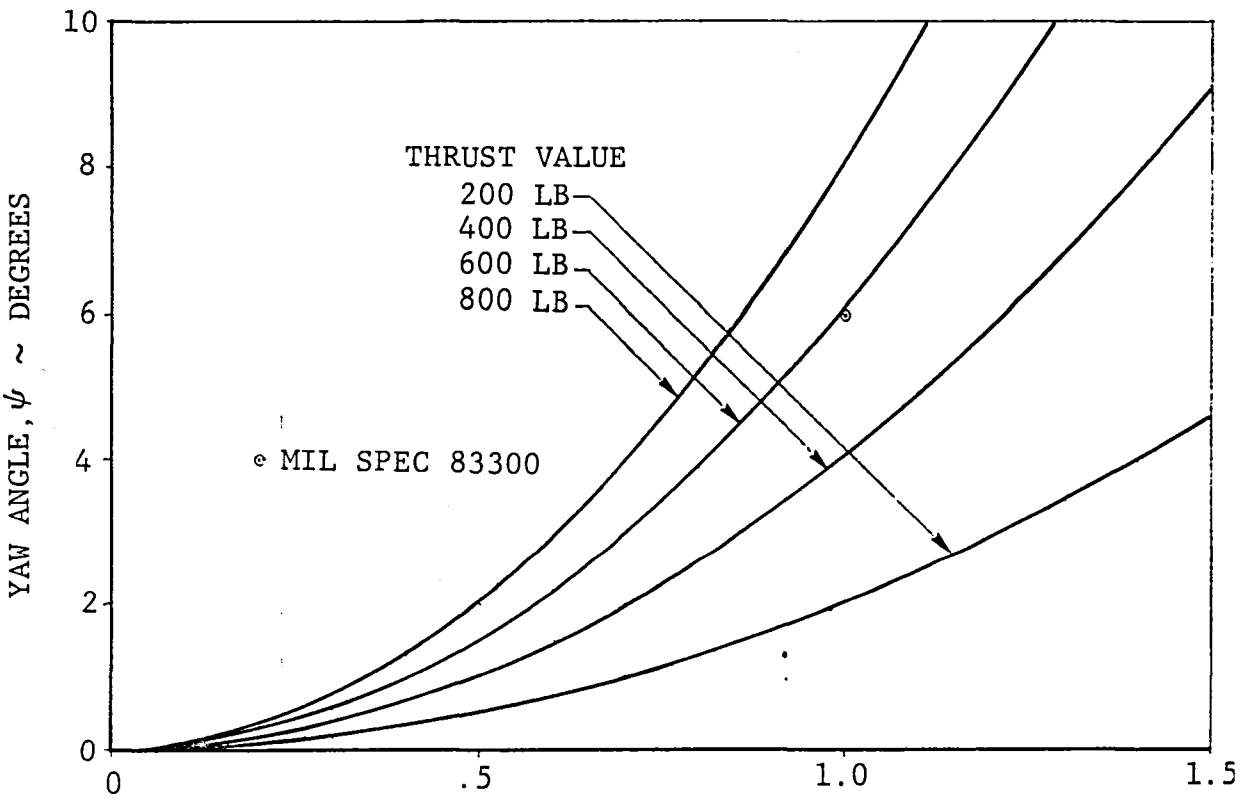

Figure 4-32 Change in Yaw Angle for a Step RCS Input

ROLL ANGLE VARIATION
FOR A STEP RCS INPUT

1-D, UNCOUPLED ANALYSIS

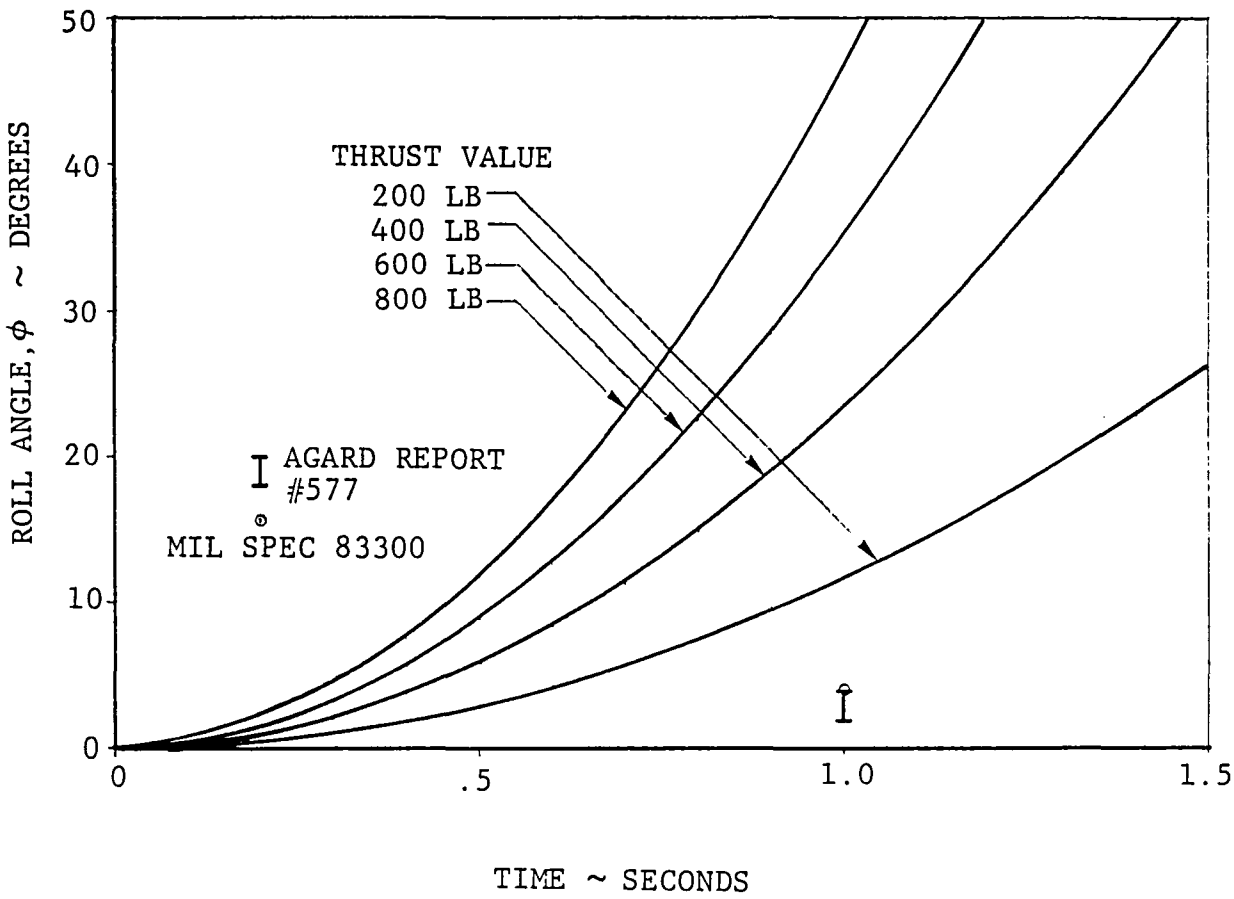

Figure 4-33 Change in Roll Angle for a Step RCS Input

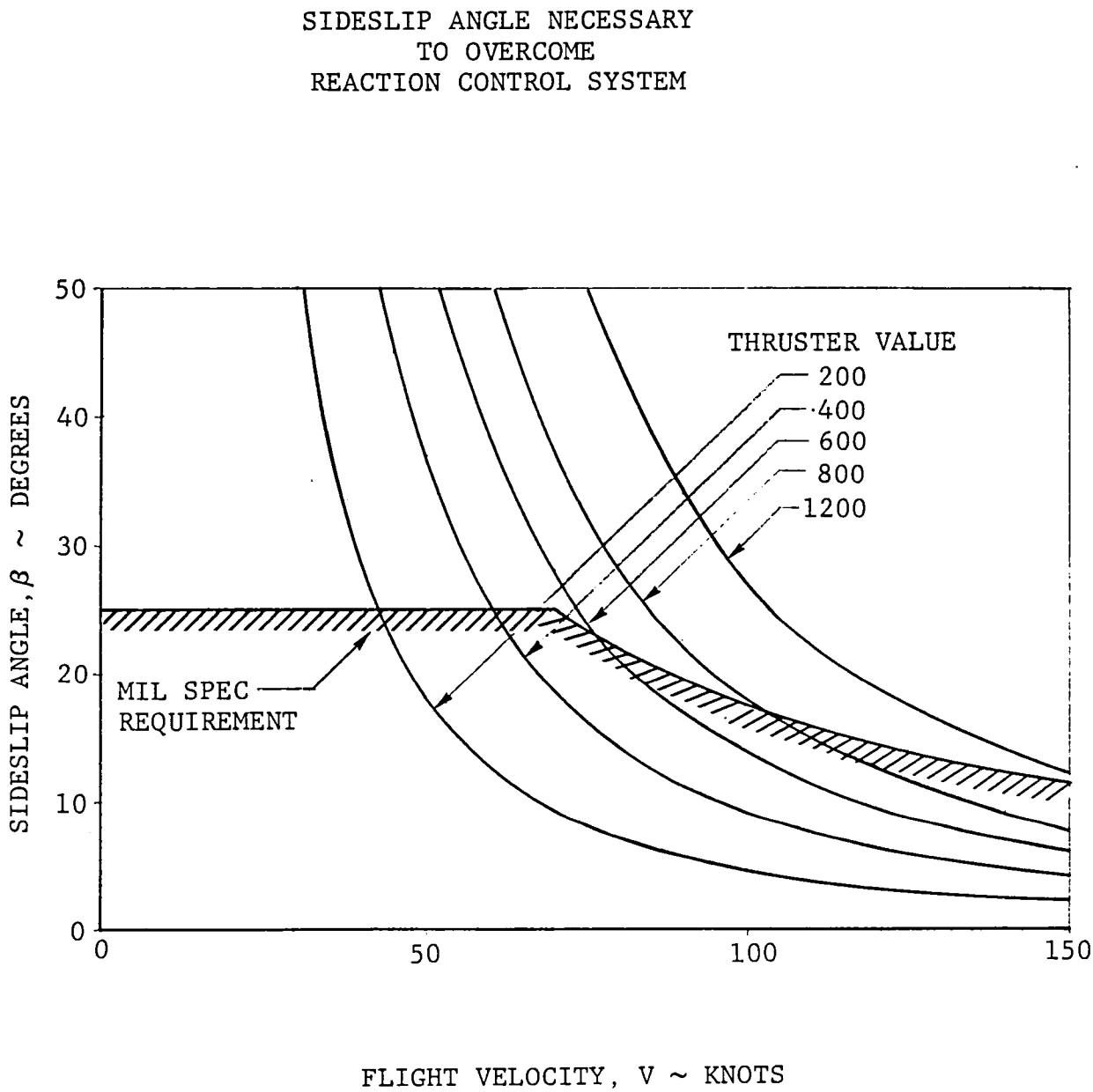

Figure 4-34 Maximum Sideslip Angle Capability Versus Airspeed for Fixed Values of Roll Thruster

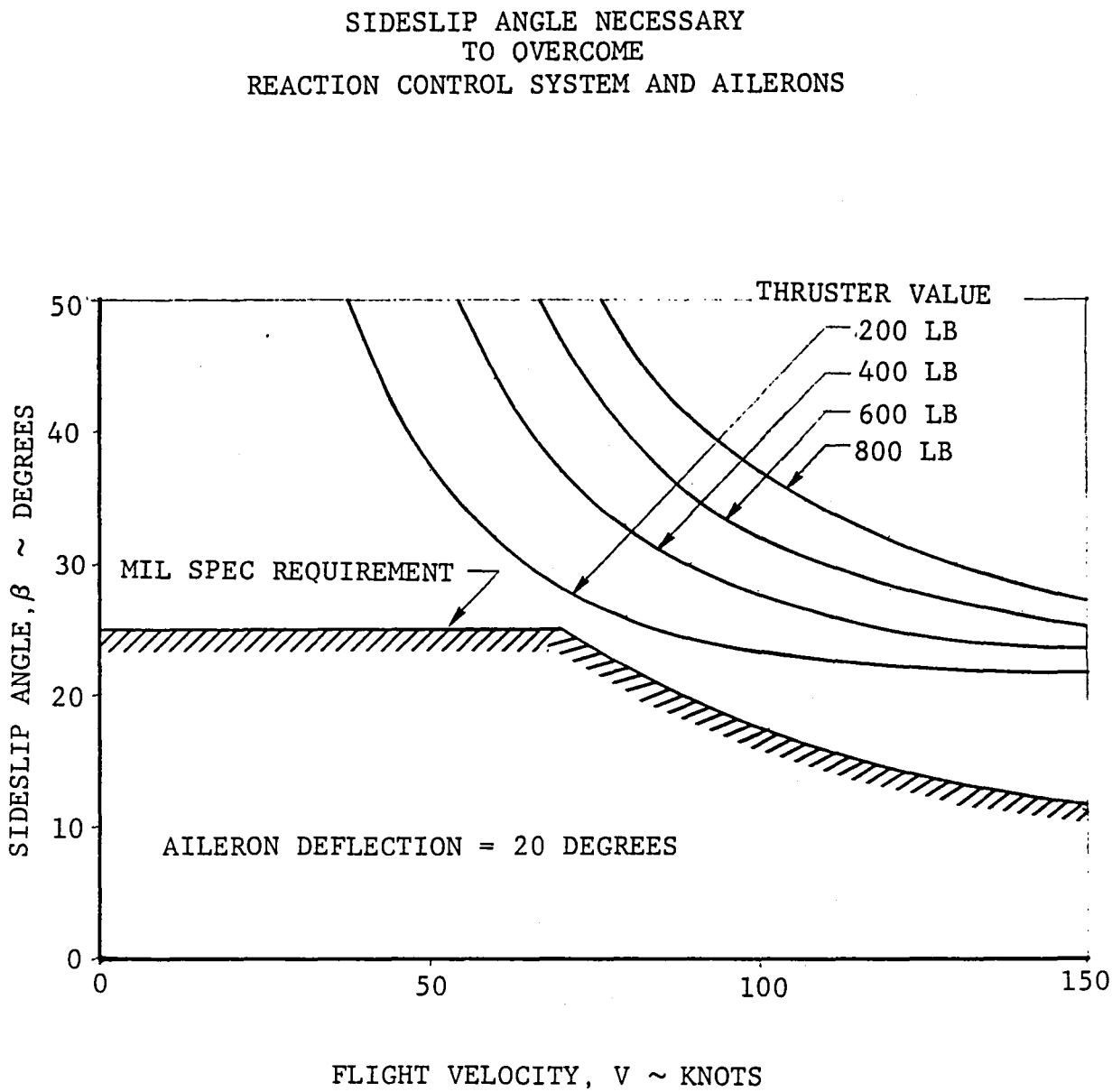

Figure 4-35 Maximum Sideslip Angle Capability Versus Airspeed for Fixed Values of Roll Thruster plus 20 degrees Aileron Deflection

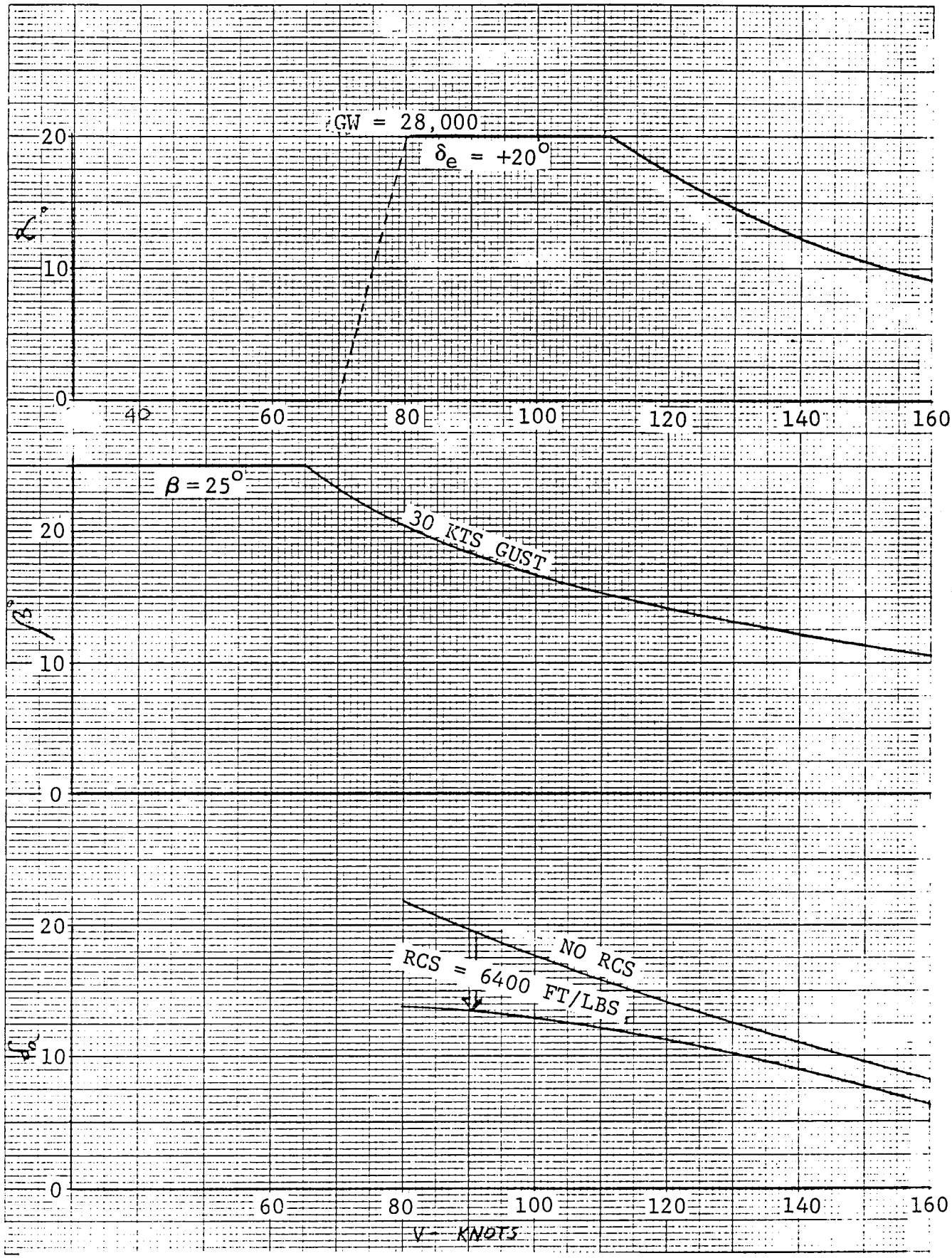

Figure 4-36 Angle of Attack, Angle of Sideslip and Aileron Deflection during Takeoff with 30 kts Sidegust

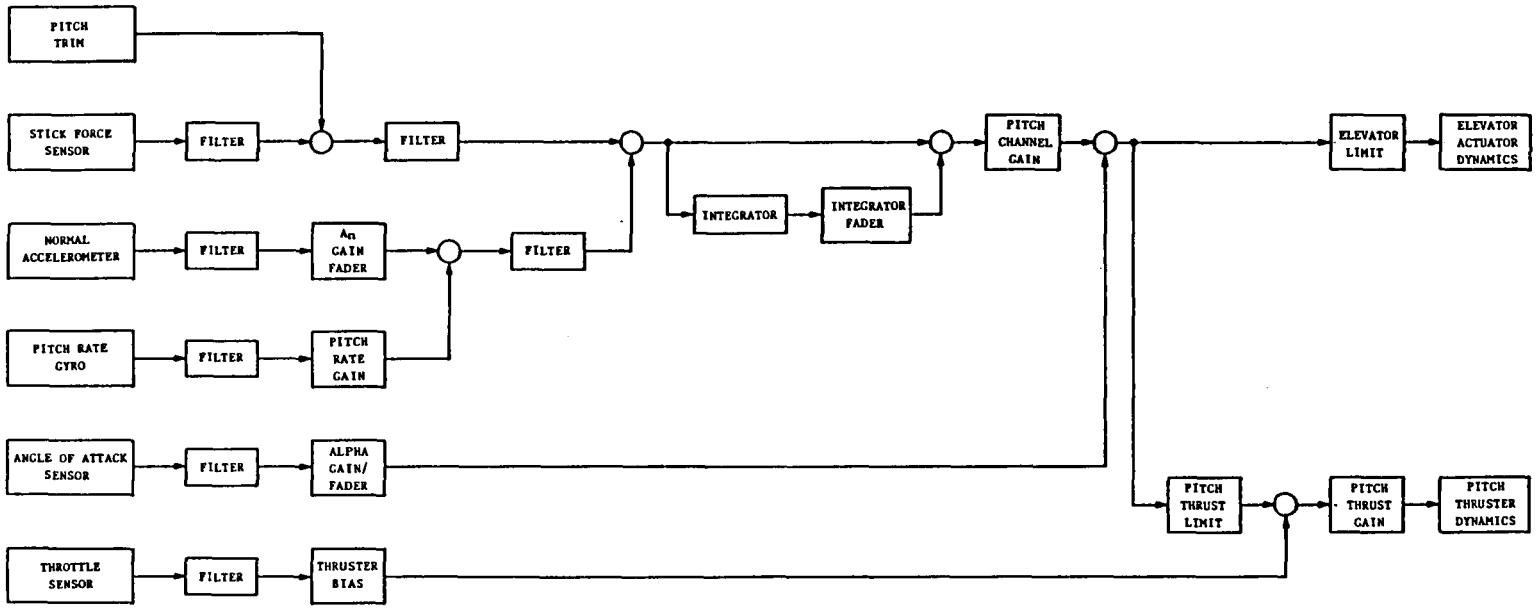

Figure 4-37 STOVL Longitudinal 3 DOF Model

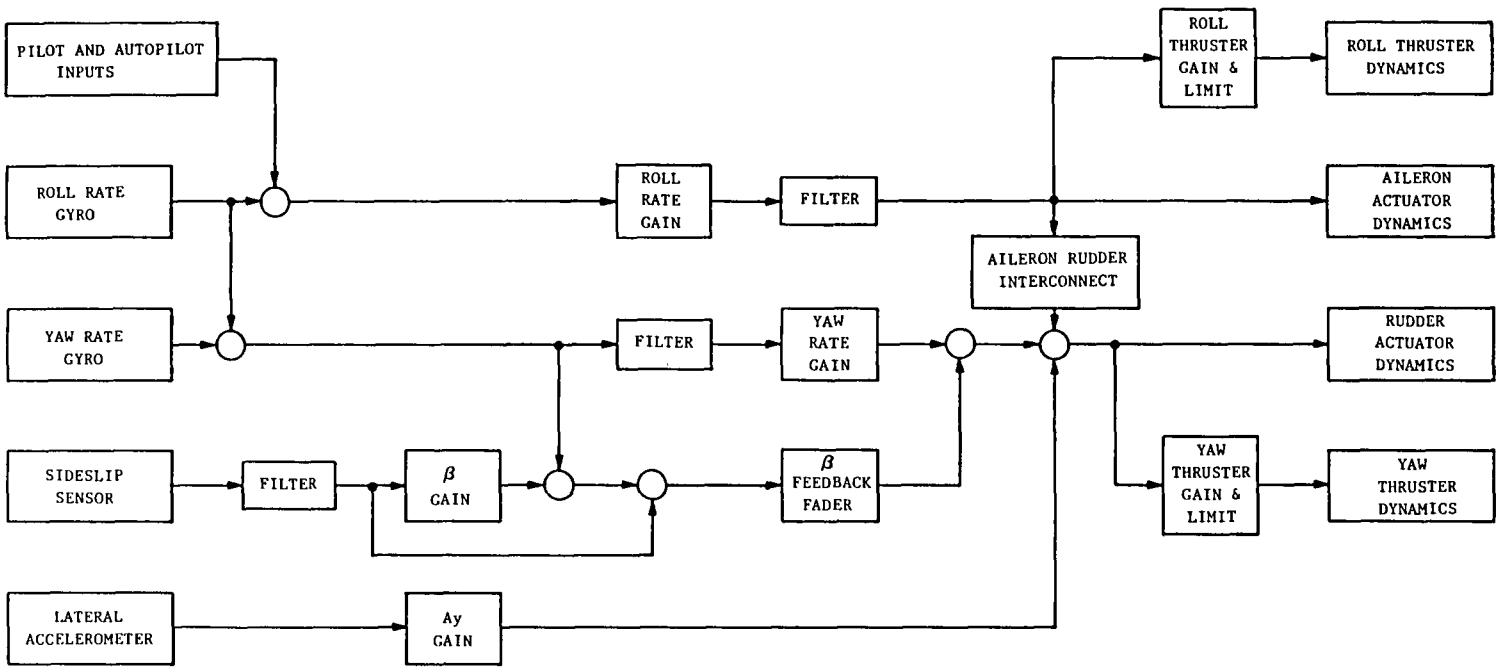

Figure 4-38 STOVL Lateral Directional 3 DOF Model

4.5 SUMMARY OF TRIMMED AERODYNAMIC CHARACTERISTICS

Trimmed lift and drag characteristics described in Section 4.1 and 4.2 are summarized in Figures 4-39 through -41.

Maximum usable trimmed lift coefficient is given as a function of Mach number in Figure 4-42. Subsonically this maximum results from limiting the angle of attack to 25 degrees, and supersonically by elevon deflection available to trim (25 degrees).

Estimated buffet characteristics are given in Figure 4-43. These are based on F-106A flight test buffet characteristics which are expressed as a function of angle of attack in Reference 28. The E-7 trimmed lift curves were used to express these buffet levels in terms of lift coefficients for E-7.

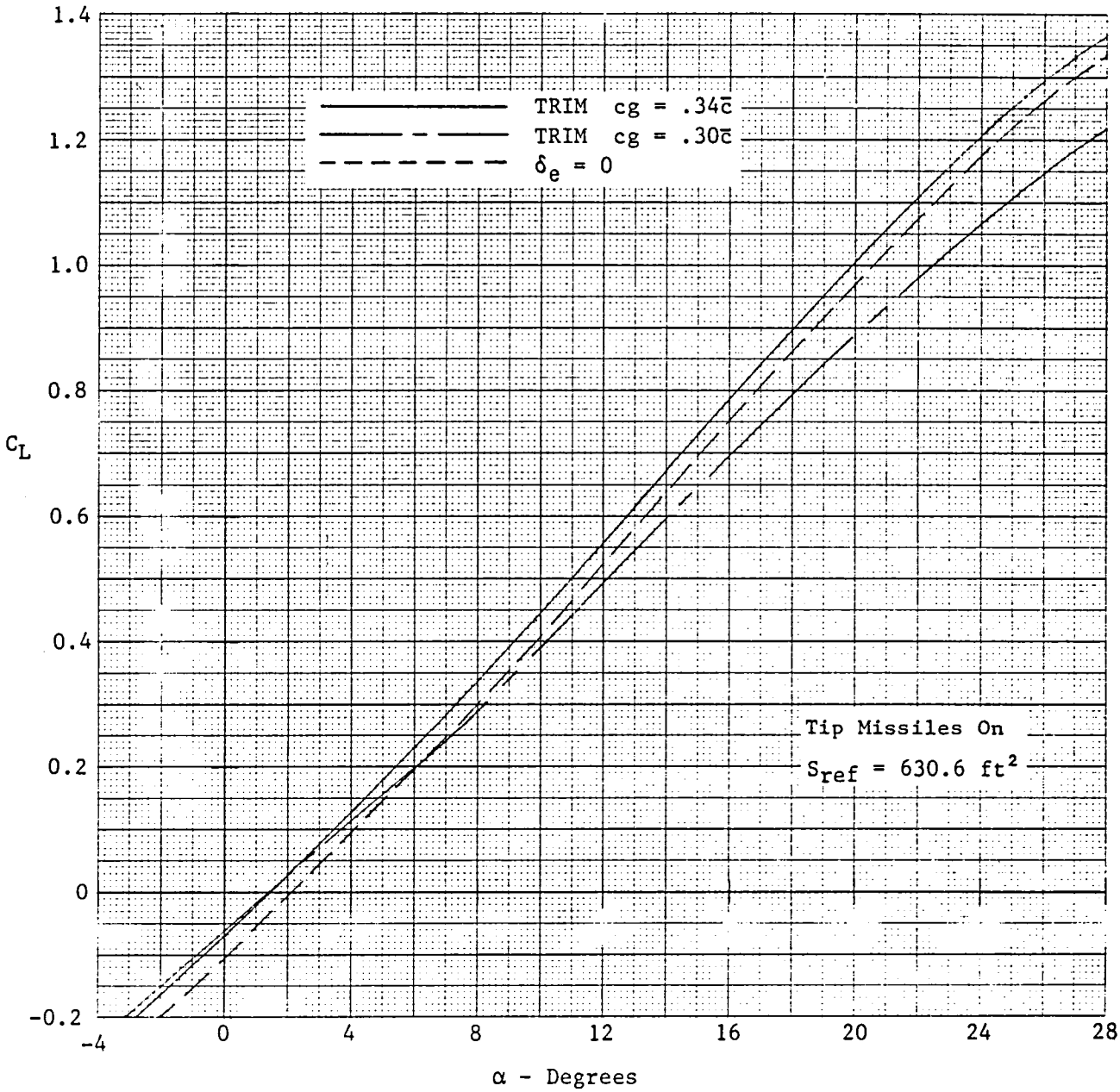

a) M = 0.6

Figure 4-39 Variation of Lift Coefficient with Angle of Attack

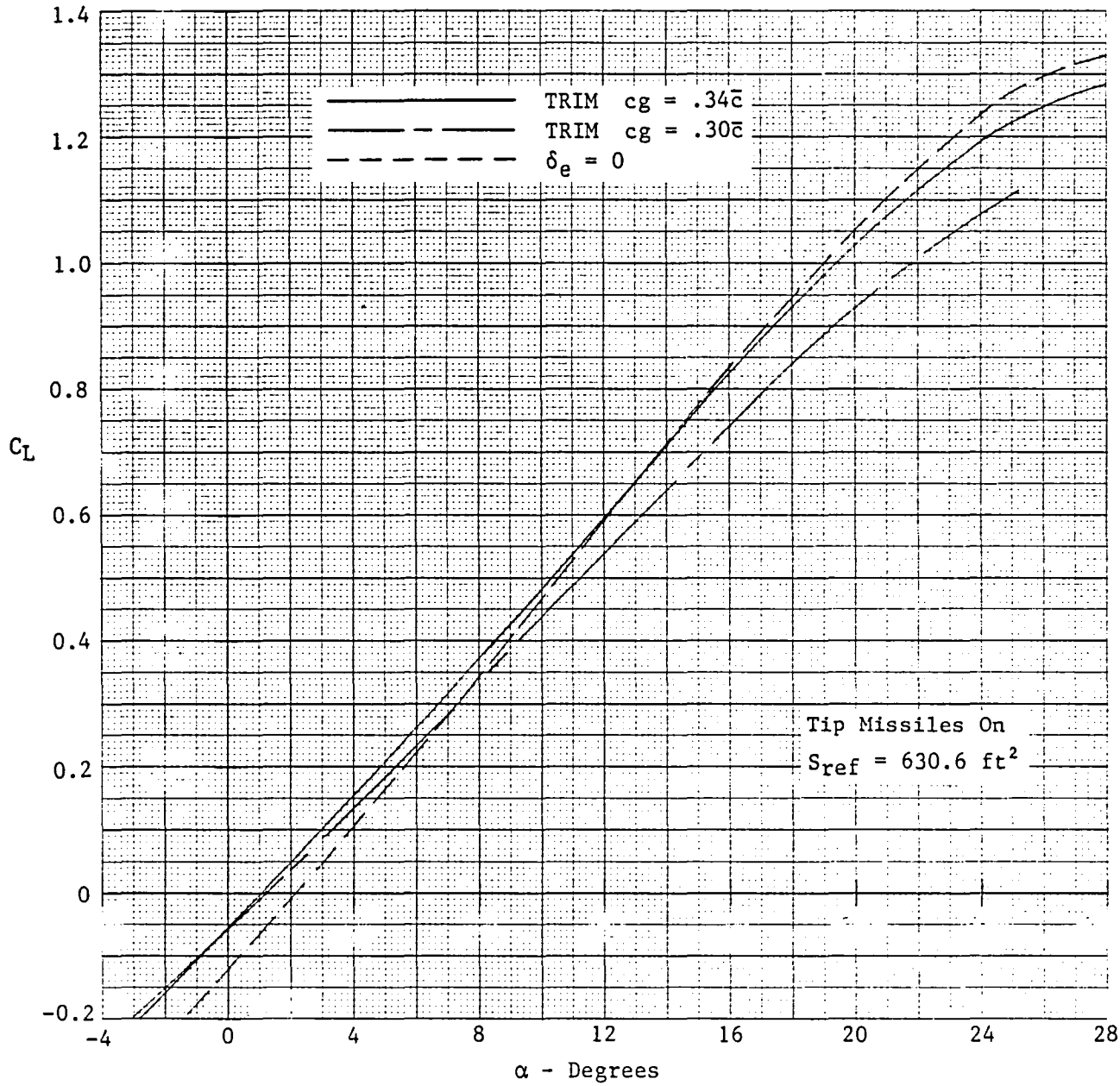

b) M = 0.9

Figure 4-39 Continued

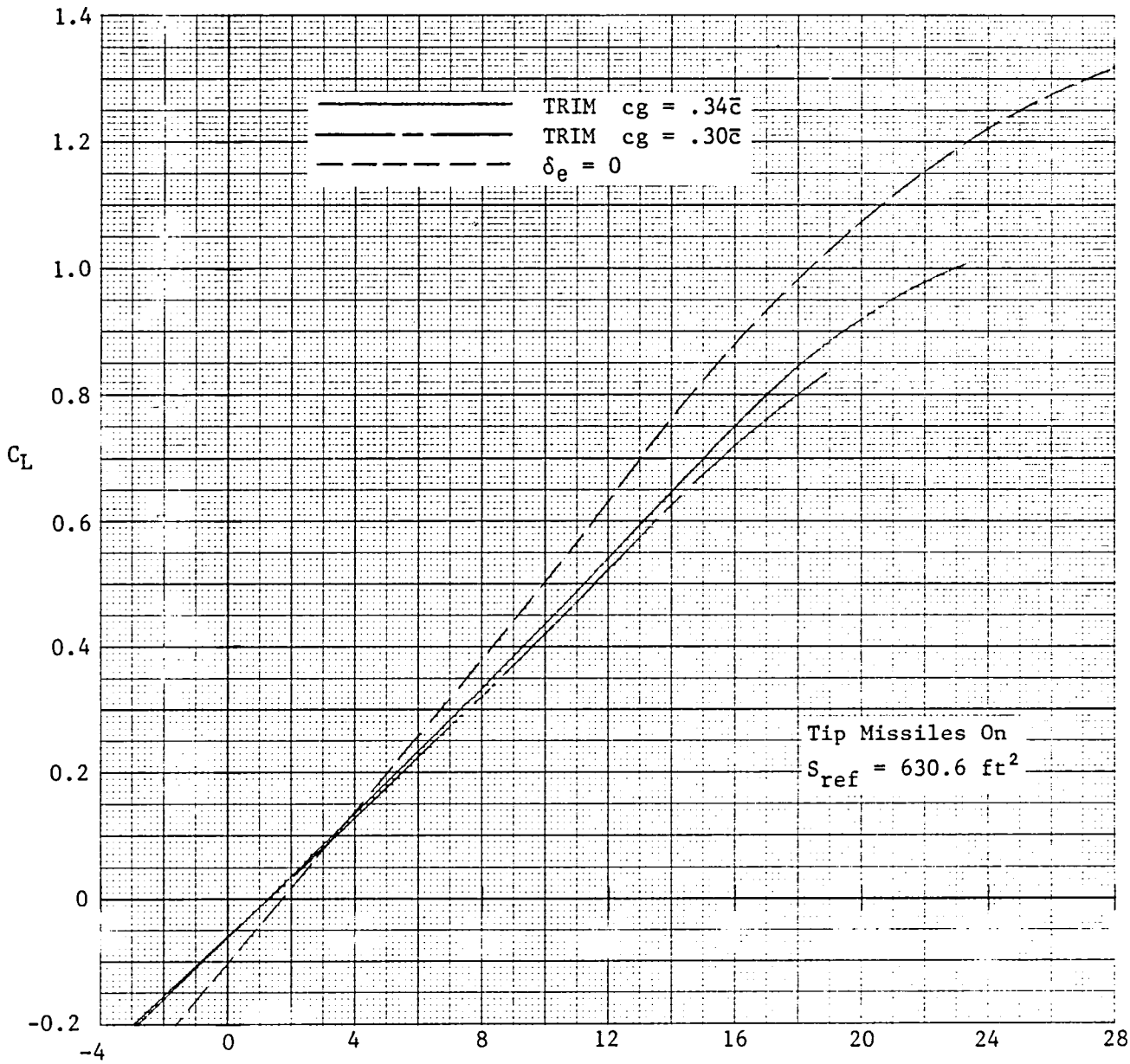

c) M = 1.2

Figure 4-39 Continued

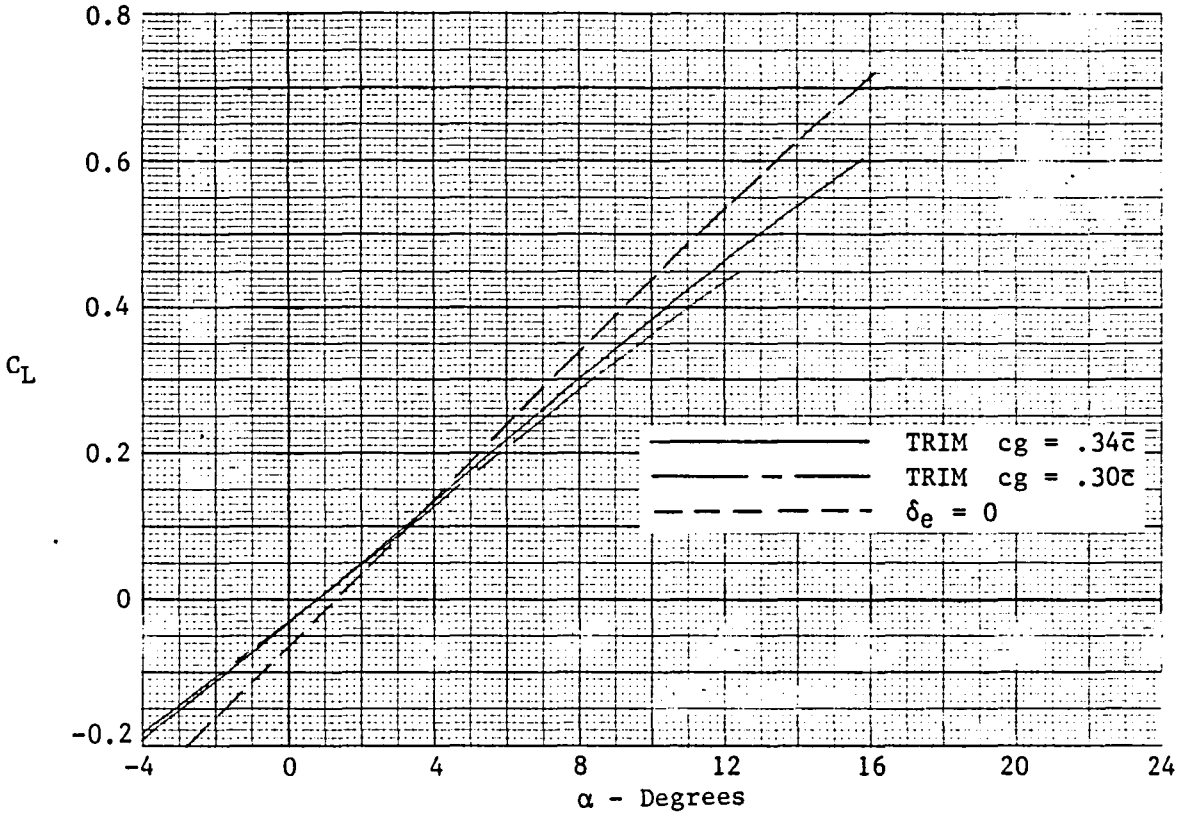

d) M = 1.6

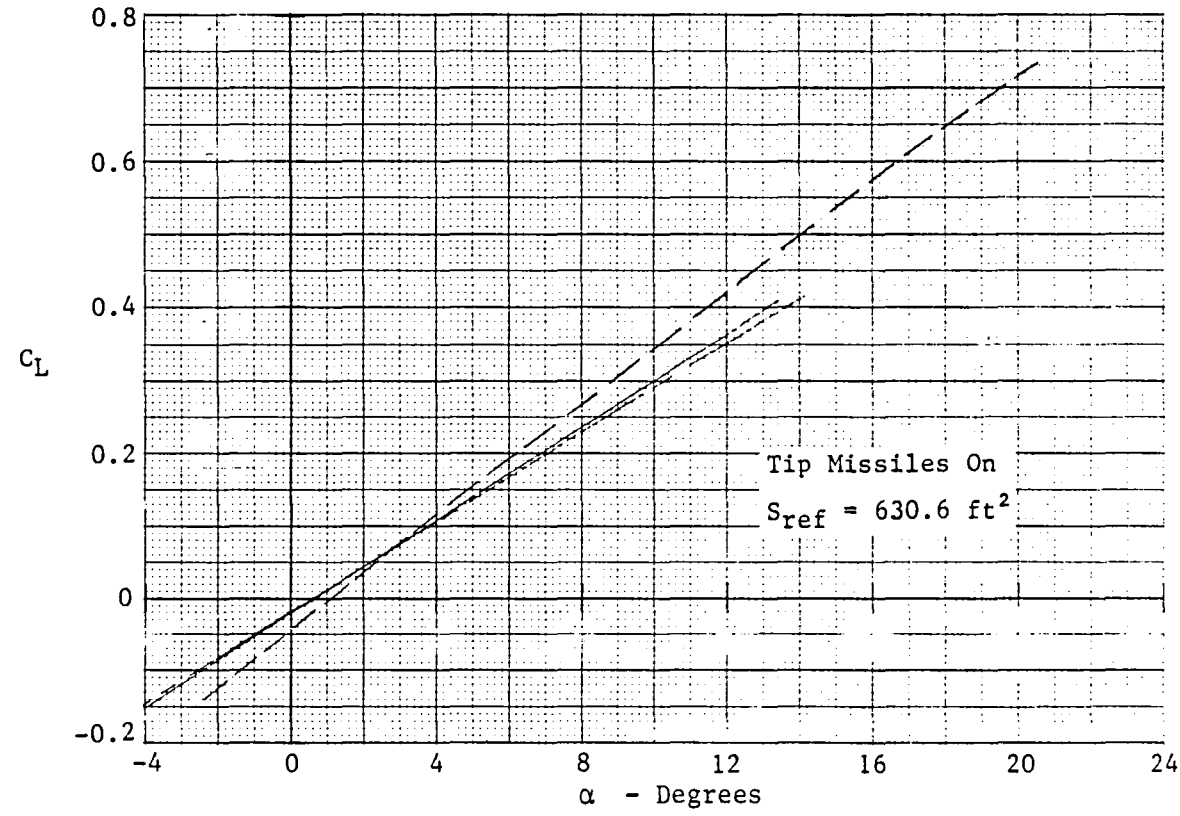

e) M = 2.0

Figure 4-39 Concluded

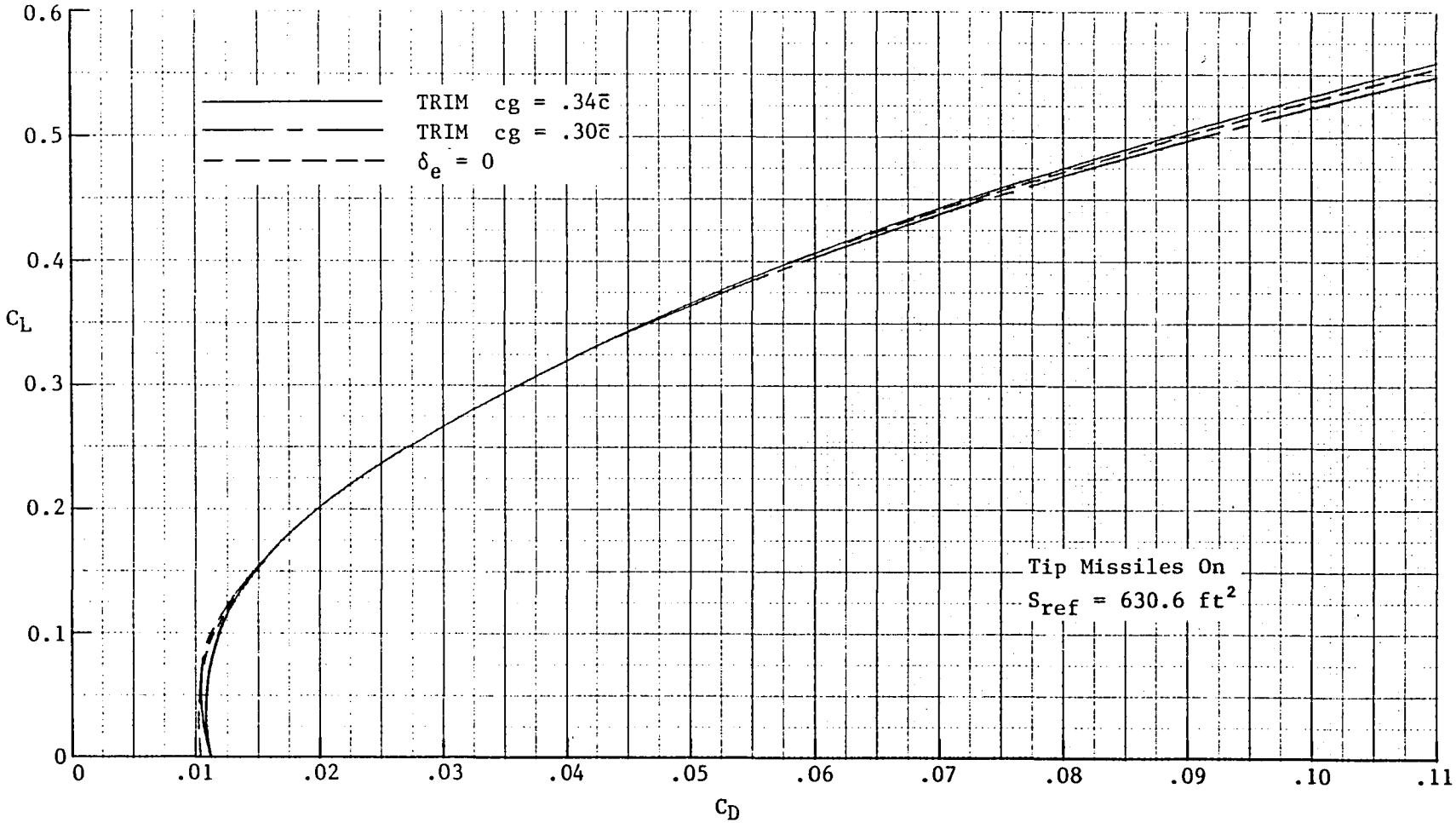

a) M = 0.6

Figure 4-40 Variation of Drag Coefficient with Lift Coefficient

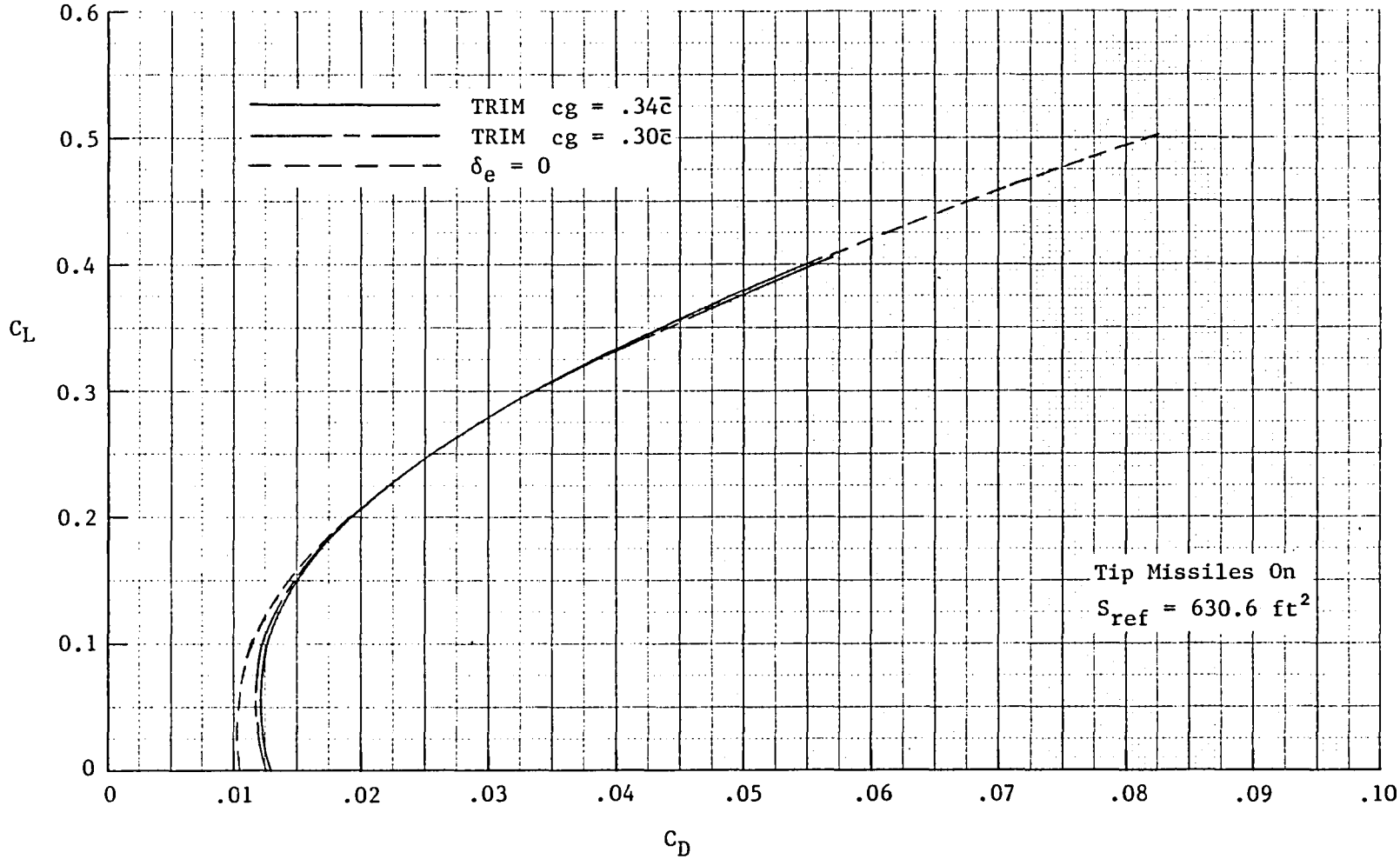

b) M = 0.9

Figure 4-40 Continued

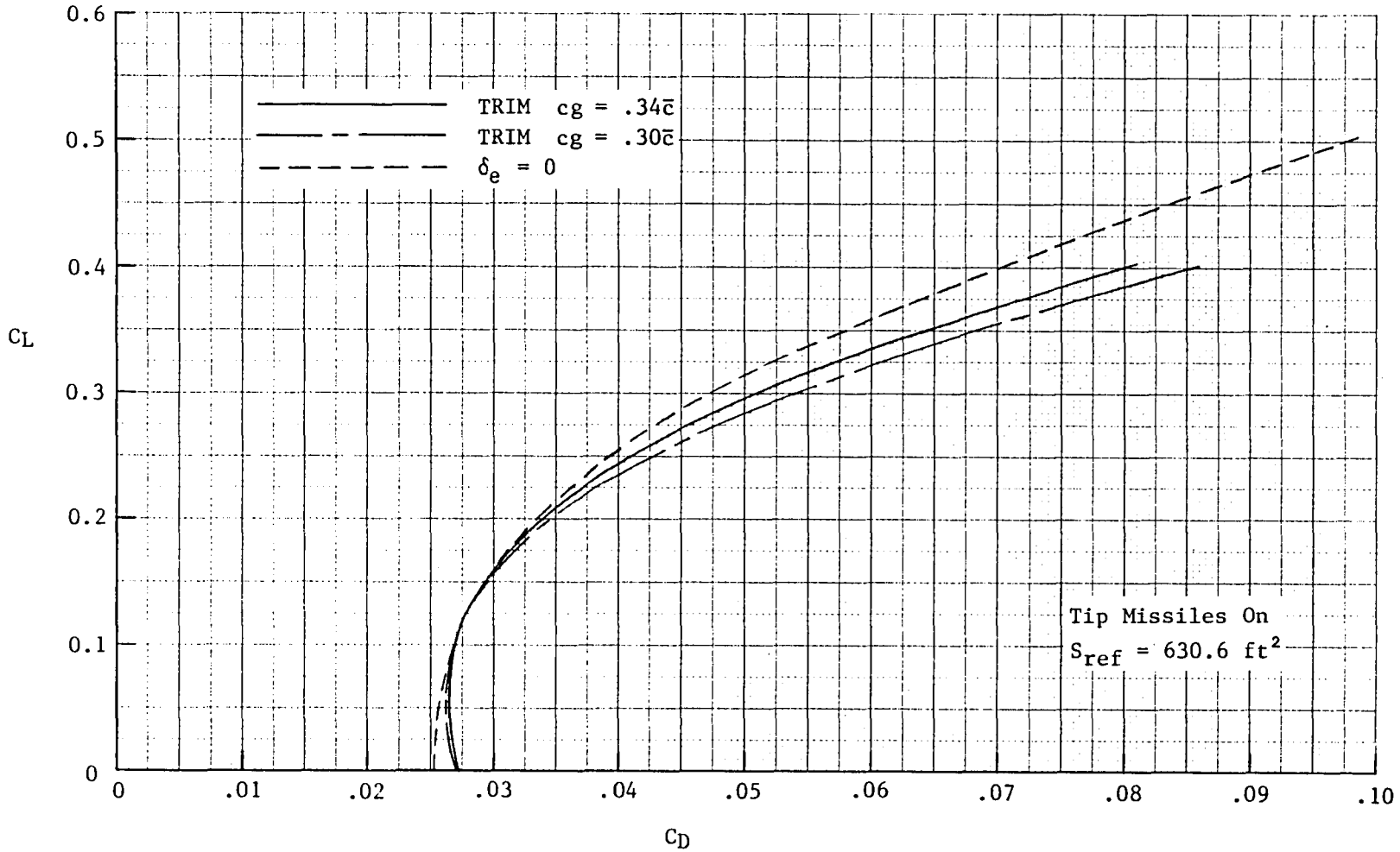

c) M = 1.2

Figure 4-40 Continued

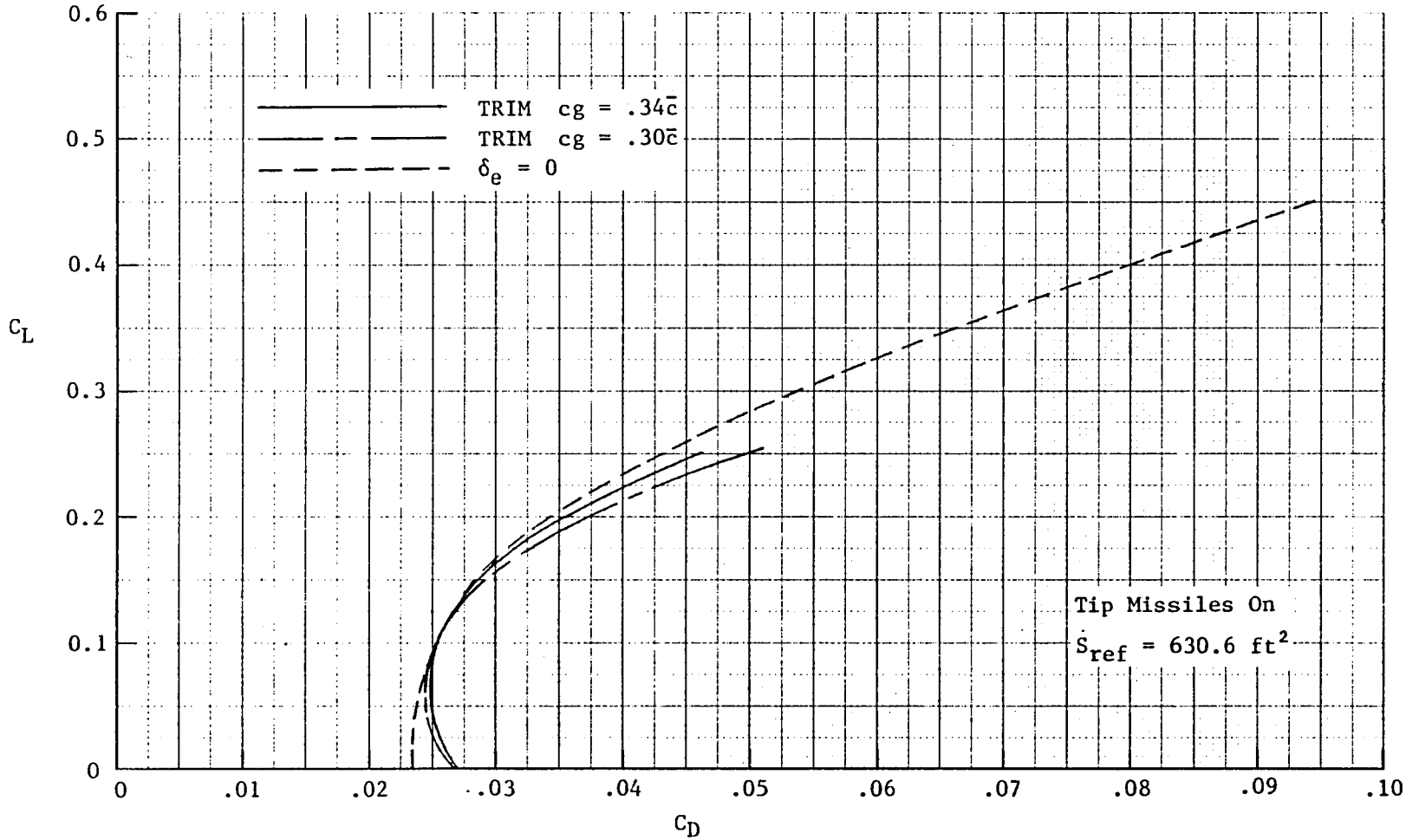

d) M = 1.6

Figure 4-40 Continued

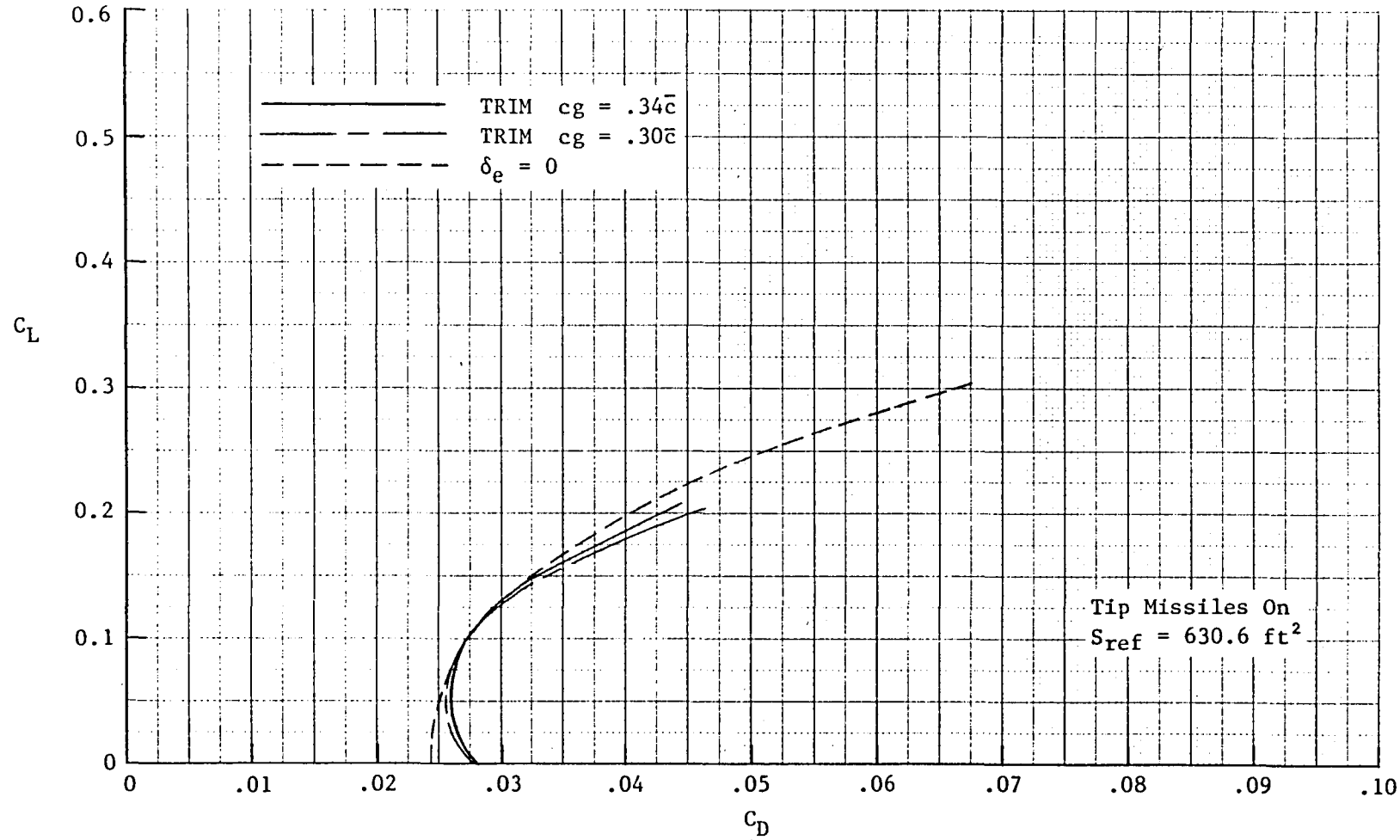

e) M = 2.0

Figure 4-40 Concluded

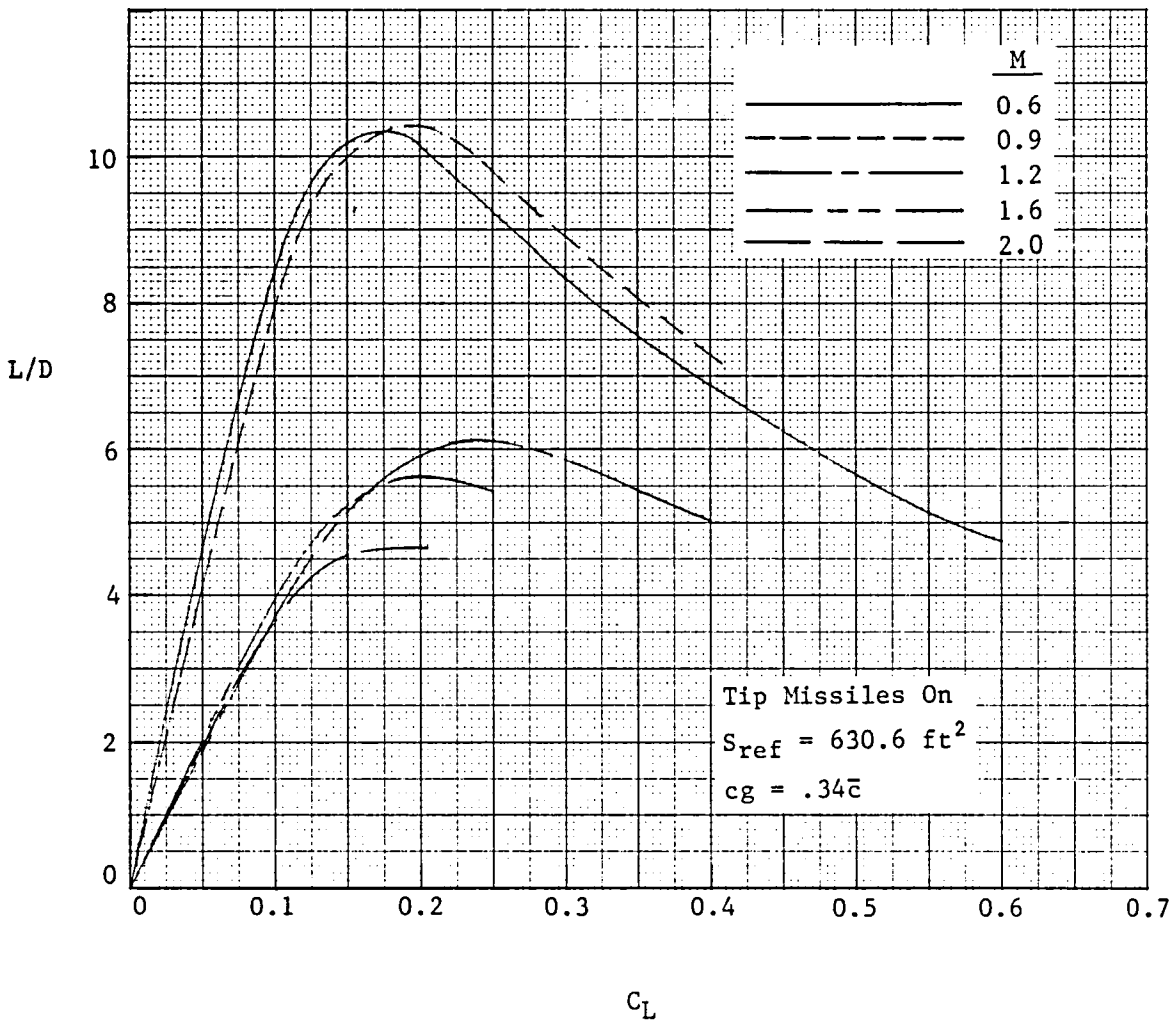

Figure 4-41 Variation of Trimmed Lift-to-Drag Ratio with Lift Coefficient

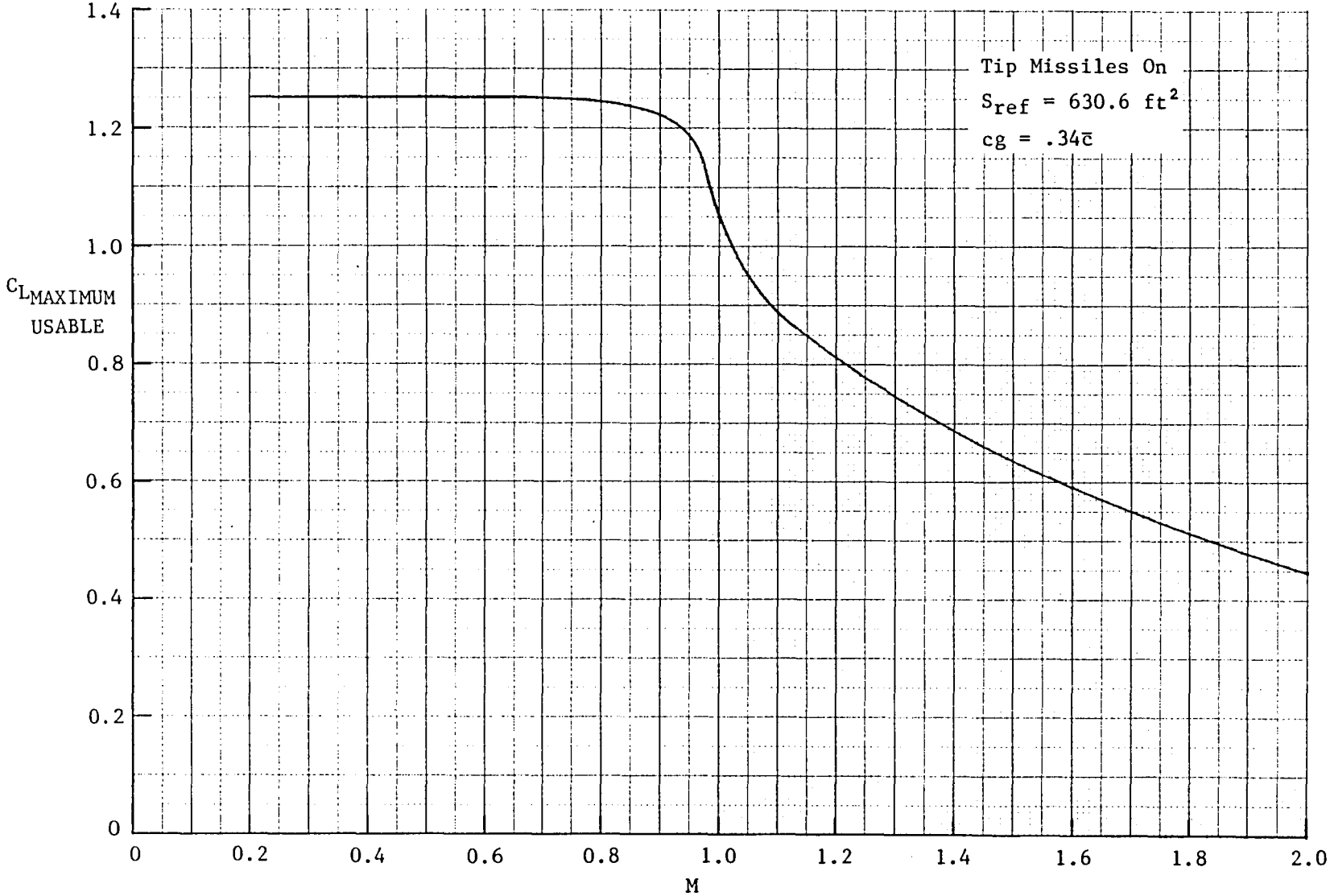

Figure 4-42 Variation of Maximum Usable Trimmed Lift Coefficient with Mach Number

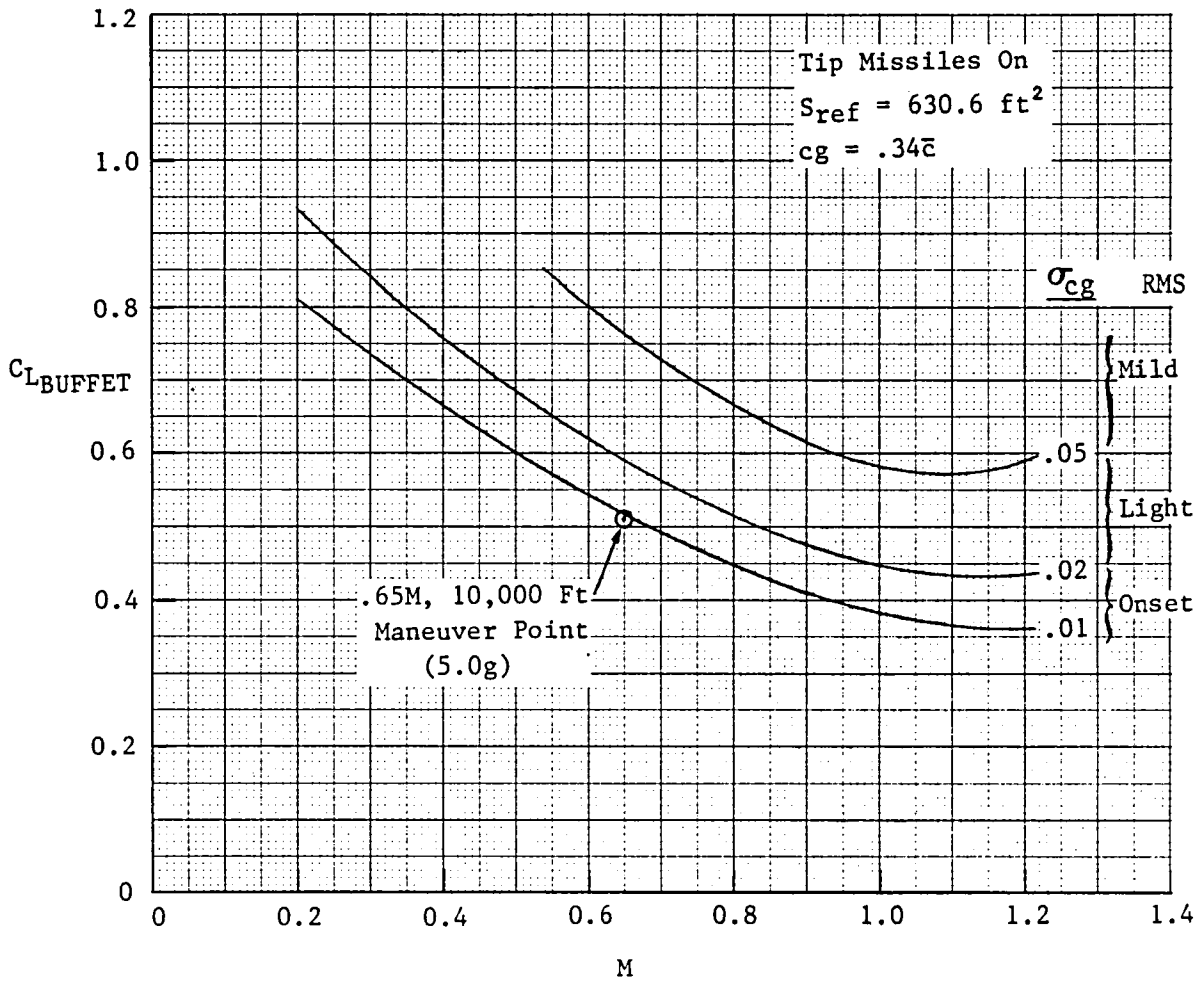

Figure 4-43 Buffet Characteristics

This Page Intentionally Left Blank

5. PROPULSION

5.1 OPERATIONAL AIRCRAFT PROPULSION SYSTEMS

5.1.1 Main Engine

The baseline powerplant is the F101/DFE engine, rated at 270 lbm/sec corrected airflow. The baseline corresponds to an engine scale factor of 1.0. Once baseline engine performance was determined, an engine scale factor of 1.09 was applied to thrusts and fuel flows, keeping engine geometry and weight constant, in order to evaluate up and away performance for the growth aircraft. The 9 percent thrust growth is possibly conservative, but is consistent with present assumptions for the near-term (1985) growth versions of the F101/DFE. However, the thrust requirement in hover for the threshold aircraft dictates an engine scale factor for hover of 1.15, which represents a reasonable growth in thrust for a fifteen year period. (Figure 5-1 presents a thrust growth history of selected U.S. gas turbine engines as percentage increase in max thrust over a baseline thrust as a function of time measured from a baseline year.) The goal aircraft requires an engine scale factor of 1.32, which is probably beyond what could be expected for normal growth.

In the demonstrator configuration, the F101/DFE engine could retain its core engine and low spool, but the afterburner duct will be removed and the bypass flow will be routed through a collector and sent either to a set of Ames/DeHavilland ejector nozzles or to an aft variable-area convergent-divergent nozzle, depending on whether the aircraft is deploying its ejectors for takeoff, transition, or hover, or whether the ejectors are stowed for up-and-away flight. For transition, the flow can be divided up in any desired ratio of ejector to aft mass flow by modulating the throat area of the aft nozzle and simultaneously throttling the flow to the ejector nozzles.

The ejectors are of the Ames/DeHavilland type, with a diffuser area ratio of 1.6 and throat-area-to-primary-nozzle-area ratio of 25.0. The most notable aspect of this type of ejector is the diffuser half angle of 6 degrees, which provides a much more stable flow than ejectors with large diffuser angles. Performance for these ejectors has been substantiated in tests at the 40- by 80- Wind Tunnel at NASA/Ames. While ejector augmentation ratios of 1.73 have been obtained, the current design assumes an augmentation of 1.63; the conservatism allows for degredations in performance which might be encountered due to design compromises in fitting the ejector to the aircraft.

The operational aircraft will require an afterburner to achieve its supersonic performance requirements. Performance calculations were based on engine thrust with a dual afterburner - both fan stream and core stream equipped with afterburning capability.

The assumed engine requirements are shown in Table 5-1; a detailed discussion can be found in Reference 5.

5.1.2 Starting System, Emergency Power, and Reaction Control System for Operational Aircraft

The operational aircraft will be equipped with a jet fuel starter (JFS) to give both a ground and air start capability. We have assumed that an F-16 type JFS will be used. The accessory gearbox will be redesigned to accommodate any increase in power extraction from the main engine for driving an RCS load compressor, as is presently envisioned.

The optimum reaction control system for both operational aircraft will require that the main engine be modified for either increased horsepower extraction or for increased high-pressure bleed extraction with minimal thrust degradation. The choice of the option to be pursued will be dictated by the engine manufacturer. Installed RCS thrust levels of 1200 lbf (threshold aircraft) and 1400 lbf (goal aircraft) are required.

Emergency power will be provided by a cartridge augmented ram air turbine similar to the system suggested in the F-16 Model 260 naval strike fighter aircraft proposal.

Table 5-1 E-7 POWERPLANT REQUIREMENTS

✔ FLIGHT DEMONSTRATOR:	PRESENT F101/DFE ENGINE (Baseline, T/W = 4.98*) + AL5512 APU	
✔ THRESHOLD OPERATIONAL:	UP-AND-AWAY	1.09 ESF
	HOVER	1.15 ESF + H.P. BLEED OR POWER EXTRACTION SUFFICIENT TO PROVIDE 1200 LBS INSTALLED R.C.S. THRUST + FAN AIR A/B + T/W = 5.72*
✔ GOAL OPERATIONAL:	UP-AND-AWAY	1.09 ESF MINIMUM
	HOVER	1.32 ESF WITH A FAN P.R. OF 4.5 + H.P. BLEED OR POWER EXTRACTION SUFFICIENT TO PROVIDE 1400 LBS INSTALLED R.C.S. THRUST + FAN A/B + T/W = 6.57*

**INT. POWER*

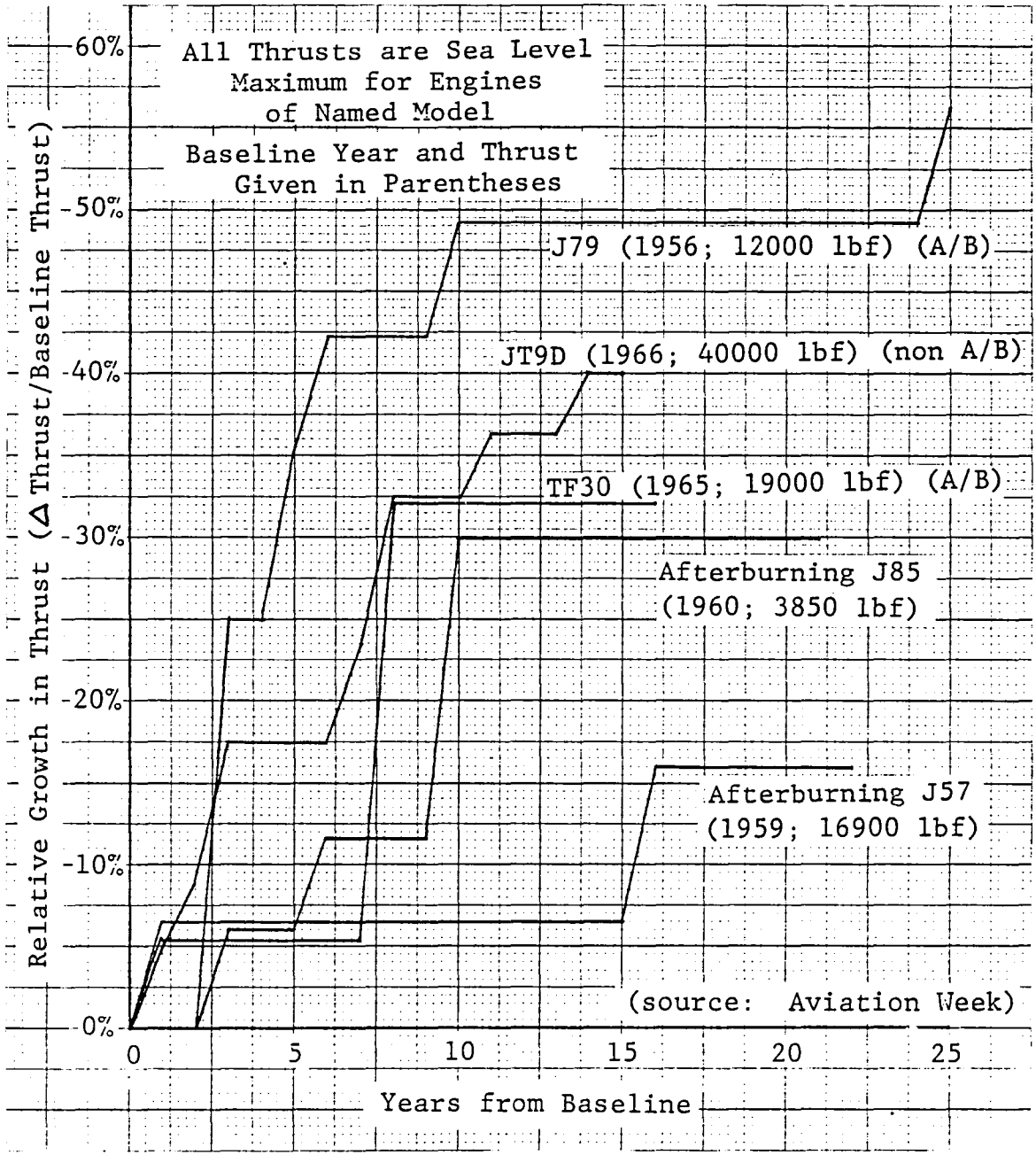

Figure 5-1 Percentage Thrust Growth of Selected U.S. Gas Turbine Engines

5.2 FLIGHT DEMONSTRATOR PROPULSION SYSTEM

5.2.1 Main Engine

The flight demonstrator aircraft propulsion system is similar in most respects to the operational aircraft propulsion system, but the main powerplant is a F101/DFE engine without any additional growth in installed thrust. The flight demonstrator will not have a supersonic flight requirement, and therefore will not require an afterburner. The aft nozzle for the bypass stream will be a fixed-area nozzle. However, the flow going to the aft nozzle during transition of the aircraft must still be modulated, and performance calculations for the fixed area aft nozzle configuration took into account the throttling loss required to match flow conditions at fan exit and nozzle exit.

5.2.2 Starting and Emergency Power

The flight demonstrator aircraft will have an air turbine starter for ground start capability only. An air turbine start system is simpler and more reliable than a jet fuel starter, although it is more dependent on ground support. The support requirements and the lack of airstart capability make this system undesirable for an operational carrier-based aircraft.

The flight demonstrator will also have a hydrazine powered emergency power unit similar to the EPU on the F-16 aircraft, which is acceptable for a non-carrier based aircraft.

5.2.3 Flight Demonstrator RCS

A detailed analysis of the reaction control system has been carried out for the flight demonstrator aircraft. Both the aircraft configuration and the technology level available for the main and RCS powerplants are better defined here than for the operational aircraft.

The basic RCS concept around which various configurations were built consisted of a central supply of high-pressure gas ducted through a junction box and thence to any combination of five RCS nozzles (one forward downward-directed for pitch control, two aft side-directed for yaw control, and two wingtip mounted downward-directed for combined pitch and roll control).

The first option considered for providing the RCS thrust was the direct utilization of main engine bleed. However, our ground rule for the RCS duty cycle is that 1050 lbf of thrust should be available continuously during the entire approach and vertical-landing sequence. The F101/DFE powerplant as installed experiences more than a 20% loss of thrust at the maximum high-pressure bleed extraction condition at tropical day conditions, which is unacceptable for maintaining hovering thrust.

The next RCS concept to be examined was the utilization of a main engine powered load compressor to provide the high-pressure gas needed for ducting around the airframe. In order to maintain a reasonable RCS nozzle size, we estimate that a nozzle pressure ratio of at least 7 is required. Unfortunately, a large penalty in power required to achieve the target thrust level is exacted for the high pressure requirement. Once all the various system losses are accounted for, we estimate that the power required to drive a load compressor to provide 1000 lbf thrust at the required nozzle pressure ratio is approximately 2400 hp. The F101/DFE has a maximum power extraction capability of 438

HP, and it is unlikely that the DFE will be uprated in power extraction capability by the required factor by the time the flight demonstrator is to be completed, so that the direct horsepower extraction approach appears to be unfeasible at this time.

The leading candidate for the RCS configuration at this time is a system consisting of a load compressor driven by a small gas turbine which also acts as an auxiliary power unit. The AVCO Lycoming AL5512 turboshaft engine can generate 4075 HP and fits into a cylinder 24 inches in diameter and 48 inches long. We presently plan to install the AL5512 above and aft of the main engine in the flight demonstrator.

6. PERFORMANCE

6.1 HOVER PERFORMANCE

The hover thrust budget for the demonstrator and operational aircraft is shown in Table 6-1. The derivation of the hover installed thrust may be found in Reference 5.

Table 6-1 HOVER THRUST BUDGET

	FLIGHT DEMO	OPERATIONAL THRESHOLD	OPERATIONAL GOAL
HOVER INSTALLED THRUST (LBF)	18939	21780	25000
RCS THRUST (LBF)	1050	1200	1400
TOTAL VERTICAL THRUST (LBF)	20139	22980	26400
MAXIMUM HOVER WEIGHT (LBF)	18939	21780	25000
ZERO FUEL WT. (LBF)	17404	19976(1)	23247(2)
MAX FUEL AVAILABLE FOR HOVER (LBF)	1435	1704	1753
HOVER TIME (Min.)	8.06	8.31	7.49

(1) INCLUDES (2) AIM-9 & (2) AMRAAM

(2) INCLUDES (2) AIM-9 PLUS 4000 LBS

6.2 PERFORMANCE - OPERATIONAL AIRCRAFT

6.2.1 Mission and Point Performance

According to the definition of the threshold and goal operational aircraft discussed in Section 1, the only difference between the two is in the area of hover performance. Thus, the up-and-away performance of the two are the same.

Point performance parameters are shown the first column of Table 6-2. The second column shows the performance calculated at 60 percent of full fuel weight in accordance with TS 169. The E-7 configuration meets or exceeds all performance thresholds. The radius for the escort mission is 217 miles greater than that required by the specification, and is a direct result of sizing to meet the interdiction mission with internal fuel. The performance values given in the third column are calculated at 88 percent VTOLGW. They have no meaning in a military sense, but are included to provide a measure of performance for comparison with NASA guidelines shown in the last column.

The 1-g flight envelope is shown on Figure 6-1, and the acceleration time histories on Figure 6-2. Figure 6-3 displays sustained load factors vs. Mach number, while Figure 6-4 shows P_S vs. load factor for 10,000 ft, 20,000 ft, and 30,000 ft altitudes. All mission and point performance were calculated using the General Dynamics MAPS computer code (Reference 29).

6.2.2 STO Performance

All STO performance was calculated using the General Dynamics MAPS, option 80, computer code (Reference 29) which is a full six degree-of-freedom routine. The takeoff performance in 400 ft, zero wind is shown in Figure 6-5. The escort weight can become airborne with a 400 ft roll, while at interdiction weight the aircraft would require a 6-degree NAEC (Reference 30) ramp. The escort trajectory and time histories are shown in Figures 6-6, while those for the interdiction, 6-degree ski-jump, are shown in Figures 6-7. The sequence of events and control rates assumed are shown below.

SEA LEVEL, TROPICAL

CONTROLS	RANGE	RATE
Elevon Deflection:	$-20^o \leq \delta_e \leq 20^o$	at 60 deg/sec
ADEN vectoring:	$0 \leq \delta_n \leq 90^o$	at 90 deg/sec
Mass Split Factor:	$0 \leq k \leq 1$	at 1.33/sec
Tail A/B control:	off to on	at 1/sec

SEGMENT	DESCRIPTION
1.	From beginning of deck, accelerate with both A/B's, $\delta_e = \delta_n = 0$, $k = 1$, until airspeed is 15 kts $> V_{stall}$
2.	Initiate rotation. Set k to constant. Fan A/B cuts out. Use k and δ_n to pitch up to $\theta = 19.5^o$. Maintain until 40 ft from end of deck (use δ_n to prevent overrotation)

3. Stop rotation and fly away. $\delta_e = 10^o$. Use δ_n to maintain $\theta = 19.5^o$. Begin transition at t = 10 sec.

4. Start transition. Begin cutting off ejector flow $\delta_e = 10^o$. Use δ_n to maintain $\theta = 20^o$.

5. Continue transition. Continue shutting off ejector. $\delta_n = 0$. Trim with δ_e until k = 1.

6. Fly away. Relight A/B as desired, close ejector doors, retract gear.

While not a part of the present conceptual study, it must be mentioned that the aircraft will require an integrated flight/propulsion system and, probably, a microprocessor to assist the pilot in takeoff. For instance, pitch can be controlled five separate ways when using powered lift (ejector, core vector, elevon, and both pitch and roll RCS). The number of control variables, and the speed with which they must be varied, represent an unacceptable pilot workload in a pure direct-control flight mode.

Figures 6-8 through -10 show the effect of ski jump, deck length, and wind on STO weight; these figures are intended to show the overload potential of the aircraft, and so 10 foot sink over bow (10 foot sink from apogee for the ski-jump cases) are shown.

Table 6-2 POINT PERFORMANCE

	NOTE 1	NOTE 2	NOTE 3	NOTE 4
PT. PERFORMANCE WEIGHT	25267	27341	19228	19228
ESCORT MISSION				
FUEL (Lb)	9657	12275		
TOGW (Lb)	30130	32251		
RADIUS (N.Mi)	400	617		
INTERDICTION MISSION				
FUEL (Lb)		12275		
TOGW (Lb)		35522		
RADIUS (N.Mi)		551		
MAXIMUM MACH				
35 KFT, MAX THRUST	1.73	1.73	1.73	1.6
10 KFT, INT. THRUST	1.02	1.02	1.02	
COMBAT CEILING, INT. THRUST		45200		
LEVEL FLIGHT ACCEL @ 35 KFT				
M .8 TO 1.2	35	37	25	
M .8 TO 1.6	85	88	62	
TURN LOAD FACTOR				
M .60, 10 KFT			6.9	6.2
M .65, 10 KFT	5.5	5.3	7.6	
P_S @ 1 g, M .9, 10 KFT	777	747	1059	900
SPECIFIC RANGE (NMI/LB)				
ESCORT – 60% FUEL	.182	.175		
INTERDICTION – WITH STORES – 85% FUEL	.140	.143		
W/O STORES – 70% FUEL	.218	.213		

NOTES: (1) PT. PERF. @ 60' ESCORT FUEL WT. (2) PT. PERF. @ 60°, FULL FUEL WT. (3) PT. PERF. @ 88°, VTOL WT. (4) NASA GUIDELINES

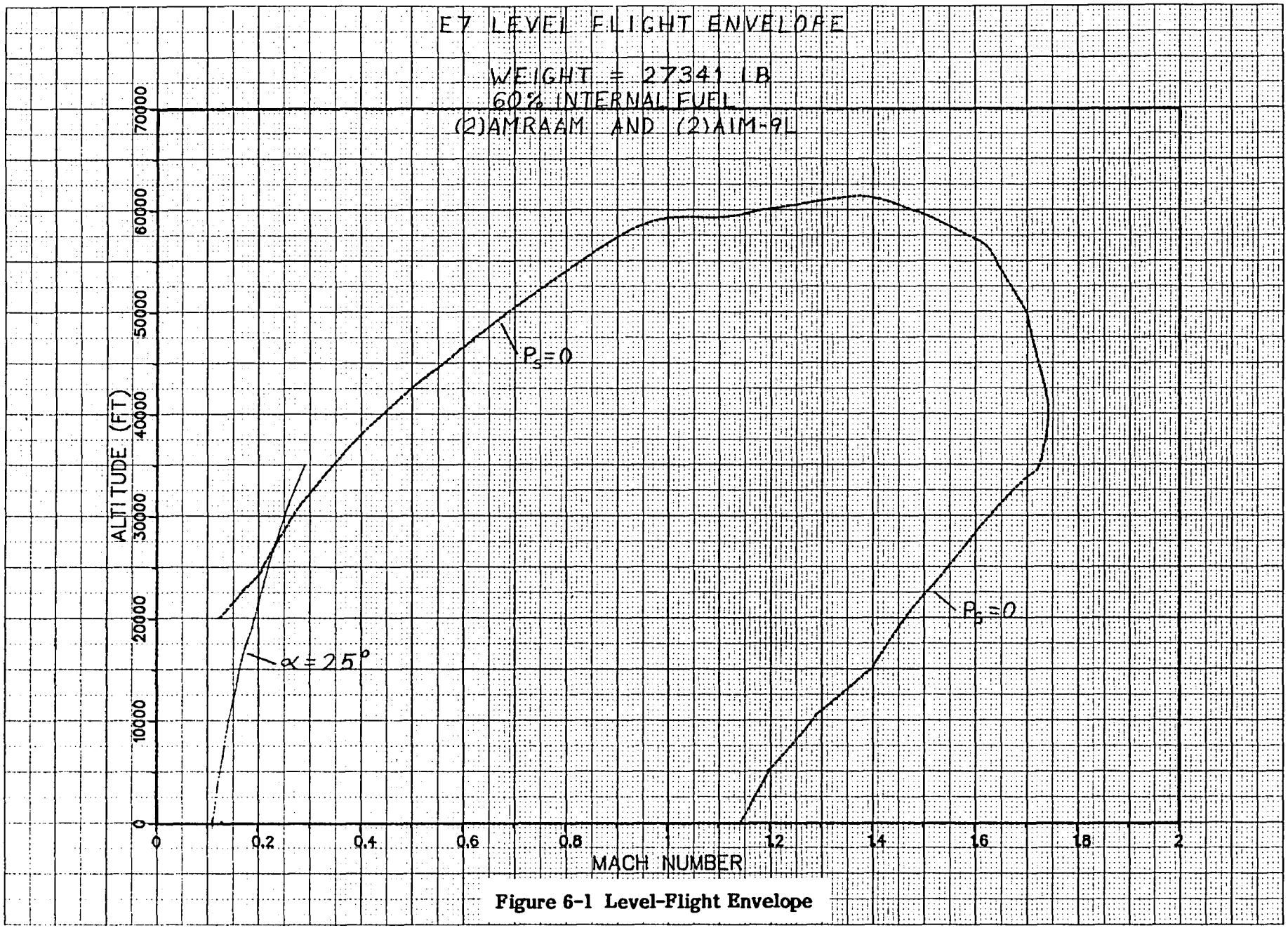

Figure 6-1 Level-Flight Envelope

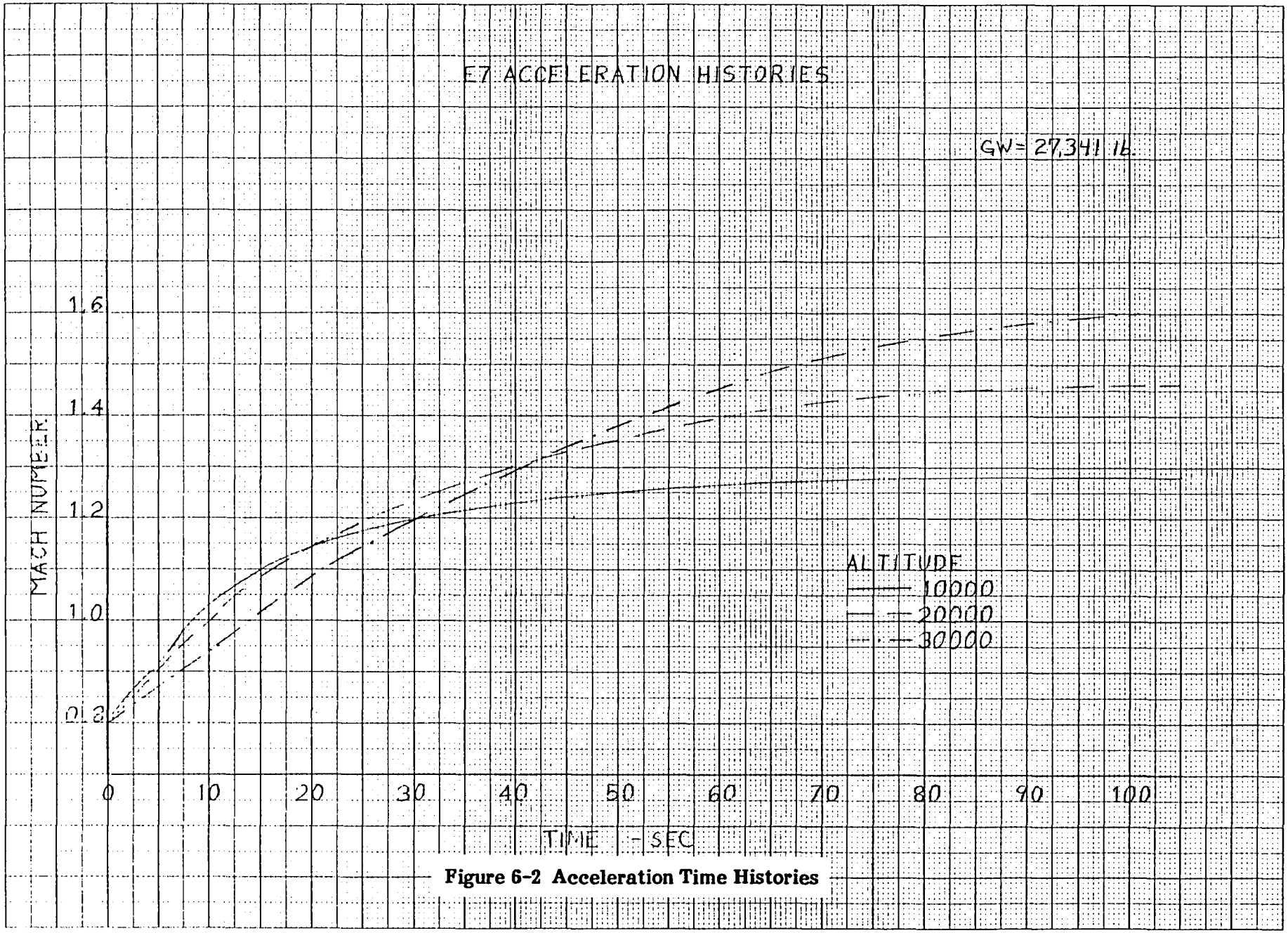

Figure 6-2 Acceleration Time Histories

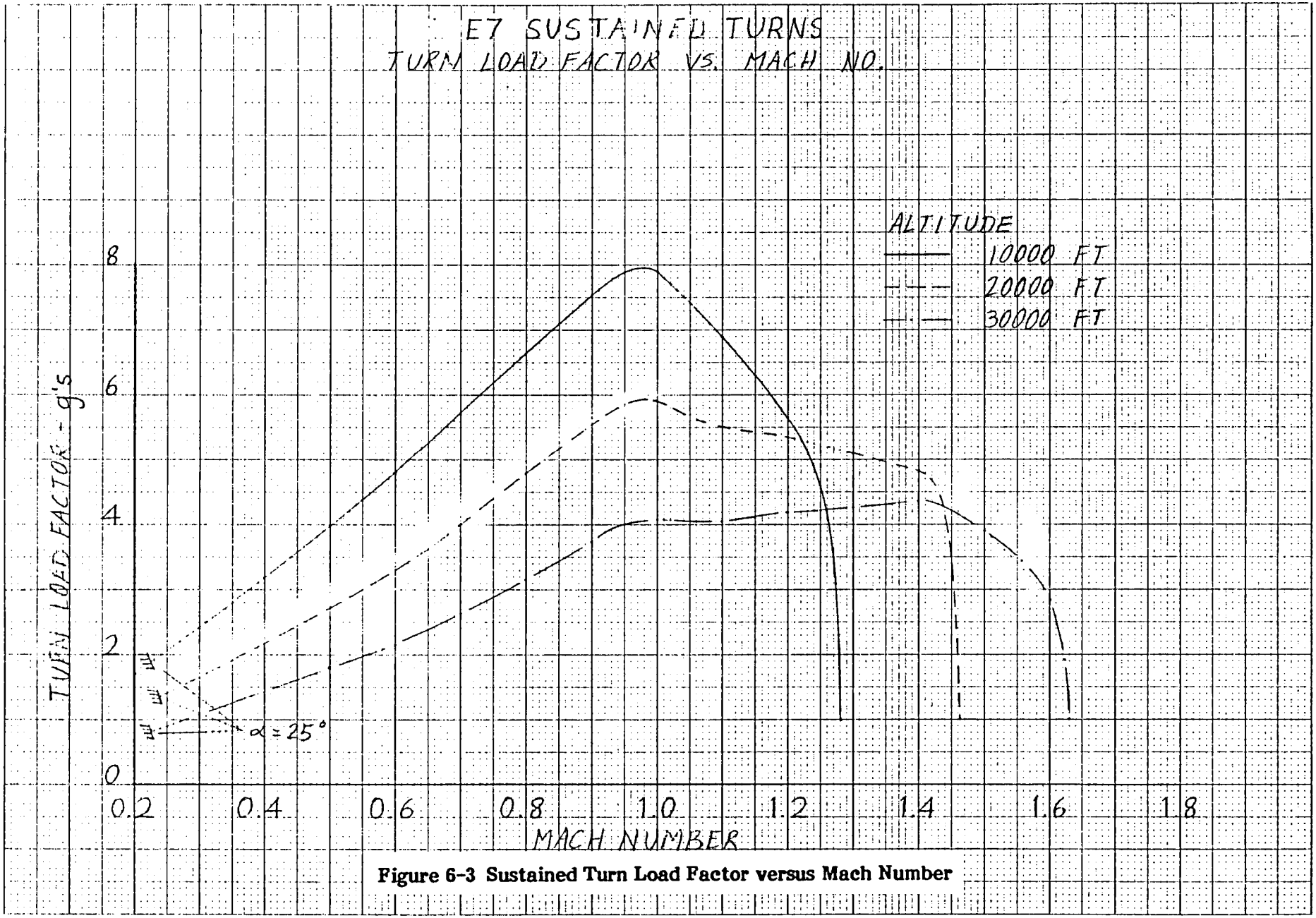

Figure 6-3 Sustained Turn Load Factor versus Mach Number

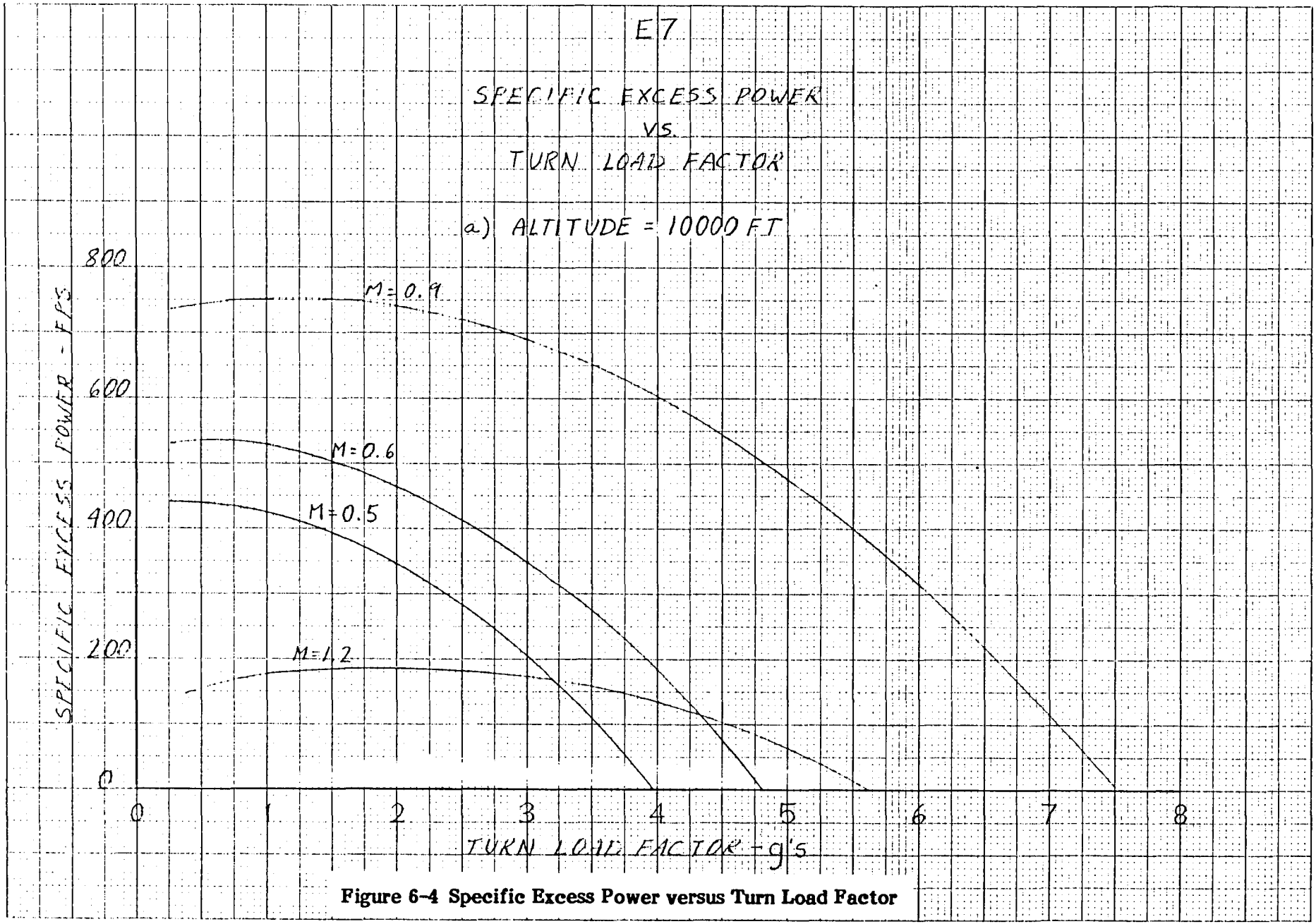

Figure 6-4 Specific Excess Power versus Turn Load Factor

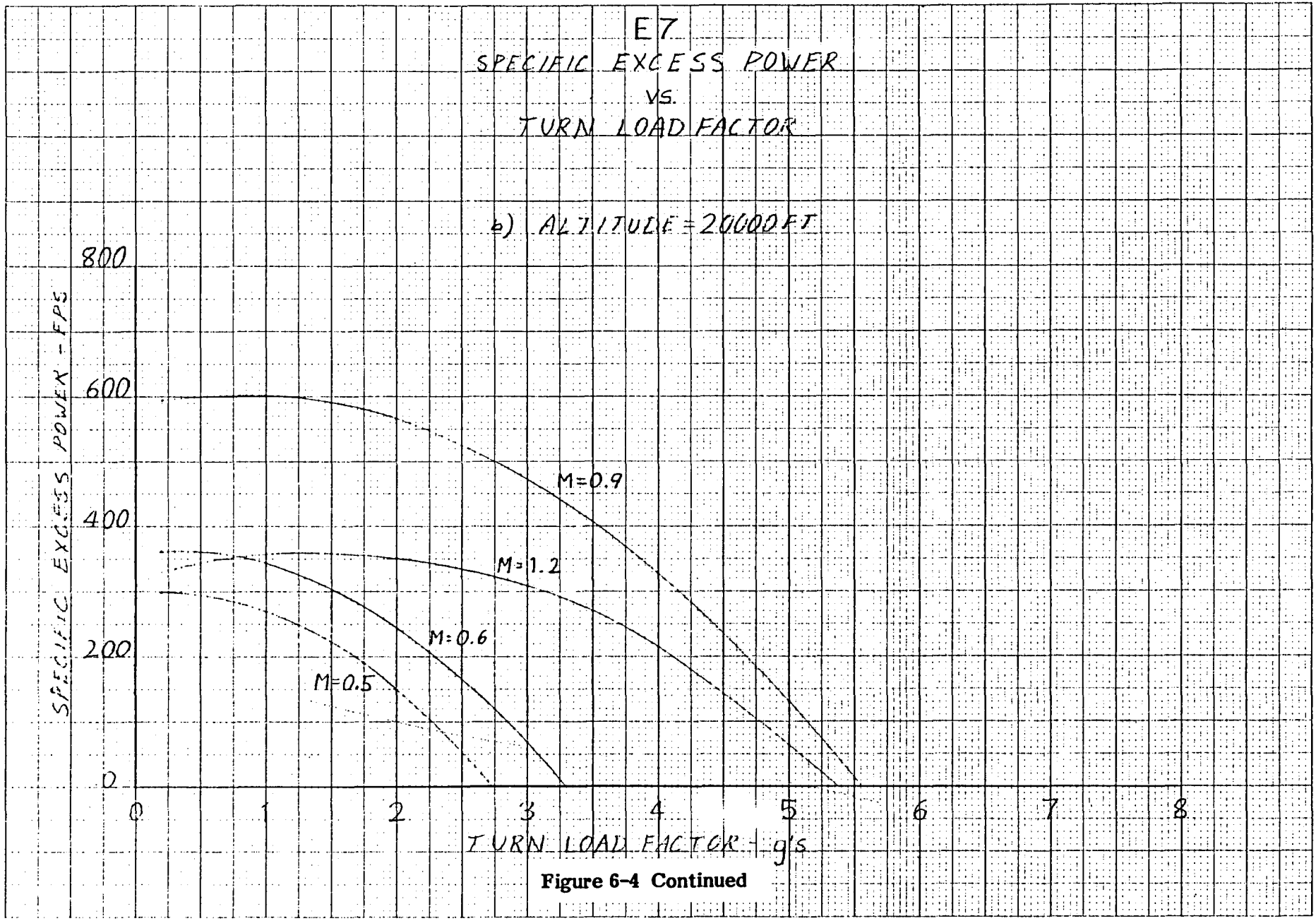

Figure 6-4 Continued

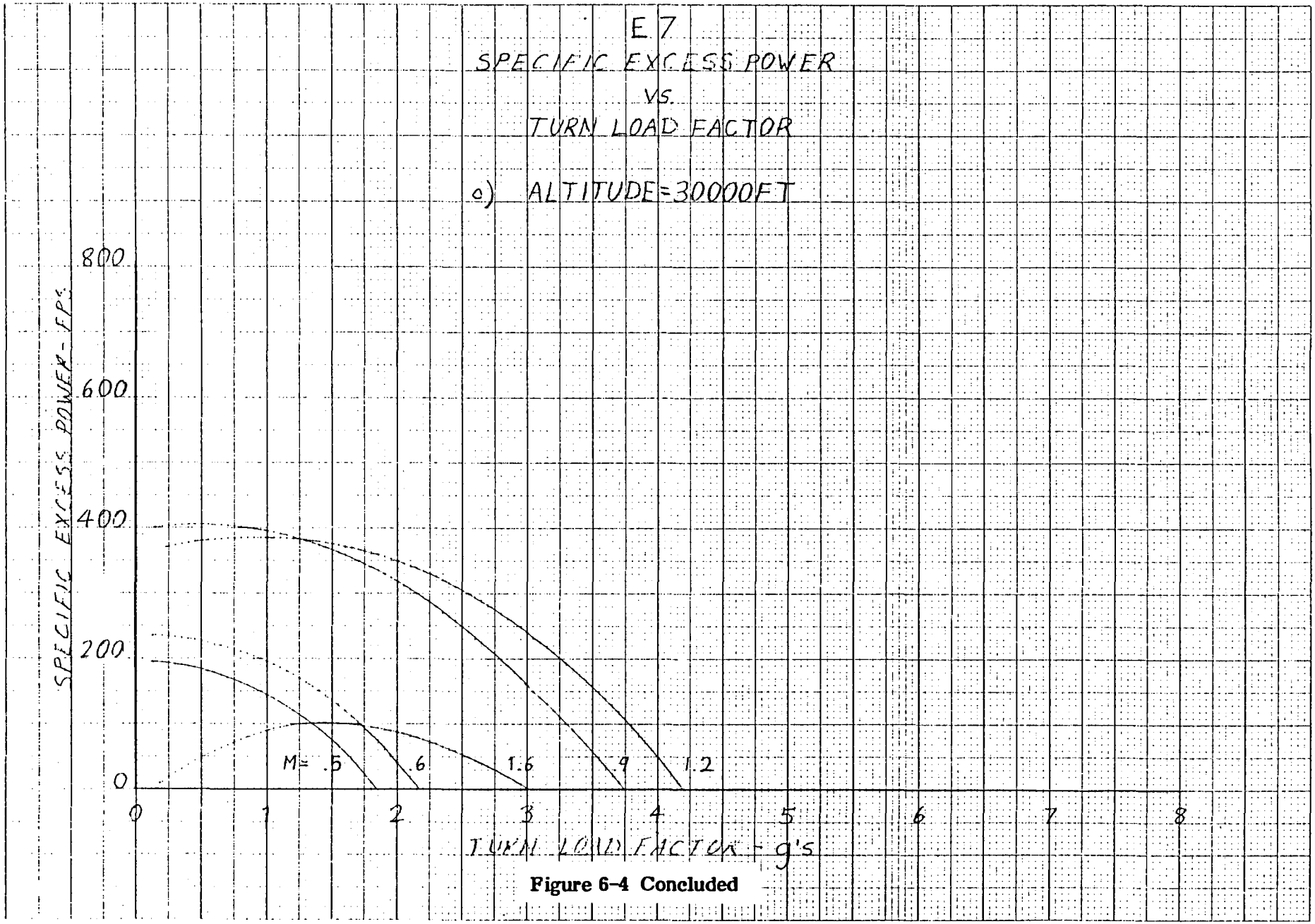

Figure 6-4 Concluded

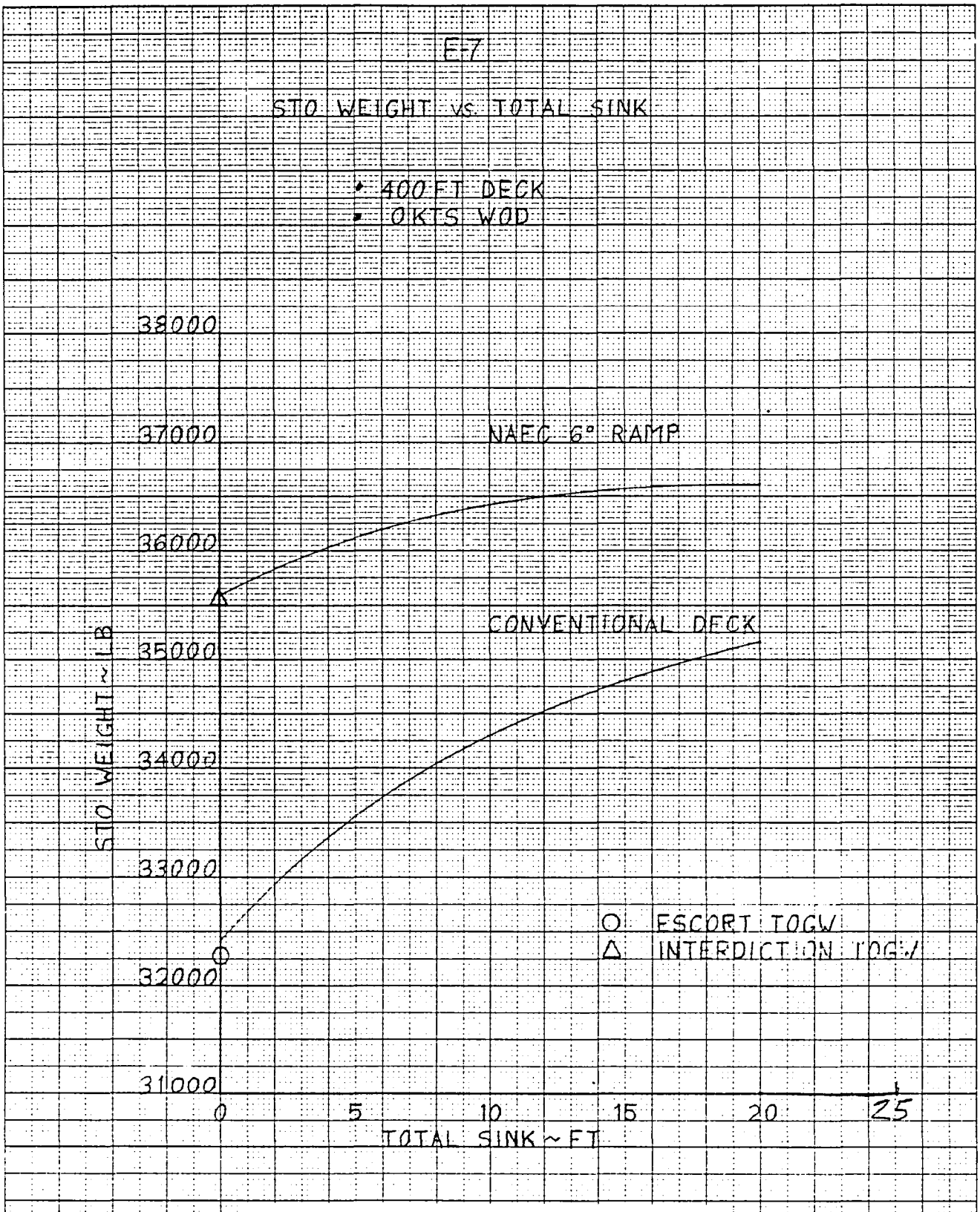

Figure 6-5 STO Weight versus Sink Over Bow

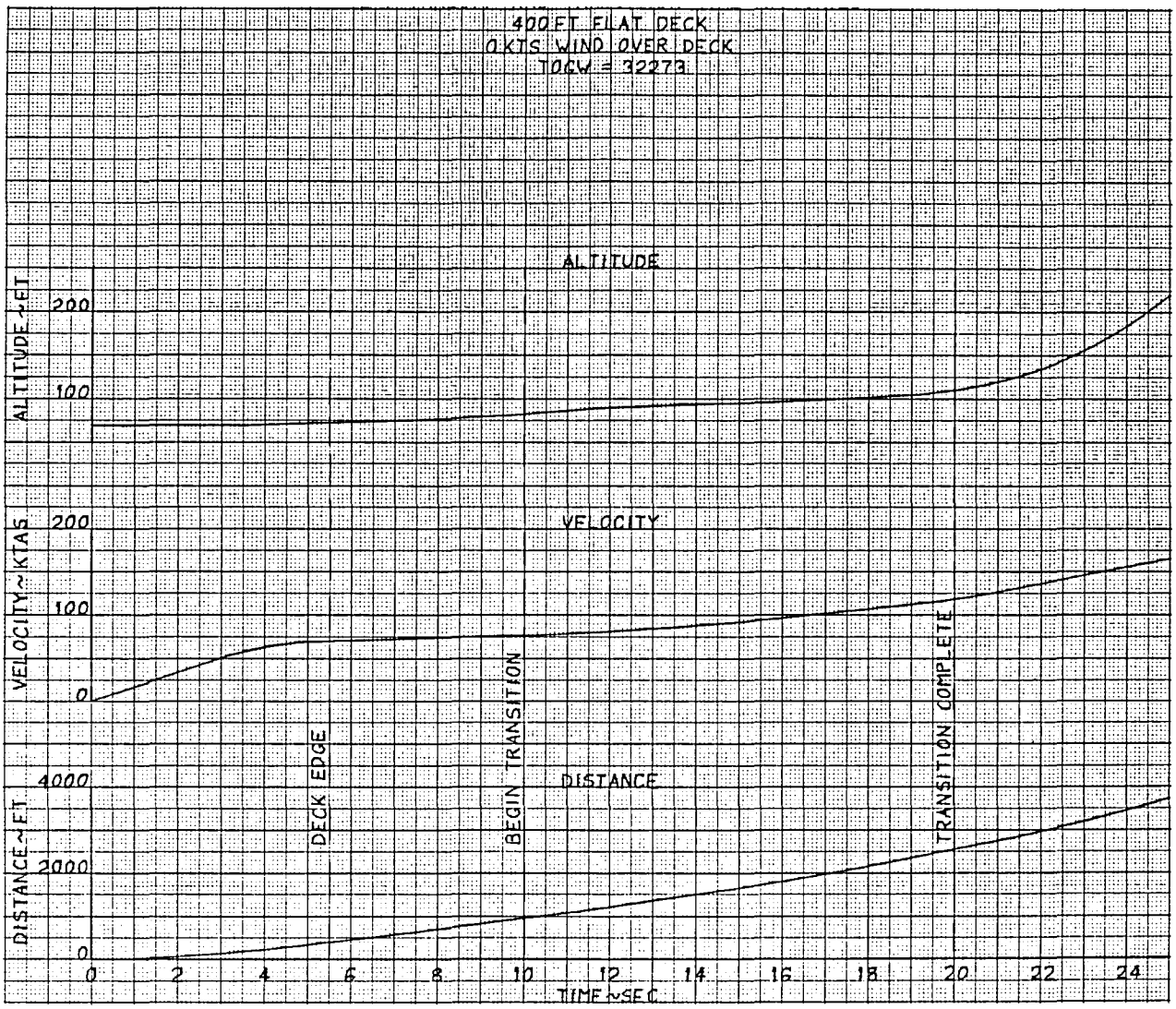

Figure 6-6 Takeoff and Transition Time Histories - Conventional Deck

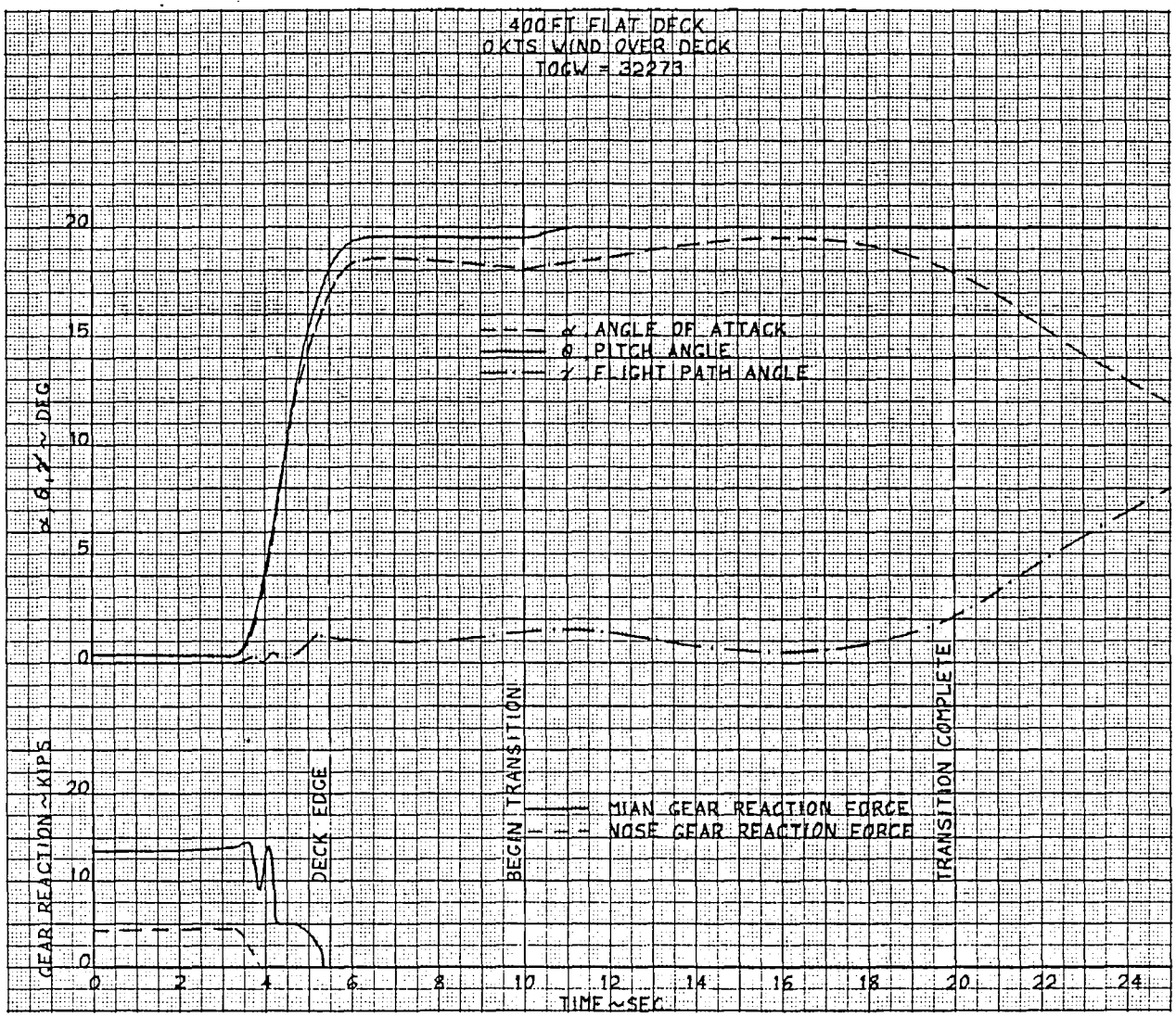

Figure 6-6 Continued

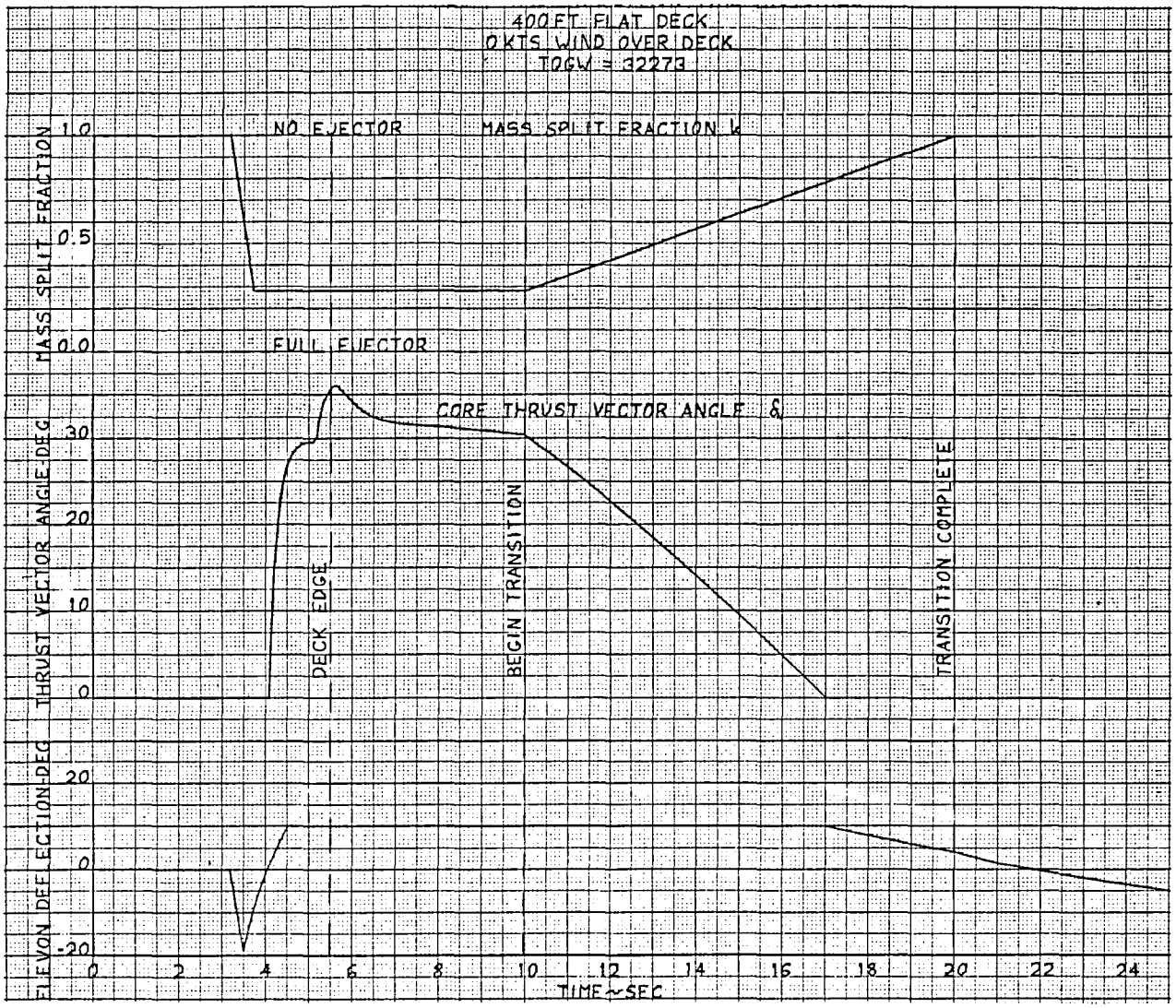

Figure 6-6 Concluded

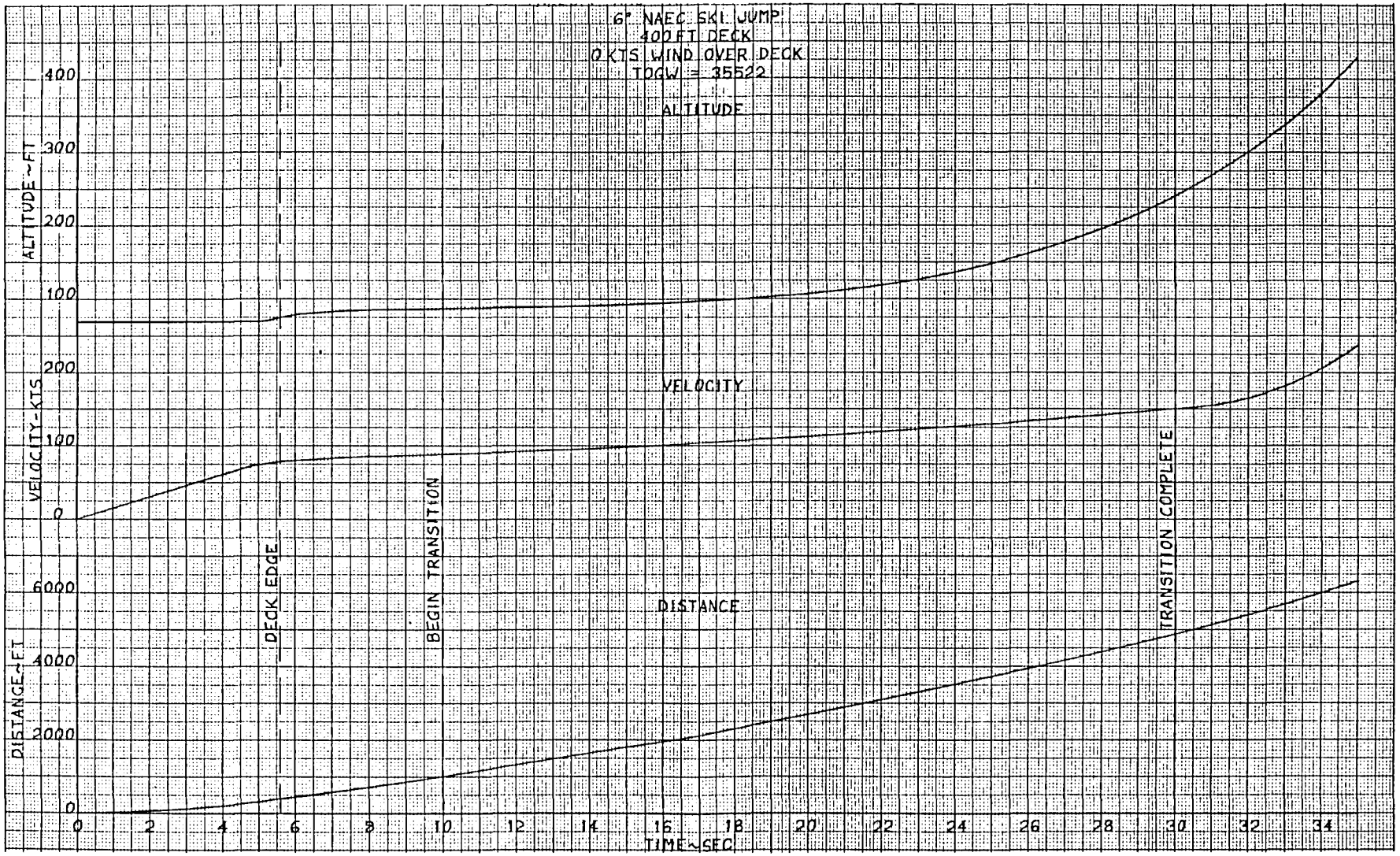

Figure 6-7 Takeoff and Transition Time Histories - 6-Degree Ski Jump

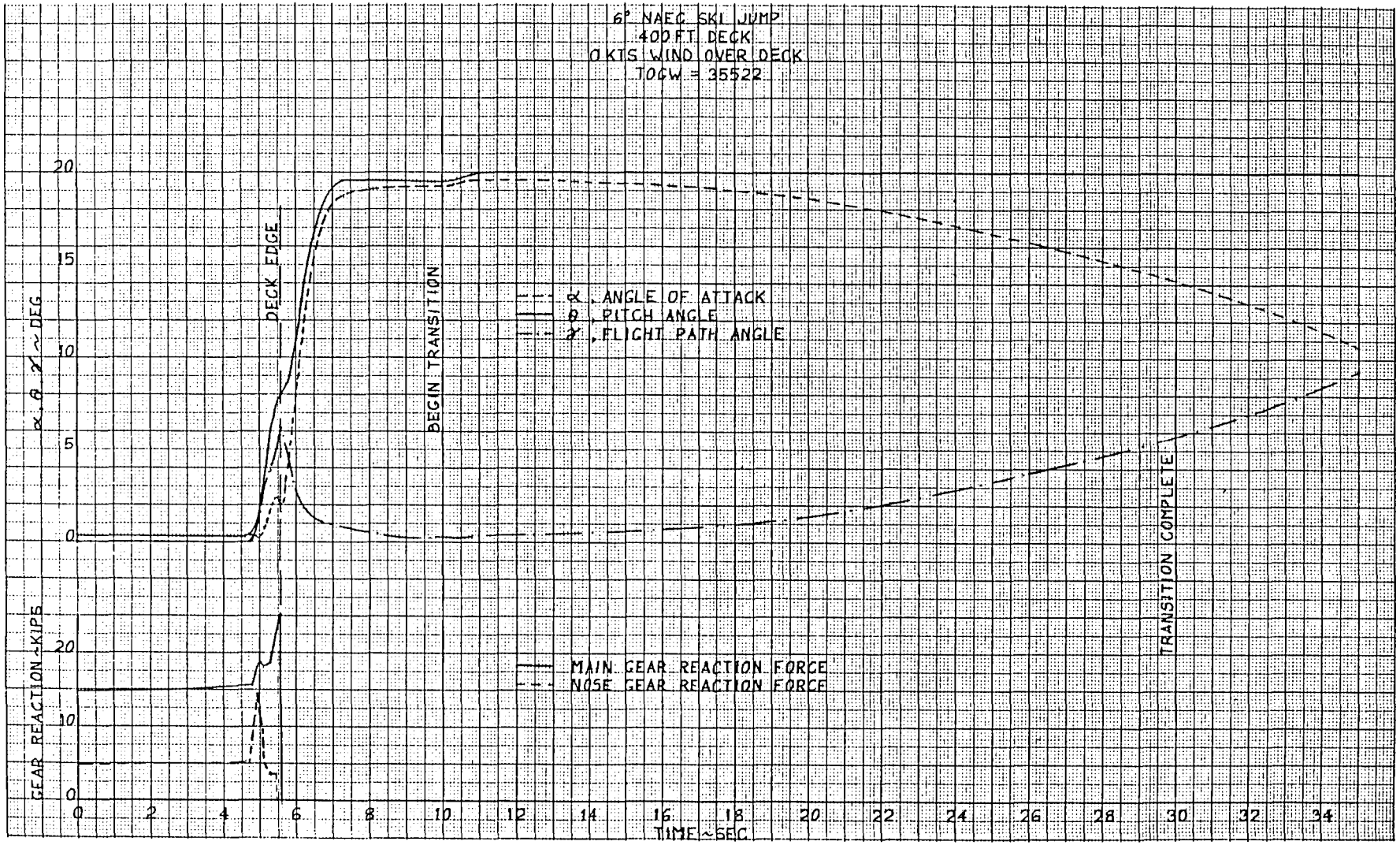

Figure 6-7 Continued

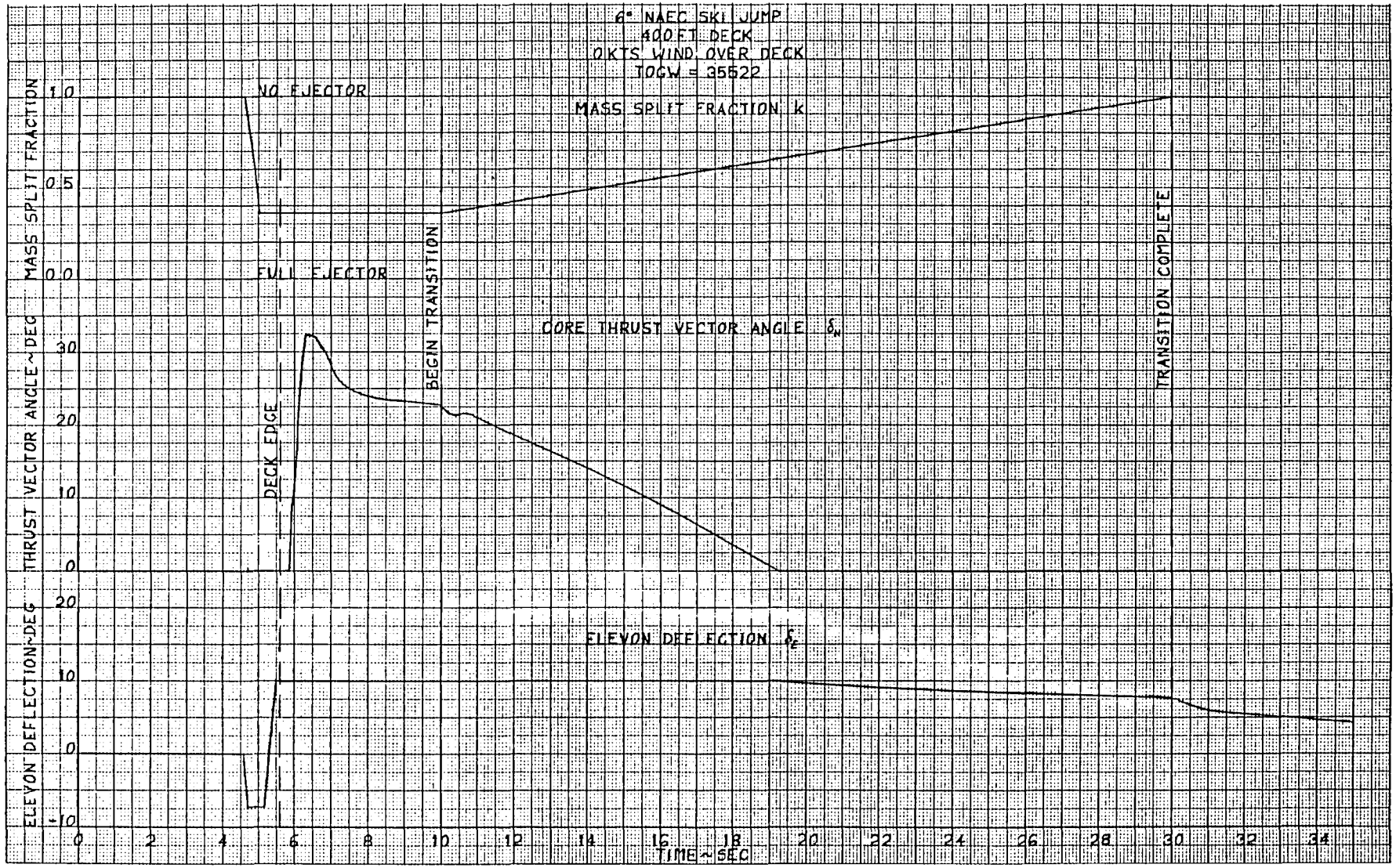

Figure 6-7 Concluded

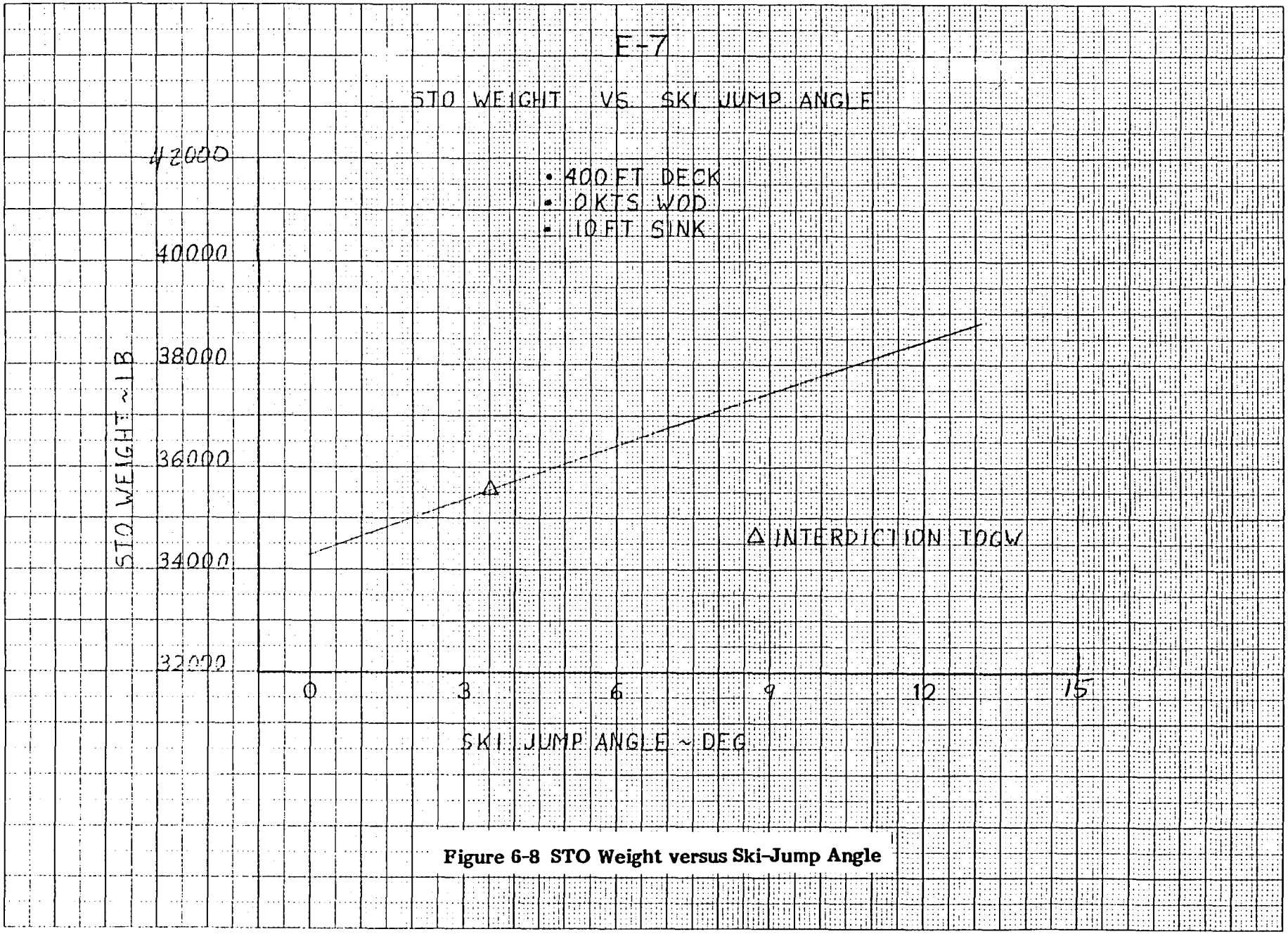

Figure 6-8 STO Weight versus Ski-Jump Angle

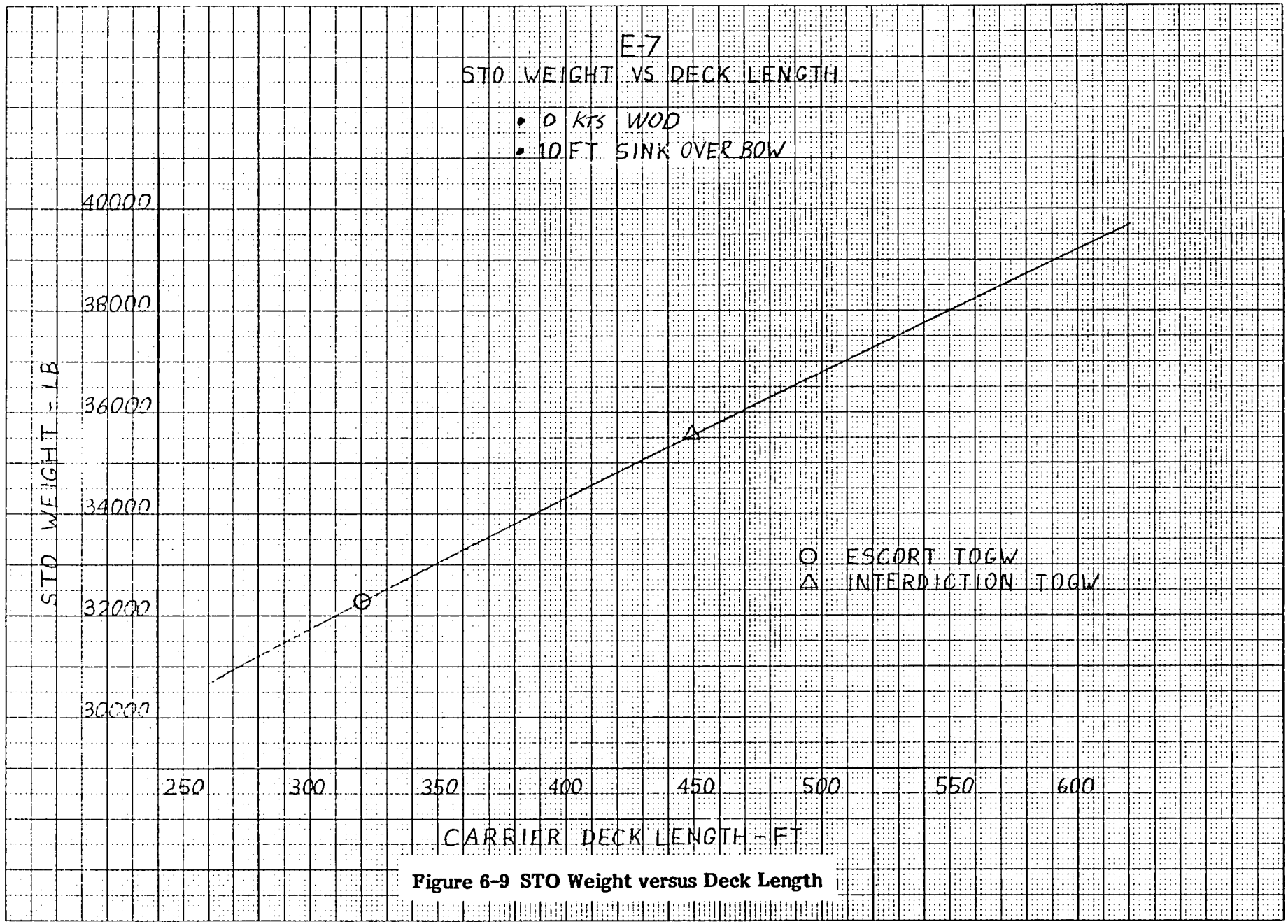

Figure 6-9 STO Weight versus Deck Length

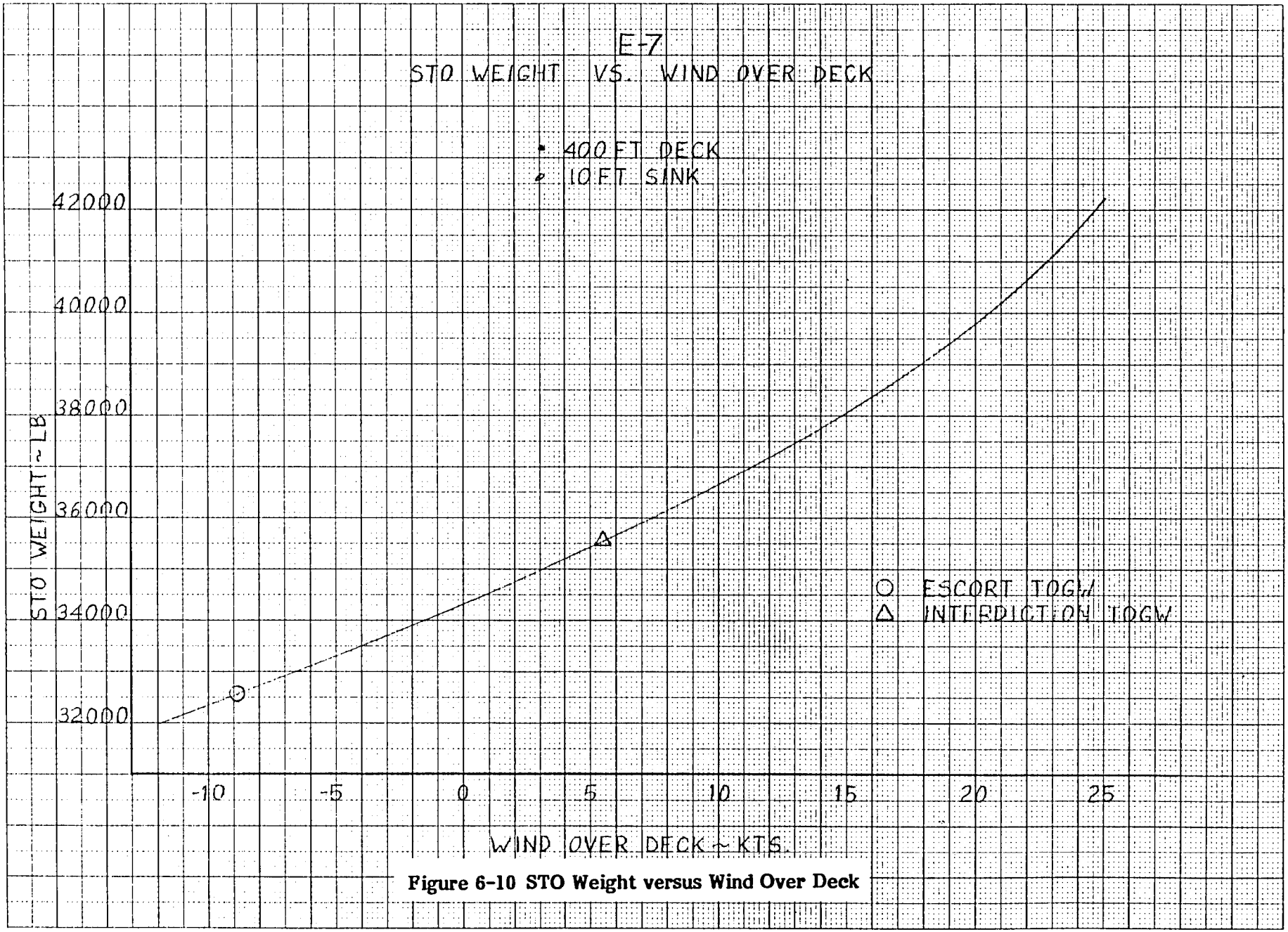

Figure 6-10 STO Weight versus Wind Over Deck

6.3 PERFORMANCE - FLIGHT DEMONSTRATOR

Because the flight demonstrator's purpose is to demonstrate hover and the low-speed end of flight at a minimum of cost, no afterburners are installed. Therefore, calculation of mission and point performance is inappropriate. The calculated STO performance is shown in Figure 6-11; sea level, tropical day, zero wind, and zero sink are assumed. The takeoff sequence is the same as for the operational aircraft with the exception of afterburner use.

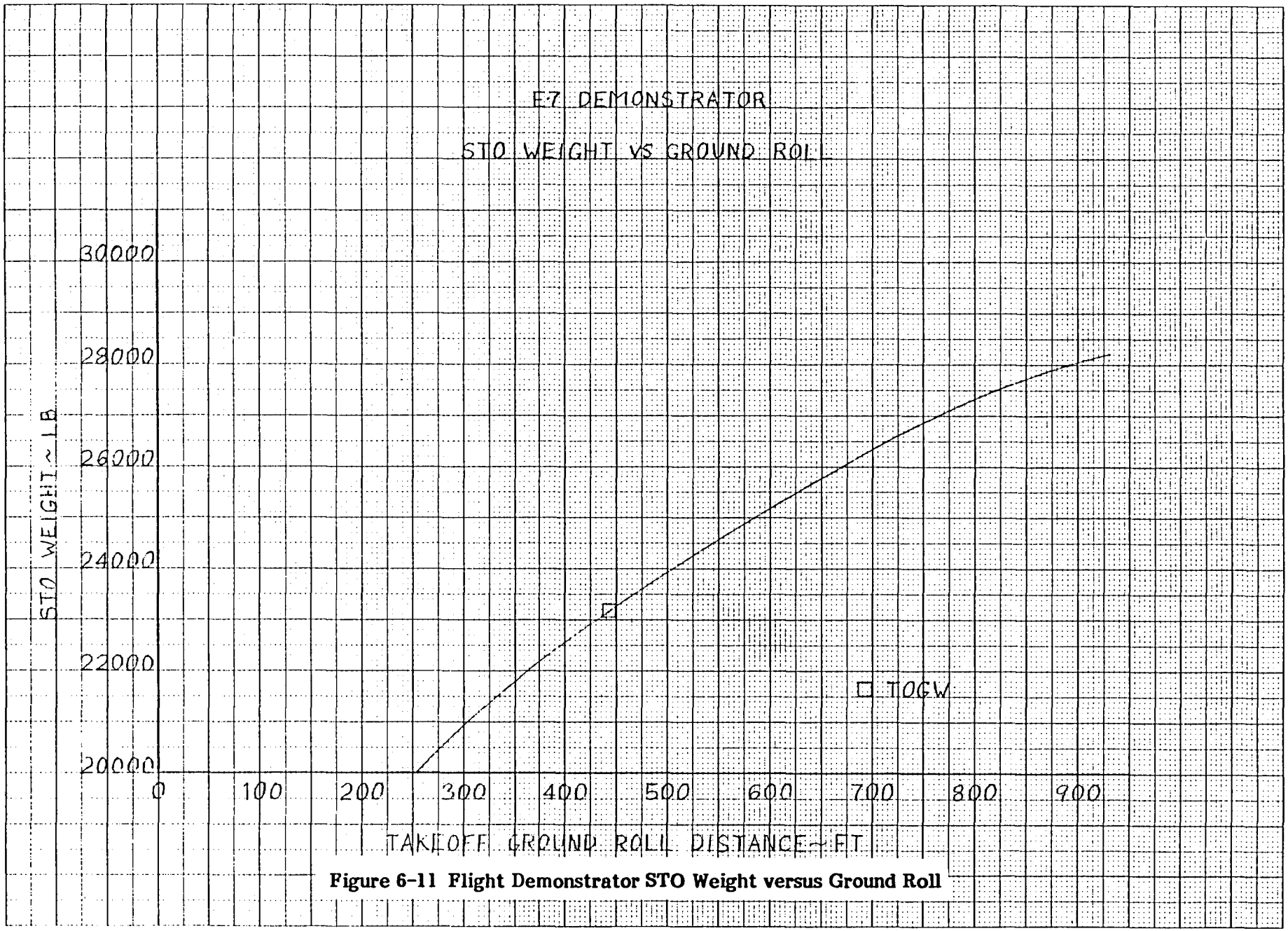

Figure 6-11 Flight Demonstrator STO Weight versus Ground Roll

7. AERODYNAMIC UNCERTAINTIES

7.1 STABILITY AND CONTROL

The stability and control derivatives estimated thus far have been for the clean configuration only. There are no acceptable methods of evaluating the derivatives with the ejector operating and this situation will continue until wind-tunnel tests on powered models can be conducted.

The handling qualities and criteria for operation of short takeoff and vertical landing aircraft from ships must be carefully addressed. The magnitude of the crosswind with superimposed gusts and the type of gust drastically influence the sizing of the reaction control system and the aerodynamic controls. The different classes of ships react differently to various wind conditions and sea states, and maneuvering and pilot workload and techniques may be different for all of these situations.

All electronic flight control systems will be utilized. This approach will allow the study of a large variation in the flight control geometry to be considered in order to keep the pilot workload at acceptable levels for the various flight modes. This approach will require integration of flight and propulsion controls (IFPC). This is a long lead study since requirements must be timely enough to be given to the engine manufacturer so that integration into the engine controls can be assured.

Stability and control characteristics of the proposed planform up to very high angles of attack must be determined. Wind tunnel testing must be accomplished in sufficient detail to evaluate both longitudinal and lateral-directional stability and controllability at high angles-of-attack. The fuselage presents a large, slab-sided, area forward of the center of gravity because it forms the inboard ejector diffuser surface. The main gear fairings form twin keelsons aft of the c.g. These contribute to the lateral-directional stability uncertainties.

7.2 WING-BORNE FLIGHT

The estimated drag polars for E-7, Figure 4-40, reflect wing camber effects that are based on the F-16E, which was the subject of an extensive wing development program by General Dynamics and NASA Langley Research Center. E-7 camber in the wing root area is restricted by the requirement to house the ejector; this will require modifications to the wing sections that are beyond the present data base.

The unique integration of the 2-D core nozzle with the fuselage creates an uncertainty with afterbody force and moment predictions. Plume entrainment will create a negative pressure region on the upswept aft fuselage. The magnitude of the adverse effect on drag and pitching moment is difficult to predict.

The current E-7 design carries AIM-9 missiles and launchers on the wing tips. In this manner, a favorable aspect ratio effect is achieved because of the end plate effect of the missiles. This is offset to some extent by the unfavorable effect on trim caused by the aft shift in aerodynamic center. It is possible that a net improvement can be achieved by extending the basic wing span to a true delta planform and mounting the missles on a short pylon under the wing. The subsonic polar efficiency and the supersonic drag penalty of the wing-tip extension will largely depend upon correct choice of the camber distribution. This trade needs to be evaluated in the wind tunnel at transonic and supersonic aspects.

Buffet onset predictions are difficult without test data, particularly on highly swept wings where the amount of camber has a strong influence on the buffet levels. The E-7 buffet predictions of Figure 4-43 are based on F-106 flight and wind-tunnel tests. The F-106 has a different camber distribution than the F-16E-type camber assumed for E-7. Since the .65-Mach-number maneuver design point is at the buffet onset lift coefficient, this is an important area for test verification.

7.3 STO AND TRANSISTION

As discussed in Section 7.1, the stability characteristics are uncertain. In addition, while it is known from References 1 through 4 that there will likely be an interaction between the ejector propulsive flow and the wing aerodynamics, E-7 is sufficiently different from the NASA/DeHavilland configuration that the results of the previous tests probably do not apply here. There are no analytic codes or procedures which can accurately predict these interactions; they remain a subject which can only be addressed by test.

Ground effects during takeoff are probably of little concern during carrier operations where the deck edge is some sixty feet above the ocean, but they could be a consideration during land-based operations. Here again there is no data base for applicable analytic methods.

7.4 HOVER

As shown in Figure 7-1, the lines of the NASA/DeHavilland ejector have been modified to accomodate the configuration. While it is hoped that these modifications will not adversely influence performance, this is by no means certain. The exact ejector performance is, thus, not fully known and must be validated by test.

The other area of uncertainty during hover is ground effects. While the data of Reference 3 have been used to determine the influence of ground proximity on ejector performance, there is no base from which to predict the interaction between the hot, high speed core exhaust and the cool, slower, but much more massive ejector exhaust.

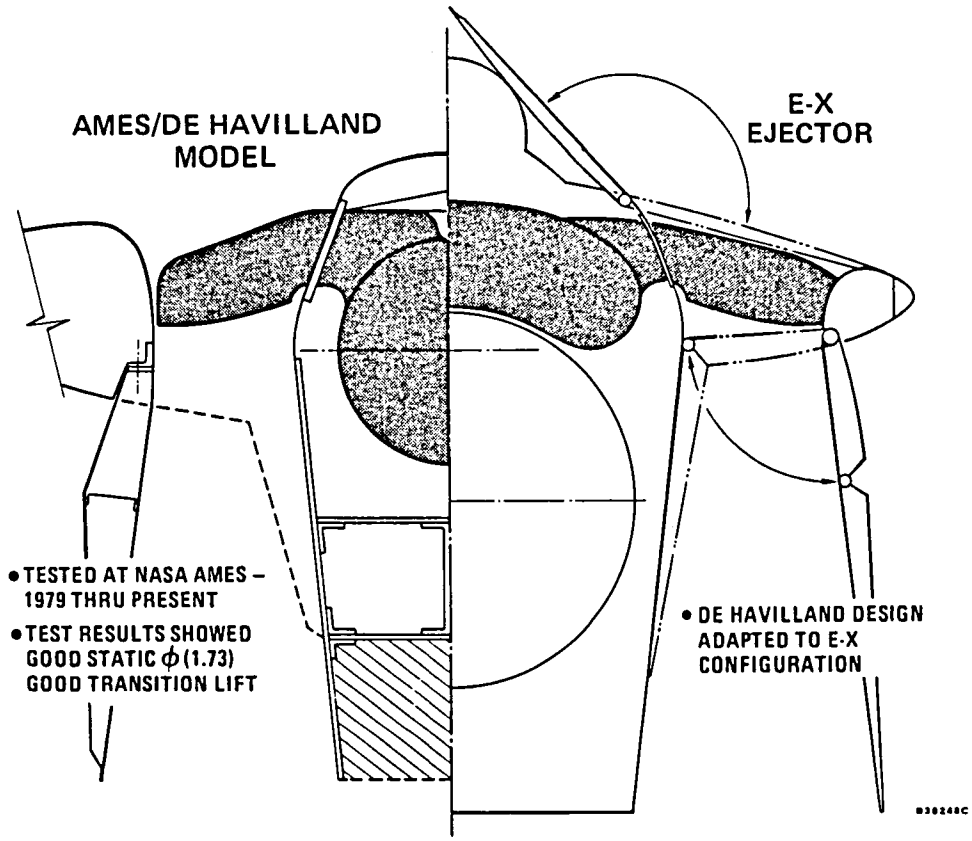

Figure 7-1 E-7, DeHavilland Ejector Comparison

This Page Intentionally Left Blank

8. PROPOSED RESEARCH PROGRAM

8.1 WIND TUNNEL TEST PLAN

A wind tunnel test program is proposed to investigate the aerodynamic uncertainties associated with up-and-away or wing-borne flight (Figure 8-1). It is envisioned that a 1/9-scale model be fabricated and tested over a Mach-number range from 0.2 to 2.0 using the NASA/Ames Unitary and 12-Foot Wind Tunnels. The proposed run schedule (Table 8-1) is designed to measure the effects of camber variation and wing-tip extension on longitudinal aerodynamic characteristics and to verify predicted stability and control and buffet characteristics of the configuration.

Two sets of wings will be constructed, each with a different camber design. The first wing set (camber no. 1) will have removable elevon parts with brackets for up and down deflections of 10, 20 and 30 degrees. Provisions will also be made for an extended (delta) tip or a tip missile. Removable main-landing-gear fairings will be made to fit the first wing contour. The second wing set will have no elevons, main-landing-gear fairings, extended tip or tip-missile provisions. The incremental aerodynamic effects of these components will be measured using the first wing and these increments applied to the second wing characteristics.

Both sets of wings will have complete buffet instrumentation including wing-tip accelerometer and wing-root bending-moment gage.

A small strake will be tested on the forward fuselage to determine its effectiveness in improving high-angle-of-attack directional stability by fixing body vortex position.

Lateral/directional stability contributions of the vertical tail and main-landing-gear fairings will be determined using sideslip sweeps at various angles of attack.

A conceptual sketch of the high-speed model is shown in Figure 8-2. The inlet airflow will be split into two streams which exit the core and fan air nozzles respectively. Internal duct drag losses will be measured using total pressure rakes at each exit plane. flow angularity corrections will be determined by measuring model forces with the model upright and inverted at each Mach number.

Table 8-1 PRELIMINARY WIND-TUNNEL TEST PLAN

CONFIGURATION	δ_e deg	δ_r deg	α deg	β deg	MACH NUMBER									COMMENT
					12 Ft	11 Ft						9x7 Ft		
					Ø.2	Ø.6	Ø.8	Ø.9	Ø.95	1.1	1.2	1.6	2.Ø	
Camber Number 1 with tip missiles and mlg fairings	Ø	Ø	V	Ø	P	P	P	P	P	P	P	P	P	Rake
	Ø	Ø	V	Ø	F	F	F	F	F	F	F	F	F	Inverted
	Ø	Ø	V	Ø	F,B	F,B	F,B	F,B	F,B	F,B	F,B	F,B	F,B	Longitinal
	Ø	Ø	Ø	V	F	F		F			F	F	F	Lateral/
	Ø	Ø	5	V	F	F		F			F	F	F	Direct-
	Ø	Ø	15	V	F	F		F			F			ional
	Ø	Ø	25	V	F									
	Ø	Ø	3Ø	V	F									
	Ø	Ø	35	V	F									
	-3Ø	Ø	V	Ø	F,B	F,B		F,B			F,B			Pitch
	-2Ø	Ø	V	Ø	F,B	F,B		F,B			F,B	F,B	F,B	Control
	-1Ø	Ø	V	Ø	F,B	F,B		F,B			F,B	F,B	F,B	and
	1Ø	Ø	V	Ø	F,B	F,B		F,B			F,B	F,B	F,B	Trim
	2Ø	Ø	V	Ø	F,B	F,B		F,B			F,B	F,B	F,B	
	3Ø	Ø	V	Ø	F,B	F,B		F,B			F,B			
	Ø/-1Ø	Ø	V	Ø	F	F		F			F			Roll
	Ø/-2Ø	Ø	V	Ø	F	F		F			F			Control
	Ø	5	V	Ø	F	F		F			F			Yaw
	Ø	1Ø	V	Ø	F	F		F			F			Control
	Ø	2Ø	V	Ø	F	F		F			F			
Camber number 1 with tip missiles and mlg fairings vertical tail off	Ø	Ø	Ø	V	F	F		F			F	F	F	Vertical
	Ø	Ø	5	V	F	F		F			F	F	F	Tail
	Ø	Ø	15	V	F	F		F			F			Effects
	Ø	Ø	25	V	F									
	Ø	Ø	3Ø	V	F									
	Ø	Ø	35	V	F									

Table 8-1 Continued

CONFIGURATION	δ_e deg	δ_r deg	α deg	β deg	MACH NUMBER									COMMENT
					12 Ft	11 Ft						9x7 Ft		
					Ø.2	Ø.6	Ø.8	Ø.9	Ø.95	1.1	1.2	1.6	2.Ø	
Camber Number 1 with tip extension and mlg fairings	Ø	Ø	V	Ø	F,B	F,B	F,B	F,B	F,B	F,B	F,B	F,B	F,B	Extended Tip Effects
	Ø	Ø	Ø	V	F	F		F			F	F	F	
	Ø	Ø	5	V	F	F		F			F	F	F	
	Ø	Ø	15	V	F	F		F			F			
	Ø	Ø	25	V	F									
	Ø	Ø	3Ø	V	F									
	Ø	Ø	35	V	F									
	-3Ø	Ø	V	Ø	F,B	F,B		F,B			F,B			
	-2Ø	Ø	V	Ø	F,B	F,B		F,B			F,B	F,B	F,B	
	-1Ø	Ø	V	Ø	F,B	F,B		F,B			F,B	F,B	F,B	
	1Ø	Ø	V	Ø	F,B	F,B		F,B			F,B	F,B	F,B	
	2Ø	Ø	V	Ø	F,B	F,B		F,B			F,B	F,B	F,B	
	3Ø	Ø	V	Ø	F,B	F,B		F,B			F,B			
	Ø/-1Ø	Ø	V	Ø	F	F		F			F			
	Ø/-2Ø	Ø	V	Ø	F	F		F			F			
Camber Number 1 with mlg fairings	Ø	Ø	V	Ø	F,B	F,B	F,B	F,B	F,B	F,B	F,B	F,B	F,B	Tip-Missile Effects
	Ø	Ø	Ø	V	F	F		F			F	F	F	
	Ø	Ø	5	V	F	F		F			F	F	F	
	Ø	Ø	15	V	F	F		F			F			
	Ø	Ø	25	V	F									
	Ø	Ø	3Ø	V	F									
	Ø	Ø	35	V	F									
	-3Ø	Ø	V	Ø	F,B	F,B		F,B			F,B			
	-2Ø	Ø	V	Ø	F,B	F,B		F,B			F,B	F,B	F,B	
	-1Ø	Ø	V	Ø	F,B	F,B		F,B			F,B	F,B	F,B	
	1Ø	Ø	V	Ø	F,B	F,B		F,B			F,B	F,B	F,B	
	2Ø	Ø	V	Ø	F,B	F,B		F,B			F,B	F,B	F,B	
	3Ø	Ø	V	Ø	F,B	F,B		F,B			F,B			
	Ø/-1Ø	Ø	V	Ø	F	F		F			F			
	Ø/-2Ø	Ø	V	Ø	F	F		F			F			

Table 8-1 Concluded

CONFIGURATION	δ_e deg	δ_r deg	α deg	β deg	MACH NUMBER									COMMENT
					12 Ft	11 Ft						9x7 Ft		
					Ø.2	Ø.6	Ø.8	Ø.9	Ø.95	1.1	1.2	1.6	2.Ø	
Camber Number 1	Ø	Ø	V	Ø	F,B	F,B	F,B	F,B	F,B	F,B	F,B	F,B	F,B	Camber and MLG Fairing Effects
	Ø	Ø	Ø	V	F	F		F			F	F	F	
	Ø	Ø	5	V	F	F		F			F	F	F	
	Ø	Ø	15	V	F	F		F			F			
	Ø	Ø	25	V	F									
	Ø	Ø	3Ø	V	F									
	Ø	Ø	35	V	F									
	-3Ø	Ø	V	Ø	F	F		F			F			
	-2Ø	Ø	V	Ø	F	F		F			F	F	F	
	-1Ø	Ø	V	Ø	F	F		F			F	F	F	
	1Ø	Ø	V	Ø	F	F		F			F	F	F	
	2Ø	Ø	V	Ø	F	F		F			F	F	F	
	3Ø	Ø	V	Ø	F	F		F			F			
	Ø/-1Ø	Ø	V	Ø	F	F		F			F			
	Ø/-2Ø	Ø	V	Ø	F	F		F			F			
Camber Number 1 with strakes	Ø	Ø	V	Ø	F,B	F,B	F,B	F,B	F,B	F,B	F,B	F,B	F,B	Strake Effects
	Ø	Ø	Ø	V	F	F		F			F	F	F	
	Ø	Ø	5	V	F	F		F			F	F	F	
	Ø	Ø	15	V	F	F		F			F			
	Ø	Ø	25	V	F									
	Ø	Ø	3Ø	V	F									
	Ø	Ø	35	V	F									
Camber Number 2	Ø	Ø	V	Ø	F,B	F,B	F,B	F,B	F,B	F,B	F,B	F,B	F,B	Camber Effects
	Ø	Ø	Ø	V	F	F		F			F	F	F	
	Ø	Ø	5	V	F	F		F			F	F	F	
	Ø	Ø	15	V	F	F		F			F			
	Ø	Ø	25	V	F									
	Ø	Ø	3Ø	V	F									
	Ø	Ø	35	V	F									

DATA TYPES: F - FORCE (6-Component Balance)
B - BUFFET (Wing-Tip Accelerometer and Wing-Root Bending-Moment Gage)
P - PRESSURE (Total-Pressure Rake at Nozzle Exit Planes for Internal Drag Measurements)

V - VARIABLE

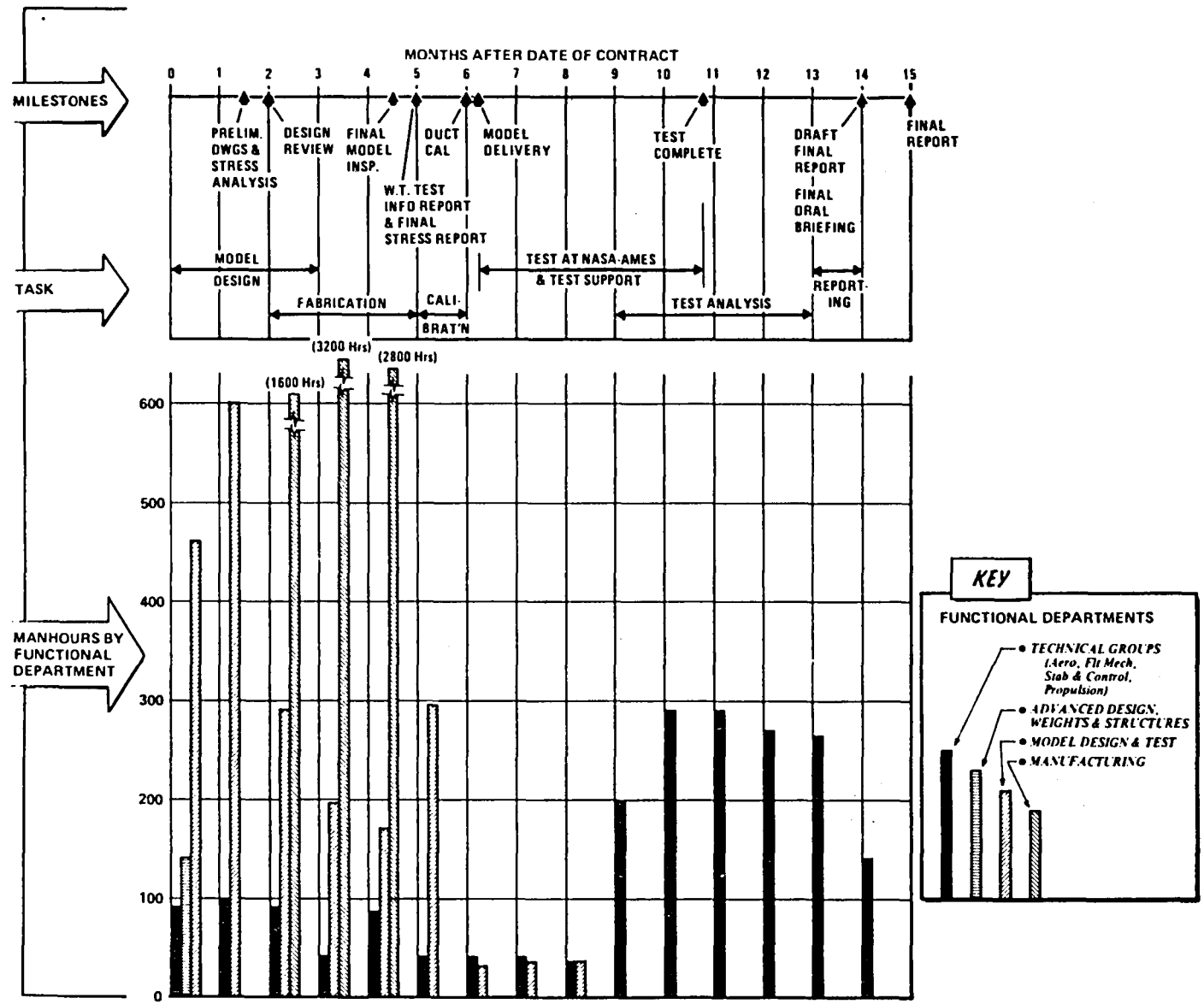

Figure 8-1 Proposed Test Program Schedule

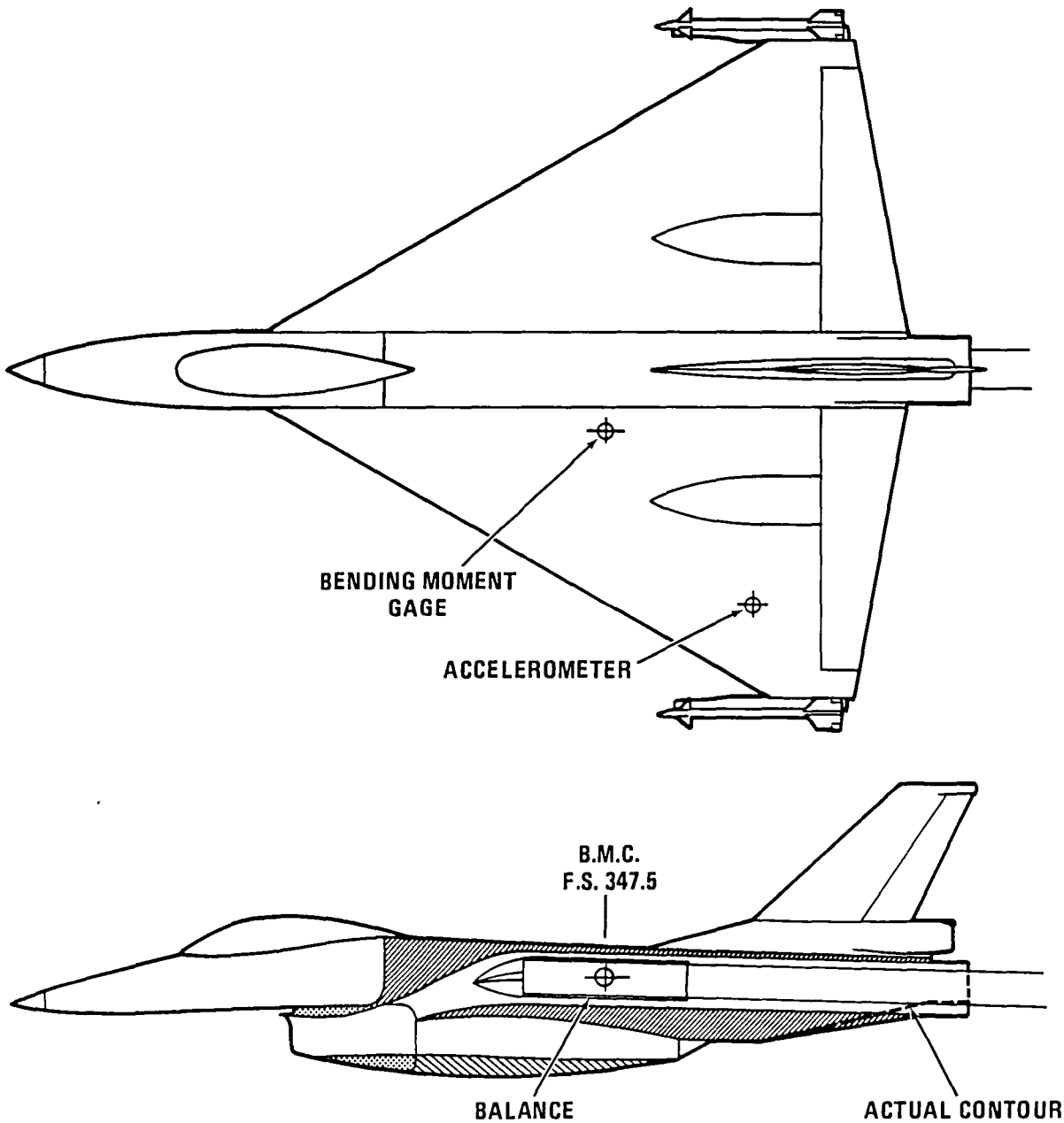

Figure 8-2 Conceptual Sketch of High-Speed Model

8.2 MODEL AND STING CONCEPT

8.2.1 Support System

In the sting design, angles of attack of up to 25 degrees in the 11-Foot tunnel, 15 degrees in the 9- by 7-Foot tunnel, and 90 degrees in the 12-Foot tunnel will be tested. The sting will be designed to minimize flow interference with the model. Angles of attack corresponding to maximum lift will also be used to design the sting, considering low dynamic pressures. In the NASA/Ames 11-Foot Tunnel, this sting support will be used along with an existing Ames bent adapter and sting extension. In the 9- by 7-Foot Tunnel, the sting will mount directly to the tunnel support system. Previous experience in the Ames 12-Foot Tunnel indicates that use of a floor-mounted pitch mechanism will be necessary to achieve angles of attack up to 90 degrees. Because of the pitch range limit with this system, two sting adapters (one straight and one bent) will be required to achieve the desired zero to 90-degree angle-of-attack range. Possible installations in the specified facilities are shown in Figure 8-3. These concepts will provide the desired angle-of-attack range and tunnel flowfield.

After specific model requirements are determined, an effort will be made to locate an existing sting to support the model. If an adequate sting can be found so that it is not necessary to fabricate a new sting and tunnel adapter, a reduction in the proposed fabrication costs to the government will result.

The material used in the support sting will be high-heat-treat steel with proper balance and support tapers machined at each end. The sting material will be ultrasonically inspected before machining and magnetic-particle or penetrant-dye inspected (depending on material used) after final machining.

8.2.2 Model Design and Fabrication

Within seven weeks following the start of Phase II General Dynamics will furnish preliminary detailed manufacturing drawings and a stress analysis of the model and support structure design for written approval by the contracting officer. An informal review of the design approach will be held one week later. Fabrication will not begin until such approval has been obtained by General Dynamics. Changes in the design that may be proposed by General Dynamics after the start of fabrication will not be implemented until such changes have received the approval of the contracting officer.

The model will be fabricated over a 3-month period following approval of the NASA Technical Monitor at the informal design review. The model will be fabricated in the Fort Worth Division Model Shop. The techniques used in model manufacturing are well-established as a result of many years of experience. The shop has the equipment and skilled personnel required for the manufacture of a high-quality model that duplicates the airplane geometry and has a good surface finish.

Model contours will be derived from pencil line drawings and tabulated geometry. Templates made from pencil line drawings (fuselage, nacelle) will be accurate to within 0.015 inch. Those templates made from tabulated geometry (wings, elevons, and vertical tail) can be made to within 0.03 inch. All templates will fit the model contour to within 0.006 inch.

All parts will be fitted and contoured with mating surfaces and contours so that no fillers are necessary to fill cracks or joints when the model is assembled. No joint will have a gap width greater than 0.015 inch.

The exterior surface of the model will have a surface finish of 32 rms microinch. The nacelle internal duct surface from the inlet aft to the throat will also have a finish of 32 rms. The remainder of the duct will have a surface finish of 125 rms or better.

8.2.3 Instrumentation

Force measurements will be made using a six-component balance such as the Task Corp. 2.5-inch balance. Buffet instrumentation includes both a wing-root bending moment gage and wing-tip accelerometer. Fluctuating wing bending moments are to be measured by a Kulite diffused semiconductor four-arm-gage sensor. The gage will be located on the wing part at the root at approximately 50 percent chord. Fluctuating wing-tip accelerations may be measured using an EGA-125-100D accelerometer. It is anticipated that the accelerometer will be GFE; alternatively an Endevco 2222B accelerometer may be supplied by General Dynamics.

8.2.4 Strength Analysis

The maximum loads that will be experienced by the model will be estimated on the basis of (1) operation in the Ames 11-Foot Wind Tunnel at Mach 0.9, maximum angle of attack, and a dynamic pressure of 1450 psf, and (2) the starting loads encountered in the Ames 9- by 7-Foot Wind Tunnel. For the latter tunnel, the model will be positioned in a wings-vertical attitude to minimize the starting loads. The model will be designed to be capable of withstanding these estimated loads and will have a safety factor of 5, based on the ultimate strength of the material, or 3, based on yield strength, whichever is the more conservative. To obtain the required model strength it is anticipated that heat-treated steel will be necessary for the fuselage center section, wings, vertical tail, and the various deflection brackets. Other model components will be fabricated from aluminum and various plastic materials.

8.2.5 Dimensional Verification and Documentation

The General Dynamics Program Manager will notify the Ames Contracting Officer two weeks prior to the expected date of model completion and final inspection. Government representatives will witness the final inspection at the Fort Worth facility, and General Dynamics agrees that the acceptance of the model by the government shall depend upon satisfactory completion of the inspection. The inspection shall consist of complete assembly and measurement of all model components and supporting structure, including model installation on the sting support with required wiring and tubing routed as appropriate. An acceptable fit between the model and a government furnished master-balance gage will be demonstrated. At least 80 percent contact between all sting and balance taper joints will also be demonstrated during the inspection by use of appropriate government furnished gages.

A model and sting dimensional verification document will be furnished the government representatives, at the time of the final inspection, comparing appropriate measured dimensions and contours to those specified in the manufacturing drawings. The provisions of NASA/Ames specification RQ002 will be met.

In addition to the final inspection, quality assurance during the construction of the model will be conducted by inspectors in the Model Manufacturing Department. The

entire inspection task will be administered by the lead model test engineer, who will work full time on the program during the fabrication phase and who will report on a day-to-day basis to the program manager.

The inspections will be made with the normal mechanical instruments. In addition, a Cordax surface comparator will be used to verify airfoil contours. Should model complexity require it, inspections will also be made with stereo-optic/photographic equipment in use at the Fort Worth facility.

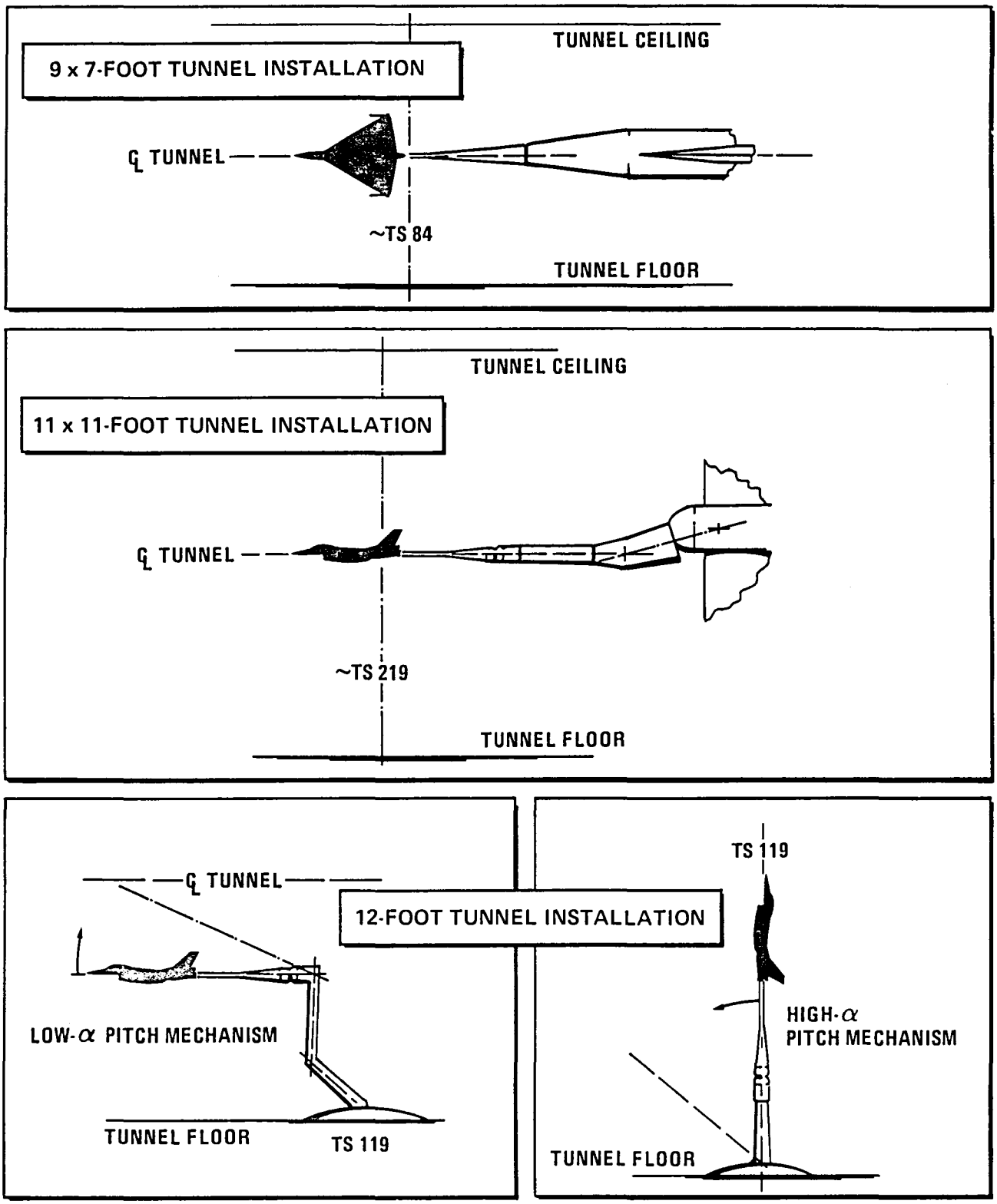

Figure 8-3 Installation Sketches for the Unitary and 12-Foot Wind Tunnels

8.3 WIND TUNNEL TEST INFORMATION REPORT

The wind tunnel test information report, to be submitted 12 months ADC Phase II, will contain as a minimum the following:

1. Test scope and objectives.

2. Description of test articles, including the basic model, component variables, surface deflections, and additional components.

3. Geometry summary of the model horizontal and vertical control surfaces, wing, and flaps, including locations, dimensions, areas, sweeps, aspect ratios, taper ratios, mean aerodynamic chords, incidence angles, dihedral, airfoils, and hinge lines.

4. Plots of wind tunnel model cross-sectional area distribution versus length.

5. Proposed test matrix and operating conditions (Mach number, Reynolds number, dynamic pressure, angle-of-attack, and sideslip range) for each tunnel.

6. Plots of dynamic pressure versus angle of atack showing boundaries due to model, sting, or tunnel support system load limits and sting divergence limits. These plots will be at Mach numbers representative of the most critical load conditions.

7. Suggested grit location and microbead diameter for the various tunnels.

8. Description of instrumentation, including balance selection, pinning position, and pressure pickups in the base, balance cavity, and duct exit rakes.

9. Data reduction requirements, including model reference lengths and areas, moment reference center, balance center, and moment transfer distances, as well as any non-standard data reduction equations and output formats.

10. Reduced-size copies of the final manufacturing drawings of the model and sting support, including an index to these drawings.

8.4 WIND TUNNEL TEST SUPPORT

Before delivery, General Dynamics will calibrate the model flow-through duct to provide a duct exit-rake calibration factor for internal drag determination during the wind tunnel tests. This calibration will be done at the General Dynamics Flow Laboratory located at the Fort Worth facility.

General Dynamics will supply a model design engineer for a period of two weeks to familiarize Ames personnel with the model, to assist with the installation and instrumentation of the model, and to assist Ames personnel with assuring the validity of the test results. General Dynamics will also send the program aerodynamicist to Ames for a period of up to two weeks to become familiar with the facilities, test techniques, and data content, and to assist the model design engineer with assuring the validity of the test results.

8.5 DATA ANALYSIS

8.5.1 Task Descriptions

The tasks to be accomplished by General Dynamics during the Phase II data analysis effort are as follows:

1. Plot selected test data in a form needed for engineering analysis appropriate to the objectives of the study.

2. Analyze the longitudinal aerodynamic data obtained from tests of the configuration, including comparisons with theoretical estimates where appropriate. This analysis will include at least the following:

   a. Estimation and application of corrections to the predicted results of Phase I to account for differences in geometry between the flight vehicle and wind-tunnel model, as well as differences in flight and test conditions. This will result in a set of predicted longitudinal characteristics for the wind-tunnel model at the test Reynolds number.

   b. Comparison of predicted and test untrimmed longitudinal characteristics for the baseline configuration, including a model component build-up. Plotted results will include at least C_L vs. α, C_L vs. C_D, C_L vs. C_m, C_{D_o} vs. M, and a.c. vs. M. Buffet characteristics will also be included.

   c. Summary of the trimmed characteristics for the baseline configuration considering variations in wing camber and trailing-edge flap deflection as well as wing-tip extension and tip-missile effects.

3. Analysis of the lateral/directional aerodynamic data obtained from tests of the configuration, including comparison with theoretical estimates where appropriate. This analysis will be for the baseline configuration or another configuration depending on results of the tests. The results will show the effect on C_l, C_n, and C_Y of variations in β and vertical tail deflection with various combinations of wing camber, trailing-edge flap deflection, and presence of the strake.

4. Recommendations, on the basis of the foregoing analysis of the wind-tunnel test results, of any additional testing required to complete the investigation of the aerodynamic uncertainties. This will include any new problem areas uncovered during the previous testing and data anlaysis and may include recommended new model hardware or combinations of new and/or existing hardware. Also, on the basis of the foregoing analysis, weaknesses in the theoretical prediction methods will be identified and modifications to existing methods and/or new techniques will be recommended.

8.5.2 Data Management

The analysis of the wind tunnel data will be accomplished with the aid of computer procedures currently available or developed specifically to process the wind tunnel data results supplied from Ames Research Center. The wind tunnel test data will be supplied to General Dynamics by Ames in at least tabular form and on magnetic tape in a mutually agreeable format. All data processing will be performed using the Fort Worth Division

DEC VAX 11/780 computer, including the development of trimmed aerodynamic characteristics.

8.5.3 Reports

The proposed reports and briefings are summarized below:

1. Monthly progress reports.

2. Preliminary manufacturing drawings and stress analysis report - 7 weeks ADC Phase II.

3. Informal design review - 8 weeks ADC Phase II.

4. Model inspection documentation - 18 weeks ADC Phase II.

5. Wind Tunnel Test Information, including final model drawings and stress report - 20 weeks ADC Phase II.

6. Final oral briefing of analysis and draft final report - 56 weeks ADC Phase II.

7. Final report - 60 weeks ADC Phase II (NASA CR).

9. CONCLUSIONS AND RECOMMENDATIONS

A conceptual design and analysis on a single-engine STOVL fighter/attack aircraft has been completed. This aircraft combines a NASA/DeHavilland ejector with vectored thrust and is capable of accomplishing the mission and point performance of Type Specification 169, and a flight demonstrator could be built with an existing F101/DFE engine.

The aerodynamic, aero/propulsive, and propulsive uncertainties have been identified, and a wind-tunnel program has been proposed to address those uncertainties associated with wing-borne flight.

While not a part of the proposed program, it is recommended that the configuration be exercised on PAN AIR so that a good indication of the stability derivatives be obtained in advance of the test results. The fact that the E-7 was designed on ComputerVision and that a computational analysis model is available will greatly speed the code input process. This effort would not only provide the capability of an early start in the design of the flight control system but will also provide an additional basis for evaluating the capability of the PAN AIR code when the tunnel data becomes available for comparison.

General Dynamics is presently constructing a .3-scale ejector model designed to aircraft lines in order to evaluate hover performance. While not part of the program discussed above, eventually a powered model of the entire aircraft of at least 1/6 scale should be built in order to address both ground effects and the STO/transition uncertainties.

This Page Intentionally Left Blank

APPENDIX

U.S. Customary Units have been used for dimensional quantities throughout the report text. This appendix provides conversion factors to the International System (SI) of units taken from Reference 31.

To Convert From	To	Multiply By
ACCELERATION		
foot/second^2	meter/second^2	3.048 E-01
AREA		
foot^2	meter^2	9.290 304 E-02
inch^2	meter^2	6.4516 E-04
DENSITY		
lbm/inch^3	kilogram/meter^3	2.767 990 5 E+04
lbm/foot^3	kilogram/meter^3	1.601 846 3 E+01
slug/foot^3	kilogram/meter^3	5.153 79 E+02
ENERGY		
British thermal unit	joule	1.055 056 E+03
foot lbf	joule	1.355 817 9

To Convert From	To	Multiply By
FORCE		
lbf (pound force, avoirdupois)	newton	4.448 221 615 260 5
LENGTH		
foot	meter	3.048 E-01
inch	meter	2.54 E-02
nautical mile (U.S.)	meter	1.852 E+03
statute mile (U.S.)	meter	1.609 344 E+03
MASS		
pound mass, lbm (avoirdupois)	kilogram	4.535 923 7 E-01
slug	kilogram	1.459 390 29 E+01
POWER		
foot lbf/second	watt	1.355 817 9
horsepower (550 foot lbf/second)	watt	7.456 998 7 E+02
PRESSURE		
atmosphere	newton/meter^2	1.013 25 E+05
inch of mercury (32°F)	newton/meter^2	3.386 389 E+03
inch of mercury (60°F)	newton/meter^2	3.376 85 E+03
inch of water (39.2°F)	newton/meter^2	2.490 82 E+02

To Convert From	To	Multiply By
inch of water (60°F)	newton/meter^2	2.4884 E+02
lbf/foot^2	newton/meter^2	4.788 025 8 E+01
lbf/inch^2 (psi)	newton/meter^2	6.894 757 2 E+03
millibar	newton/meter^2	1.00 E+02
millimeter of mercury (0°C)	newton/meter^2	1.333 224 E+02
torr (0°C)	newton/meter^2	1.333 22 E+02
SPEED		
foot/second	meter/second	3.048 E-02
kilometer/hour	meter/second	2.777 777 8 E-01
knot (international)	meter/second	5.144 444 444 E-01
mile/hour (U.S. statute)	meter/second	4.4704 E-01
TEMPERATURE		
Celsius (t_C)	kelvin (t_K)	$t_K=t_C+273.15$
Fahrenheit (t_F)	kelvin	$t_K=(5/9)(t_F+459.67)$
Fahrenheit	Celsius	$t_C=(5/9)(t_F-32)$
Rankine (t_R)	kelvin	$t_K=(5/9)t_R$
VISCOSITY		
foot^2/second	meter^2/second	9.290 304 E-02
lbm/foot second	newton second/meter^2	1.488 163 9
lbf second/foot^2	newton second/meter^2	4.788 025 8 E+01
slug/foot second	newton second/meter^2	4.788 025 8 E+01

To Convert From	To	Multiply By
VOLUME		
foot^3	meter^3	2.831 684 659 2 E-02
gallon (U.S. liquid)	meter^3	3.785 411 784 E-03
inch^3	meter^3	1.638 706 4 E-05

REFERENCES

1. Garland, D.B., Static Tests of the J-97 Powered, External Augmentor V/STOL Wind Tunnel Model, DeHavilland Report DHC-DND 77-4, February 1978.

2. Garland, D.B., Phase 1 Wind Tunnel Tests of the J-97 Powered, External Augmentor V/STOL Model, DeHavilland Report DHC-DND 79-4, September 1979.

3. Garland, D.B. and Harris, J.L., Phase 2 and 3 Wind Tunnel Tests of the J-97 Powered, External Augmentor V/STOL Model, DeHavilland Report DHC-DND 80-1, March 1980.

4. Gilbertson, F.L. and Garland, D.B., Static Tests of the J-97 Powered, External Augmentor V/STOL Model at the Ames Research Center, DeHavilland Report DHC-DND 80-2, 1980.

5. Foley, W.H. and Beard, B.B., An Engine Trade Study for a Supersonic STOVL Fighter/Attack Aircraft, NASA CR 166304, (in preparation).

6. Roland, H.L., and Neben, R.E., Aircraft Structural Weight Estimating Methods, General Dynamics Fort Worth Division Report ERR-FW-242, September 1966.

7. Roland, H.L., Cadell, W.E. and Ortiz, A., Aircraft Propulsion and Fixed Equipment System Weight Estimating Methods, General Dynamics Fort Worth Division Report ERR-FW-613, June 1967.

8. Roland, H.L., Weight Prediction Accuracy Analysis, Structure Propulsion and Fixed Equipment for Manned Aircraft to M 2.3, General Dynamics Fort Worth Division Report ERR-FW-614, 15 July 1967.

9. Advanced Development of Conceptual Hardware for the Lightweight Fighter (YF-16 Composite Fwd Fuselage) AFFDL-TR-77, April 1977.

10. A Proposal for the Advanced Development of Composite Wing/Fuselage Structures Program (F-16). General Dynamics Fort Worth Division Proposal Document FZP-1700-1, Volume 1, Book 3, 10 February 1975.

11. Schemensky, R.T., Development of an Emperically Based Computer Program to Predict the Aerodynamic Characteristics of Aircraft, Air Force Flight Dynamics Laboratory, AFFDL-TR-73-144, November 1973.

12. Schemensky, R.T., Improvements to the Far-Field Wave-Drag Methodology, General Dynamics Fort Worth Division Report FZA-476, August 1976.

13. Webb, J.B. and others, F-16 Aerodynamic Design Data Report, General Dynamics Fort Worth Division Report 16PR177, Revised November 1976.

14. Smith, C.W., ed., Aerospace Handbook, General Dynamics Fort Worth Division Report FZA-381-II, October 1972.

15. Hoerner, S.F., Fluid Dynamic Drag, Published by author, Brick Town, New Jersey, 1965.

REFERENCES (Continued)

16. Cunningham, A.M., A Steady and Oscillatory Kernel Function Method for Interfering Surfaces in Subsonic, Transonic and Supersonic Flow, NASA CR 144895, September 1976.

17. Cunningham, A.M., Prediction of Subsonic and Supersonic Aerodynamics for Highly Swept and Cambered Wings at High Angles of Attack, General Dynamics Fort Worth Division Report FZA-533 (in preparation).

18. Walker, J.J., Wind Tunnel Data Report, 1/15-Scale Model 400 Force Model, NASA Langley Research Center 4-Foot Unitary Plan Wind-Tunnel Test LRC-4-1318, General Dynamics Fort Worth Division Report FZT-383, March 1980.

19. Elbers, W.K., Wind Tunnel Data Report, 1/15-Scale Model 400-9 Force Model, Calspan 8-Foot Transonic Wind Tunnel Test TO3-623, General Dynamics Fort Worth Division Report FZT-421, November 1980.

20. Cochi, R.J., Wind Tunnel Data Report, 1/15-Scale Model 400-9 Force Model, NASA Langley Research Center 4-Foot Unitary Plan Wind Tunnel Test LRC-4-1348, General Dynamics Fort Worth Division Report FZT-413, November 1980.

21. Fox, M.C., Wind Tunnel Data Report, 1/15-Scale F-16NL Force Model, NASA Langley Research Center 4-Foot Unitary Plan Wind Tunnel Test LRC-4-1368, General Dynamics Fort Worth Division Report 400PR021, May 1981.

22. Elbers, W.K., Wind Tunnel Data Report, 1/15. Scale F-16XL Force Model, Calspan 8-Foot Transonic Wind Tunnel Test T03-643, General Dynamics Fort Worth Division Report 400PR020, May 1981.

23. Walker, J.J., Wind Tunnel Data Report, 1/15-Scale F-16XL Force Model, General Dynamics Low-Speed Wind Tunnel Test GDLST 784-4, General Dynamics Fort Worth Division Report 400PR017, March 1981.

24. Walker, J.J., Wind Tunnel Data Report, 1/15-Scale F-16XL Force Model, General Dynamics Low-Speed Wind Tunnel Test 784-0, General Dynamics Fort Worth Division Report FZT-426, March 1981.

25. Anderson, S.B. et al., V/STOL Handling-Qualities Criterion, AGARD Report No. 577, December 1970.

26. Environmental Control System Transient Analysis, AFFDL-TR-77-102, March 1977.

27. Mazta, C.J., Layton, D.M. and Schmidt, L.V., eds., Proceedings Navy/NASA V/STOL Flying Qualities Workshop, Monterey, California, April 1977.

28. Benepe, D.B., Further Analysis of Buffet Characteristics of a Canard-Delta Aircraft Configuration Based on Wing-Bending and Wing-Type Accelerometer Wind Tunnel Test Data, General Dynamics Fort Worth Division Report ARM-088, June 1972.

29. Wenham, R.J., A Flexible Mission Evaluation Technique for Operationally - Oriented Missions, General Dynamics Fort Worth Division Report ERR-FW-2040, December 1979.

REFERENCES (Concluded)

30. Lucas, C.B. and Evans, J.E., A Method for Analyzing Ski-Jump Launches of Conventional Airplanes, General Dynamics Fort Worth Division Report No. NAV-GD-0033, July 1981.

31. Mechtly, E.A., The International System of Units: Physical Constants and Conversion Factors, NASA SP-7012, 1973.

1. Report No.	2. Government Accession No.	3. Recipient's Catalog No.
NASA CR-166268		

4. Title and Subtitle	5. Report Date
STUDY OF AERODYNAMIC TECHNOLOGY FOR SINGLE-CRUISE-ENGINE VSTOL FIGHTER/ATTACK AIRCRAFT — PHASE I FINAL REPORT	February 1982
	6. Performing Organization Code

7. Author(s)	8. Performing Organization Report No.
W. H. Foley, A. E. Sheridan, C. W. Smith	
	10. Work Unit No.

9. Performing Organization Name and Address	11. Contract or Grant No.
General Dynamics — Fort Worth Division P. O. Box 748 Fort Worth, Texas 76101	NAS2-11000

12. Sponsoring Agency Name and Address	13. Type of Report and Period Covered
National Aeronautics and Space Administration, Washington, D.C. 20546 David Taylor Naval Ship R&D Center, Carderock, MD 20034 Naval Air Systems Command, Washington, DC 20361	Contractor Final Report June 1981 to February 1982
	14. Sponsoring Agency Code RTOP 505-43-01

15. Supplementary Notes Technical Monitor: D. A. Durston, W. P. Nelms, NASA/Ames, Mail Stop 227-2, Moffett Field, CA 94035 (415) 965-5855/-5879; FTS 448-5855/-5879
Point of Contact: J. H. Nichols, Jr. DTNSRDC
Point of Contact: M. W. Brown, NAVAIR

16. Abstract

A conceptual design and analysis on a single-engine STOVL fighter/attack aircraft has been completed. This aircraft combines a NASA/deHavilland ejector with vectored thrust and is capable of accomplishing the mission and point performance of Type Specification 169, and a flight demonstrator could be built with an existing F101/DFE engine.

The aerodynamic, aero/propulsive, and propulsive uncertainties have been identified, and a wind-tunnel program has been proposed to address those uncertainties associated with wing-borne flight.

17. Key Words (Suggested by Author(s))	18. Distribution Statement
VSTOL STOVL EJECTORS THRUST AUGMENTATION	~~FEDD Distribution~~ Subject Category 02

19. Security Classif. (of this report)	20. Security Classif. (of this page)	21. No. of Pages	22. Price*
Unclassified	Unclassified		

Available: NASA's Industrial Applications Centers

End of Document